

**Luminescence Dating of Aeolian Sediments –  
testing new Approaches to extend the Age Range  
beyond the Eemian**

In a u g u r a l - D i s s e r t a t i o n

zur

Erlangung des Doktorgrades  
im Fachbereich Geowissenschaften  
der Freien Universität Berlin

vorgelegt von

**Esther Dorothe Schmidt**

geb. 01.11.1979 in Dieburg/Hessen

**Berlin, 2011**

**Erstgutachter und Betreuer: Prof. Dr. Manfred Frechen**

**Zweitgutachterin: Prof. Dr. Margot Böse**

**Eingereicht am: 10.12.2010**

**Tag der Disputation: 18.02.2011**

# Table of contents

<b>List of figures</b>	<b>7</b>
<b>List of tables</b>	<b>11</b>
<b>Summary</b>	<b>12</b>
<b>Zusammenfassung</b>	<b>14</b>
<b>Chapter 1</b>	<b>16</b>
<b>Introduction</b>	<b>16</b>
1.1. Background	16
1.2. Luminescence dating	18
<i>1.2.1. Principles</i>	18
<i>1.2.2. Quartz</i>	20
<i>1.2.3. Feldspar</i>	22
1.3. Study sites	24
1.4. Outline of the thesis	27
References	29
<b>Chapter 2</b>	<b>34</b>
<b>Luminescence chronology of the upper part of the Stari Slankamen loess sequence (Vojvodina, Serbia)</b>	<b>34</b>
Abstract	34
2.1. Introduction	35
2.2. Geological setting	35
2.3. Experimental details	37
2.4. Performance tests for luminescence dating	39
2.5. Chronology of the Stari Slankamen loess sequence	41
2.6. Discussion and conclusions	45
Acknowledgments	46
References	46
<b>Chapter 3</b>	<b>50</b>

**Elevated temperature IRSL dating of the lower part of the Stari Slankamen loess sequence (Vojvodina, Serbia) – investigating the saturation behaviour of the pIRIR<sub>290</sub> signal** **50**

Abstract 50

**Chapter 4** **75**

**Luminescence chronology of the loess record from the Tönchesberg section – a comparison of using quartz and feldspar as dosimeter to extend the age range beyond the Eemian** **75**

Abstract 75

4.1. Introduction 76

4.2. Geological setting 78

*4.2.1. Profile A and B* 80

*4.2.2. Profile C* 81

*4.2.3. Profile D* 82

*4.2.4. Profile E* 82

4.3. Experimental details 83

4.4. Performance tests 85

*4.4.1. OSL* 85

*4.4.2. TT-OSL* 87

*4.4.3. Pulsed post-IR IR luminescence signal* 87

4.5. Results & Discussion 90

*4.5.1. Dosimetry, Equivalent doses and Luminescence ages* 90

*4.5.2. Weichselian deposits* 94

*4.5.3. Saalian deposits* 96

4.6. Conclusion	101
Acknowledgements	102
References	102
<b>Chapter 5</b>	<b>108</b>
<b>Elevated temperature IRSL dating of loess sections in the Eifel region of Germany</b>	<b>108</b>
Abstract	108
<b>Chapter 6</b>	<b>143</b>
<b>IRSL Signals from Maar Lake Sediments Stimulated at Various Temperatures</b>	<b>143</b>
Abstract	143
6.1. Introduction	144
6.2. Geological setting	147
6.3. Experimental details	148
6.4. Luminescence dating	149
6.4.1. OSL dating of quartz	149
6.4.2. IRSL dating of polymineral fine-grains	151
	5

6.4.2.1. <i>Post-IR IRSL measurement sequence</i>	152
6.4.2.2. <i>Luminescence characteristics and performance in SAR</i>	152
6.4.2.3. <i>Equivalent Dose (<math>D_e</math>), fading rates and age estimates</i>	158
6.5. Discussion	162
6.6. Conclusion	164
Acknowledgements	165
References	165
<b>Appendix</b>	<b>170</b>
<b>Chapter 7</b>	<b>172</b>
<b>Luminescence dating of the loess/palaeosol sequence at the gravel quarry Gaul/Weilbach, Southern Hesse (Germany)</b>	<b>172</b>
Abstract	172
7.1. Introduction	173
7.2. Loess/palaeosol sequence at the gravel quarry Gaul/Weilbach	175
7.3. Experimental details	177
7.4. Luminescence dating	178
7.4.1. <i>Post-IR IRSL measurement sequence</i>	179
7.4.2. <i>Luminescence characteristics and performance in SAR</i>	180
7.4.3. <i>Equivalent Dose (<math>D_e</math>), fading rates and age estimates</i>	182
7.5. Discussion	185
7.6. Conclusion	188
Acknowledgements	188
References	189
<b>Chapter 8</b>	<b>193</b>
<b>Conclusion</b>	<b>193</b>
8.1. Quartz	193
8.2. Feldspar	194
8.3. Chronology for the investigated Aeolian sediments	196
References	198
<b>Acknowledgements</b>	<b>202</b>

# List of figures

Figure 2.1: Map of loess distribution in the Vojvodina and adjacent regions showing locations of the investigated section and other main loess sites.	36
Figure 2.2: Lithology and luminescence ages of the Stari Slankamen loess site.	37
Figure 2.3: Results of dose recovery and preheat plateau test for sample SSK 3 (a,b) and SSK 5 (c,d).	41
Figure 2.4: Decay curves of quartz OSL, polymineral IRSL and post-IR OSL for SSK 4.	43
Figure 2.5: Dose response curves of polymineral IRSL and post-IR OSL for SSK 8.	44
Figure 4.1: Map showing the location of the Tönchesberg section in the East Eifel area.	78
Figure 4.2a: Lithology and luminescence ages of the Tönchesberg section (Weichsel, Profile A and B).	81
Figure 4.2b: Lithology and luminescence ages of the Tönchesberg section (Saale, Profile C, D and E).	82

Figure 4.3: Thermal transfer test for Sample Toe1 and Toe5.	85
Figure 4.4: Dose recovery test with different preheat temperatures for Sample Toe1 and Toe5.	86
Figure 4.5: Ratio of the measured to given dose for the routine dose recovery test for the OSL SAR protocol for all samples.	87
Figure 4.6: De preheat plateau test for sample Toe8.	88
Figure 4.7: Ratio of the measured to given dose for the routine dose recovery test for the pulsed post-IR IR protocol for all samples.	89
Figure 4.8: G-values for all samples.	90
Figure 4.9: Fading test for sample Toe7 and Toe8.	90
Figure 4.10: OSL and TT-OSL dose response curves for representative aliquots of sample Toe7 and Toe8.	92
Figure 4.11: Profile B.	93
Figure 4.12: Profile E.	98
Figure 4.13: Idealized profile of the Tönchesberg section.	99
Figure 4.14: Charcoal of larch (Larix).	100



Figure 6.1: Map showing coring locations of the dry maar of Jungfernweiher, West Eifel Volcanic Field.	145
Figure 6.2: Dose response and decay curve for sample JWS1 showing the OSL from fine grain quartz.	151
Figure 6.3: Dose response and decay curves for sample a) JWS1 and b) JWS8 showing the IR <sub>50</sub> (filled symbols) and the pIRIR <sub>225</sub> (open symbols).	154
Figure 6.4: Dose response and decay curves for sample a) JWS1 and b) JWT8 showing the IR <sub>50</sub> (filled symbols) and the pIRIR <sub>290</sub> (open symbols).	155
Figure 6.5: Dose response and decay curves for sample JWT9 showing the IR <sub>50</sub> , pIRIR <sub>225</sub> and the pIRIR <sub>290</sub> .	156
Figure 6.6: Dose recovery test (a) and the residual doses (b) for the IR <sub>50</sub> and the pIRIR <sub>225</sub> signal for all samples.	157
Figure 6.7: Fading rates for the post the IR <sub>50</sub> and pIRIR <sub>225</sub> signals for all samples. Three aliquots were measured per sample.	161
Figure 6.8: Anomalous fading of IRSL <sub>50</sub> , pIRIR <sub>225</sub> and pIRIR <sub>290</sub> signals.	162
Figure 7.1: Map showing the location of the loess/palaeosol sequence exposed at the gravel quarry Gaul/Weilbach.	173
Figure 7.2: Loess/palaeosol sequence at the gravel quarry Gaul/Weilbach with a) loess concretions of the fCc horizon with remains of brown Bt material and b) two fossil Bt-horizons near the profile of Fig. 2.	175

Figure 7.3: Terraces of the river Main in the southern foreland of the Taunus mountains. The Loess/palaeosol sequence is located close to the symbol “t4”.	176
Figure 7.4: Dose response and decay curves for samples a) Wei 6 and b) Wei 7 showing the IR <sub>50</sub> (filled symbols) and the pIRIR <sub>225</sub> signal (open symbols).	180
Figure 7.5: Dose recovery test (a) and the residual doses (b) for the IR <sub>50</sub> and the pIRIR <sub>225</sub> signal for all samples.	181
Figure 7.6: Fading rates for the post the IR <sub>50</sub> and pIRIR <sub>225</sub> signals for all samples.	184
Figure 7.7: Lithology and luminescence ages of the loess/palaeosol sequence exposed at the gravel quarry Gaul/Weilbach.	186

# List of tables

Table 2.1: Dose rate data from potassium, uranium and thorium content, as measured by gamma spectrometry.	39
Table 2.2: Equivalent dose ( $D_e$ ), recycling ratio, dose recovery, fading and luminescence ages.	42
Table 4.1: Dose rate data from potassium, uranium and thorium content, as measured by gamma spectrometry.	84
Table 4.2: Equivalent dose ( $D_e$ ), recycling ratio, dose recovery, fading and luminescence ages.	91
Table 6.1: Dose rate data from potassium, uranium and thorium content, as measured by gamma spectrometry.	149
Table 6.2: Elevated temperature post-IR IRSL measurement sequence.	152
Table 6.3: Summary of equivalent dose ( $D_e$ ), saturation level, recycling ratio, dose recovery, residual doses, fading and luminescence ages.	159
Table 7.1: Dose rate data from potassium, uranium and thorium content, as measured by gamma spectrometry.	178
Table 7.2: Elevated temperature post-IR IRSL measurement sequence.	179
Table 7.3: Summary of equivalent dose ( $D_e$ ), recycling ratio, dose recovery, residual doses, fading and luminescence ages.	183

# Summary

Aeolian sediments such as loess and lake sediments are representing one of the most detailed terrestrial archives of climate and environment change. One of the challenges in Quaternary research is to make these archives accessible by obtaining reliable chronologies to get further insight into past climate and environmental processes which are leading subsequently to a better understanding of the future climate and helping to improve the accuracy of climate change predictions.

Luminescence dating is one of the most important and most commonly used tools for determining the deposition age of Quaternary sediments. Quartz and feldspar, which are used as dosimeters to date aeolian deposits, however, both exhibit disadvantages – quartz saturates at comparatively low doses and feldspar suffers from anomalous fading resulting in an upper dating limit of 100-150 ka and age underestimation, respectively. Therefore, previous studies presented age estimates only up to about 100 ka. So far it was difficult to provide reliable chronologies for the Middle Pleistocene deposits owing to the upper dating limit. This doctoral research aims to elaborate the potential of quartz and feldspar as dosimeter for dating Middle Pleistocene aeolian deposits. New approaches in luminescence dating were tested to establish a more reliable geochronological frame for the aeolian sediments.

Loess and maar lake sediments from the Vojvodina region/Serbia (Stari Slankamen), Middle Rhine area/Germany and the southern foreland of the Taunus Mountains/Germany (Weilbach) are investigated in this thesis. The loess sections in the Middle Rhine area including the sections at Tönchesberg, Kärlich, Ariendorf, Wannenköpfe, Dachsbusch and Jungfernweiher provided independent age control by intercalated tephra layers, so that the reliability of the new techniques could be tested. This study revealed that optically stimulated luminescence (OSL) from quartz could be used to obtain age estimates up to ~70 ka. The thermally transferred OSL (TT-OSL), which uses a transfer of charge from a trap where the signal saturates at doses more than 10 times higher than the normal OSL signal, has the potential for dating older sediments. However, the TT-OSL signal was not present in most of the loess samples from the Middle Rhine area, although the presence of this signal could be used to distinguish between different sources of loess. The results of this thesis showed that the post-IR infrared stimulated luminescence (IRSL) signal from feldspar measured at 290°C (pIRIR<sub>290</sub>) as well as pulsed post-IR IRSL signal measured at 150°C (pIRIR<sub>150</sub>) signal from feldspar have the potential to date Middle Pleistocene deposits. The pIRIR<sub>290</sub> signal could be

used to calculate age estimates up to ~300 ka, while the pulsed pIRIR<sub>150</sub> signal provided age estimates up to ~200 ka. Anomalous fading could not be detected. The ages obtained in the previous dating studies generally underestimated the new luminescence ages in this thesis. For the Jungfernweiher it was shown that the dry maar lake was effectively filled up with sediments at ~250 ka, and there either been very little deposition since then, or younger sediments have been striped by erosion. There is a discrepancy between these results and the established stratigraphy, which could not be dissolved during this thesis.

It can be concluded that the results of this thesis provide a more reliable geochronological framework for the loess/palaeosol sequences of the Vojvodina region, the Middle Rhine area and the southern foreland of the Taunus Mountains as well as for the dry maar lake Jungfernweiher. This information is required to access these sensitive terrestrial archives for getting a better understanding of local and regional environmental processes and conditions for the Middle and Late Pleistocene period in Europe.

# Zusammenfassung

Äolische Sedimente, wie Löss und Seesedimente, zählen zu den am meisten gegliederten terrestrischen Klima- und Umweltarchiven. Eine der Herausforderungen der Quartärforschung ist es, diese Archive zugänglich zu machen, indem durch eine verlässliche Chronologie weitere Kenntnis über Klima- und Umweltprozesse erlangt werden kann. Dies führt zu einem besseren Verständnis des zukünftigen Klimas und ermöglicht, die Genauigkeit von Klimaprognosen zu verbessern. Die Lumineszenz ist eine der wichtigsten und am meisten verbreiteten Methoden für die Datierung von quartären Ablagerungen.

Quarz und Feldspat, die als Dosimeter für äolische Sedimente verwendet werden, besitzen beide Nachteile – Quarz sättigt schon bei vergleichsweise niedrigen Dosen, während Feldspat das Phänomen des „anomalous fading“ zeigt, was zu einer oberen Datierungsgrenze von 100-150 ka und einer Altersunterbestimmung führt. Bislang war es daher nicht möglich, eine verlässliche Chronologie für mittelpleistozäne Ablagerungen zu etablieren. Diese Dissertation hat zum Ziel, das Potential von Quarz und Feldspat als Dosimeter für die Datierung mittelpleistozäner äolischer Ablagerungen herauszustellen. Neue Methoden der Lumineszenz wurden getestet, um einen verlässlicheren geochronologischen Rahmen für die äolischen Sedimente zu etablieren.

Löss und Maarsedimente aus der Vojvodina Region/Serbien (Stari Slankamen), dem Mittelrheingebiet/Deutschland (Jungfernweiher) und dem südlichen Taunusvorland/Deutschland (Weilbach) wurden in dieser Dissertation untersucht. Die Lössaufschlüsse im Mittelrheingebiet (Tönchesberg, Kärlich, Ariendorf, Wannenköpfe und Dachsbusch) besitzen unabhängige Alterskontrolle durch zwischengeschaltete Tephralagen, so dass die Verlässlichkeit der neuen Methoden getestet werden konnte.

Diese Studie stellte heraus, dass äolische Sedimente mit der optisch stimulierten Lumineszenz von Quarz verlässlich bis zu ~70 ka datiert werden können. Das thermisch transferierte OSL Signal von Quarz, das bei bis zu 10 mal höheren Dosen sättigt als die OSL und dadurch das Potential hat, ältere Sedimente zu datieren, war bei den meisten Lössproben aus dem Mittelrheingebiet nicht vorhanden. Das Signal konnte jedoch genutzt werden, um zwischen verschiedenen Lössherkunftsgebieten zu unterscheiden. Die Ergebnisse dieser Doktorarbeit zeigen, dass sowohl das post-IR IRSL Signal gemessen bei 290°C (pIRIR<sub>290</sub>) als auch das gepulste post-IR IRSL Signal gemessen bei 150°C (pIRIR<sub>150</sub>) von Feldspat das Potential haben mittelpleistozäne äolische Sedimente zu datieren. Mit dem pIRIR<sub>290</sub> Signal

konnten Alter bis ~300 ka bestimmt werden, mit dem gepulsten pIRIR<sub>150</sub> Signal Alter bis ~200 ka. „Anomalous fading“ konnte nicht nachgewiesen werden. Die Ergebnisse frühere Studien unterbestimmen die Lumineszenzalter dieser Dissertation im Allgemeinen.

Für das Trockenmaar Jungfernweiher konnte nachgewiesen werden, dass es vor ca. 250 ka schon mit Sedimente zugeschüttet war. Seither gab es entweder nur sehr wenig Ablagerung, oder die Sedimente wurden wieder erodiert. Zwischen diesen Ergebnissen und der etablierten Stratigraphie bleibt eine Diskrepanz, die während dieser Dissertation nicht gelöst werden konnte.

Zusammenfassend kann festgestellt werden, dass die Ergebnisse dieser Doktorarbeit einen verlässlicheren geochronologischen Rahmen sowohl für die Löss-Sequenzen der Vojvodina Region, des Mittelrheingebietes und des südlichen Taunusvorlandes als auch für das Trockenmaar Jungfernweiher bereitstellen. Diese Information wird benötigt, um diese sensiblen terrestrischen Archive für ein besseres Verständnis der lokalen und regionalen Umweltprozesse und -konditionen während des Mittel- und Spätpleistozän in Europa aufzuschließen.

# Chapter 1

## Introduction

### 1.1. Background

Loess is a widespread terrestrial sediment which covers approximately 10% of the world's surface (Pécsi, 1968). The most important loess covered areas of the world are found in northern China (Loess Plateau), northwestern and central Europe, Sibiria, central Asia and northern and southern America. There are other loess areas in Alaska, New Zealand and southern Britain. This silty, yellowish sediment was deposited as wind-blown dust during the glacial periods of the Quaternary and consists mainly of quartz and feldspar. Loess deposits are in general intercalated by differently developed soils, which reflect “warm” interstadial and interglacial climate. In some regions like the Middle Rhine area (Germany) aeolian dust comprises often a very large part of the sediment inventory of volcanic depressions and crater fills such as maar lakes or scoria cones which form excellent sediment traps. Therefore loess/palaeosol sequences and aeolian derived lake sediments are sensitive terrestrial archives of climate and environmental change and provide important information on local and regional environmental processes and conditions for the Middle and Late Pleistocene period in Europe. For our knowledge about future climate and environmental change it is important to understand the processes of the past. Dust accumulation and loess formation in Europe range from the maritime areas in NW France and Belgium via Central Europe to the Ukraine and the Russian Plains with increasing continental climate from W to E (Frechen et al., 2003). This thesis concentrates on loess deposits in the Vojvodina region (Serbia), on loess/palaeosol sequences and maar lake sediments of the Middle Rhine area and the foreland of the Taunus Mountains, both latter areas situated within the Rhenish massif (Germany). The Vojvodina region is located in the south-eastern part of the Carpathian basin and is covered by loess and loess-like sediments reaching a thickness up to 55 m. The loess sequences in the Vojvodina are regarded as a key for understanding and reconstructing the palaeoclimatic and -environmental conditions in South-Eastern Europe and they can be seen as an important link between the Central European loess sites and the Central Asian and Chinese loess (Marković et al., 2008, 2009). The Middle Rhine area provides many important loess/palaeosol



sequences, among them the Kärlich section which is regarded as one of the key sections for the Middle Pleistocene stratigraphy of northwestern Europe (Boenigk and Frechen, 2001). The loess successions of the Middle Rhine area often cover the Rhine terraces or represent crater fillings of volcanoes in the East Eifel volcanic field. Many loess deposits are intercalated by volcanic layers originating from the Eifel volcanism. The southern foreland of the Taunus Mountains consists mainly of Pleistocene terraces of the river Main covered by thick loess/palaeosol sequences. The loess/palaeosol sequences in the Vojvodina region and the Middle Rhine area have been intensively investigated in many studies during the last century. However, reliable numeric age estimates are still lacking for many of the loess successions, especially for the Middle Pleistocene deposits. This makes it still difficult to interpret the terrestrial climate archives as well as to correlate the loess/palaeosol sequences with other European loess records. Therefore a dating technique is required which is applicable for a broad time range to provide a reliable chronology. Luminescence dating enables to determine the depositional age of various sediments over an age range from a few decades of years to several hundred thousand years and has been used in many studies to date loess deposits. Quartz and feldspar, which are used in most cases as dosimeters are present in all loess deposits and make this kind of sediment suitable for luminescence dating (Roberts, 2008). Unfortunately most of the previous luminescence studies provided apparently reliable thermoluminescence (TL) and infrared stimulated luminescence (IRSL) ages up to about 100 ka. These age estimates were often underestimated most likely due to anomalous fading. During the past ten years significant improvements were made in luminescence dating. In many studies the potential of new methods is investigated to extend the age range. The best way to test the reliability of a method is to apply it to sediment successions for which independent age control is available like in the Middle Rhine area. In this thesis crater fillings of scoria cones and loess/palaeosol sequences with intercalated tephra layers from this area are investigated. They form excellent sites for testing the applicability of new methods.

This thesis aims to apply and to test new luminescence dating techniques, for both minerals, quartz and feldspar. The aeolian sediments in the Vojvodina region, the Middle Rhine area and the foreland of the Taunus Mountains are investigated by luminescence dating to provide a more reliable chronological frame for the deposits in these regions.

## 1.2. Luminescence dating

### 1.2.1. Principles

Luminescence dating is a radiation dosimetric method and is based on the time-dependent accumulation of radiation damage in minerals. It is used to date the time that has passed since the last exposure of the minerals to sunlight (Aitken, 1998) which means the depositional age of the sediments. Grains of quartz or feldspar (the most common minerals) are used as natural dosimeter. They are able to store energy within their crystal structure, which is coming mainly from an omnipresent ionising radiation ( $^{238}\text{U}$ ,  $^{232}\text{Th}$  with daughters,  $^{40}\text{K}$  and  $^{87}\text{Rb}$ ) in the sedimentary environment and cosmic radiation. The electrons can be trapped and subsequently stored at structural defects or impurities in the crystal lattice for long periods (Aitken, 1985). When the sediments are transported again, they are exposed to light and the trapped electrons will be released and the “luminescence clock” will be set to zero. After the sediments have been buried again the clock starts from new and the luminescence signal will build up and grow the more time passes by. At some point a sample is collected. By applying luminescence methods the time passed since the last sunlight exposure can be determined. This is equivalent to the time passed since the last deposition of the sediment.

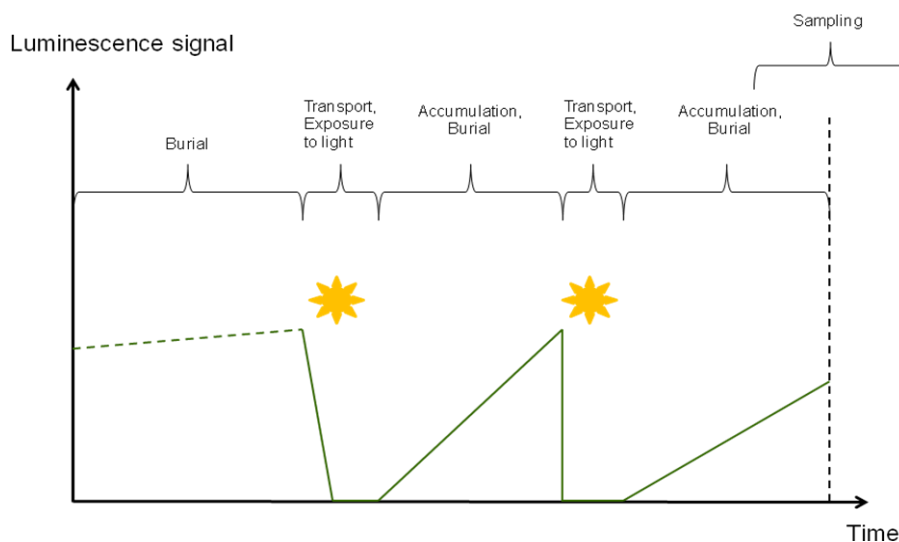


**Figure 1.1: Principle of luminescence dating**

The most important requirement is that the sediments are well bleached prior to deposition. For loess it is expected that any residual trapped charge has been removed during the aeolian transport. In the laboratory the grains are first heated, and then stimulated with IR

or blue LEDs to release the electrons from their traps. Subsequently they release their stored energy as emission of light (photon) during recombination. This light is known as the optically (or infrared) stimulated luminescence. A photomultiplier tube counts the emitted photons which are released. Then the aliquots are irradiated with different doses, often by a beta source in the laboratory and they are subsequently measured. These induced signals are used to build up a growth curve. Interpolation of the natural signal to this curve allows estimating the dose of radiation (palaeodose or equivalent dose,  $D_e$ ) which is equivalent to the energy that the crystal has absorbed since the last exposure to sunlight. Equivalent doses ( $D_e$ ) are determined using a single aliquot protocol (SAR) where all measurements can be made on one aliquot with the advantage that the  $D_e$ -values are more precise. The SAR protocol has been developed for quartz measurements (Murray and Wintle, 2000). An aliquot is first preheated and the natural signal is measured before giving a test dose, heated again and measured the test dose signal to correct the natural signal for sensitivity changes. For the next cycle a regenerative dose is given and then the aliquot is preheated and subsequently the induced OSL is measured. The same test dose as for the first cycle is administered. This cycle is then repeated several times with different given doses. To test if the sensitivity change correction is accurately measured one of the formerly given regenerative dose is repeated. The ratio of the two obtained luminescence signals (recycling ratio) should be unity. The dose response curve (growth curve) for the aliquot is obtained by plotting the sensitivity corrected OSL as a function of the given regenerative doses. Equivalent doses ( $D_e$ ) can be calculated by interpolating the sensitivity corrected natural signal to the growth curve. To test for recuperation (signal induced by heating after the OSL measurement) a zero regenerative dose is given. The ratio of the sensitivity corrected signal of this measurement and the natural OSL should then be lower than 5% (Murray and Olley, 2002). To test for the reliability of the dose measurement, laboratory experiments like thermal transfer, preheat plateau and dose recovery ratio have to be done. To check for thermal transfer (Wintle and Murray, 2006) some aliquots are bleached and subsequently measured with increasing temperatures ranging e.g. in steps of 20°C from 200°C to 300°C. After bleaching,  $D_e$  estimates should be close to zero; significant  $D_e$  value with increasing preheat temperature indicate thermal transfer of charge from thermally-shallow optically insensitive traps to the deeper OSL trap. To confirm the signal stability the dependence of equivalent dose ( $D_e$ ) on preheat temperature has to be investigated applying  $D_e$  preheat plateau tests (equivalent dose measurements using different preheat temperatures). To test the suitability of the SAR protocol, the dose recovery ratio (Murray and Wintle, 2003) has to be determined. To do this, some aliquots have first to be bleached before

giving a dose approximately equal to the natural dose. This dose is then measured as if it were a natural dose. The ratio of the measured dose to the given dose should be close to unity.

To determine the dose rate to which the sample was exposed during its burial radionuclide concentrations are obtained for example by high resolution gamma spectrometry on sediment collected from the immediate surrounding of the samples. The concentrations of uranium, thorium and potassium are converted into infinite-matrix dose rates using the conversion factors of Adamiec and Aitken (1998) and water-content attenuation factors (Aitken, 1985). As cosmic radiation is also contributing the cosmic-ray dose rate has to be calculated from knowledge of burial depth, altitude, matrix density, latitude and longitude for each sample (Prescott and Stephan, 1982; Prescott and Hutton, 1994). For the age calculation the equivalent dose,  $D_e$  is divided by the dose rate:

$$age (ka) = \frac{D_e}{D_R} \left( \frac{Gy}{Gy/ka} \right)$$

This age represents the time of the last exposure to sunlight, will say the deposition age of the sediment.

### ***1.2.2. Quartz***

The optically stimulated luminescence (OSL) of quartz has been widely used to estimate the deposition age of sediments and is usually regarded as an accurate and precise dating method (e.g. Murray and Olley, 2002). To obtain quartz grains from loess the polymineral fraction is treated with 34% fluorosilicic acid ( $H_2SiF_6$ ) for 6 days, preferentially dissolving feldspar grains, and leaving behind a quartz-rich extract. The purity of the quartz extract is checked using the IR depletion ratio during the SAR cycle (Duller, 2003); the aliquot is given a dose which is measured with blue stimulation, then the same dose is administered and the aliquot is stimulated first with infrared diodes before the blue stimulation. As the quartz is not depleting with IR stimulation the second SAR measurement cycle yield a lower sensitivity corrected signal in case of feldspar contamination. Quartz blue-stimulated OSL is detected through 7.5 mm of Hoya U-340 filter (passing 260 to 390 nm, i.e. UV). The OSL from quartz decays very fast, the fast component of quartz can be depleted in only a few minutes exposure to daylight (Godfrey-Smith et al., 1988). Fig. 1.2 shows a typical decay curve from quartz.

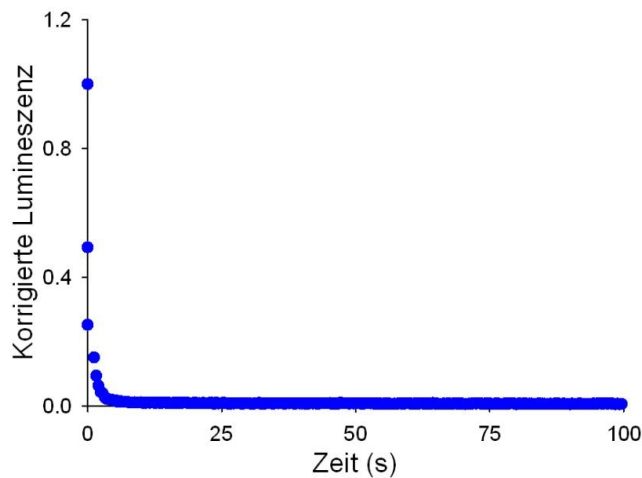


**Figure 1.2: Decay curve from quartz**

Optically stimulated luminescence (OSL) from fine grain quartz is applied in this thesis on samples from the Stari Slankamen section (Vojvodina) and from various sections in the Eifel area. A different approach to measure the OSL from quartz without treating the polymineral fine-grains with fluorosilicic acid ( $\text{H}_2\text{SiF}_6$ ) was proposed by Banerjee et al. (2001). In this protocol the  $D_e$  values are calculated using a modified SAR protocol for polymineral fine-grains, the so called Double SAR protocol based on the single-aliquot regenerative-dose (SAR) protocol for quartz (Murray and Wintle, 2000). This modified protocol involves a stimulation with IR-diodes to reduce the feldspar signal and then the aliquots are stimulated with blue LEDs (post-IR OSL signal). Two estimates of  $D_e$  are obtained; the IRSL from feldspar and the post-IR OSL which is supposed to be dominated by quartz (Roberts and Duller, 2004). This approach is applied in this thesis using polymineral fine grains from the Stari Slankamen loess/palaeosol sequence in the Vojvodina region. Unfortunately the fast component of the quartz OSL (the component normally used for dating) saturates following doses of 200-400 Gy (Wintle and Murray, 2006). This signifies an upper age limit of ~50-70 ka for loess deposits as the typical dose rate lies between 3 and 4 Gy/ka (e.g. Frechen, 1991, Roberts, 2008, Schmidt et al., 2010, in press). Thermally transferred OSL (TT-OSL; Wang, et al. 2006, 2007; Tsukamoto et al., 2008) overcomes this problem by using a thermally transferred signal to the OSL trap which saturates at doses more than 10 times higher than the OSL. This dose dependent part of the thermally transferred OSL

from quartz, which can be measured after depleting the OSL, giving a thermal treatment and then measured the signal. This signal is less light sensitive than the fast component from quartz (Tsukamoto et al., 2008; Porat, et al., 2009). As loess is supposed to be well bleached due to its aeolian transport it is hence a suitable sediment for using TT-OSL. Porat et al. (2009) proposed a simplified single aliquot TT-OSL protocol. Variations of this approach are tested to optimise the signal intensity (Schmidt et al., 2009).

### ***1.2.3. Feldspar***

The luminescence signals from feldspars grow to much higher doses than those from quartz, which offers the possibility of significantly extending back the age range. Luminescence dating focused for a long time on quartz due to the stability of the signal. In contrast, the electrons from traps in feldspars are less stable; the minerals suffer from a spontaneous loss of signal, which leads consequently to an underestimation of the age. This phenomenon is called anomalous fading (Wintle, 1973) which is most likely caused by quantum-mechanical tunnelling (Visocekas, 1985). Many studies show that the IRSL ages consistently underestimated the quartz OSL ages most likely due to anomalous fading (e.g. Schmidt et al., 2010). Hence the fading rate (g-value) (Aitken, 1985) has to be determined and the ages are corrected. Several methods of age corrections have been proposed (e.g. Huntley and Lamothe, 2001; Lamothe et al., 2003) and many studies show corrected IRSL ages which are in good agreement with quartz OSL ages in between the uncertainty. But there is no general consensus which correction method should be used and furthermore the correction method is only valid for the 'linear part' of the dose response curve (Huntley and Lamothe, 2001). Luminescence dating of loess is often carried out on polymineral fine-grains (with a diameter of 4-11  $\mu\text{m}$ ). Fine-grain TL dating was first proposed by Zimmerman (1971). Polymineral fine-grains consist normally of quartz, feldspars, mica, different kind of clay minerals (mainly illite, kaolinite, montmorillonite), and other minerals (Krbetschek et al., 1997). The luminescence characteristics of such polymineral fractions are very complex and therefore luminescence dating on fine-grains has been criticised (Krbetschek et al., 1997). However, polymineral fine-grain dating has often been successfully applied e.g. to establish loess chronologies. Roberts (2008) gives an overview about the development and application of luminescence dating techniques to loess deposits. In this study the polymineral fine grain fraction of the aeolian sediments was used to determine the equivalent doses ( $D_e$ ). Feldspar

IRSL signals are detected through Schott BG-39 and Corning 7-59 filters (passing between 320 and 460 nm; i.e. blue). Fig. 1.3 shows a decay curve from feldspar.

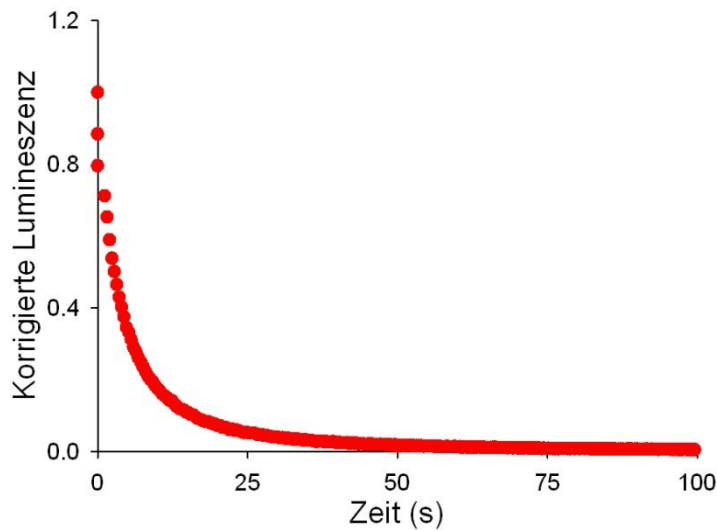


**Figure 1.3: Decay curve from feldspar**

Feldspar dating is normally carried out using a SAR protocol with 50° C IR stimulation with detection in the blue (-violet) spectrum; sometimes with an extra cleanout step to reduce the recuperation. Previous studies presented reliable age estimates for loess up to ~100 ka (i.g. Frechen, 1991). Recently new dating protocols were developed with the aim of extending the age range. Thomsen et al. (2008) found out, that stimulation at elevated temperatures significantly reduces the fading rate. Based on this study Buylaert et al. (2009) tested a SAR protocol, with detection in the blue (320-460 nm), this involves a stimulation with IR for 100s at 50°C (IR<sub>50</sub>) prior to an elevated temperature stimulation with IR for 100s at 225°C (pIRIR<sub>225</sub>), a so called post-IR IRSL measurement sequence. They have shown that the observed fading rates for the post-IR IRSL signal are significantly lower than from the conventional IR<sub>50</sub> and that the signal is bleachable in nature. Thiel et al. (2011) extended the post-IR IRSL protocol using a preheat of 320°C and a stimulation temperature of 290°C for the post-IR IRSL (pIRIR<sub>290</sub>) from polymineral finegrains. They found natural signals from a sample below the Brunhes/Matuyama boundary in saturation on a laboratory growth curve and they concluded that they were unable to detect fading in this field sample. A different approach was presented by Tsukamoto et al. (2006) who reported that the long-lifetime luminescence component, observed from feldspars when the stimulation light source is pulsed, is significantly more stable than shorter lifetime components. The post-IR IRSL and

pulsing approach were combined to use the off-period pulsed post-IR IRSL from polymineral fine-grains for dating purpose. Pulsed stimulation is carried out by a LED pulsing unit with an included photon-count gating circuit described by Denby et al. (2006). This provides a counting window within the off-period of each pulse cycle. The pulsed measurements are conducted using 50  $\mu$ s on, and 150  $\mu$ s off, with the gating the counts were only recorded during the off-periods, when the stimulation LEDs have completely turned off from the PM. The  $D_e$  values are obtained using a pulsed post IR IRSL measurement sequence with stimulation with IR for 100 s at 50°C prior to a pulsed elevated temperature stimulation with IR for 400 s at 150°C.

### 1.3. Study sites

The loess/palaeosol sequences in the Vojvodina region (Fig. 1.4) are among the oldest and most complete loess records in Europe covering a long time period (Marković et al., 2009).

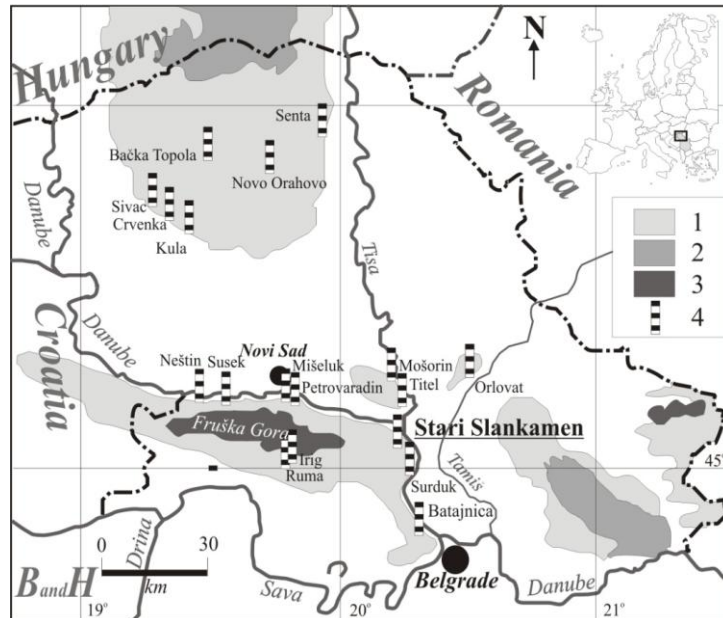


**Figure 1.4:** Map of loess distribution in the Vojvodina and adjacent regions showing locations of the investigated section and other main loess sites (modified from Marković et al., 2004). Key: 1. Loess plateau; 2. Sandy area; 3. Mountain; 4. Investigated exposures.



The Vojvodina region is situated in the south-eastern part of the Pannonian basin in the area of the confluence of the rivers Danube, Sava and Tisza. More than 60% of this lowland area is covered by loess and loess-like sediments up to 55 m thickness (Marković et al., 2004, 2006, 2007). The loess stratigraphy of the Vojvodina is quite uniform because of the plateau character of this region (Marković et al., 2006). The loess records provide important information for the comparison of the European stratigraphies (Marković et al., 2006) and furthermore they can be seen as an important link between Central European loess sites and the Central Asian and Chinese loess provinces (Marković et al., 2009). The Stari Slankamen section, the profile under study, is located in the north-eastern part of the Srem Loess Plateau and exposes an about 40 m thick series of loess intercalated by at least nine pedocomplexes. Optically stimulated luminescence (OSL) is carried out for the first time at this section to establish a more reliable chronostratigraphical framework. The other focus of this thesis lies on loess/palaeosol sequences and maar lake sediments of the Eifel region/Middle Rhine area and the foreland of the Taunus Mountains, both areas located within the Rhenish massif.

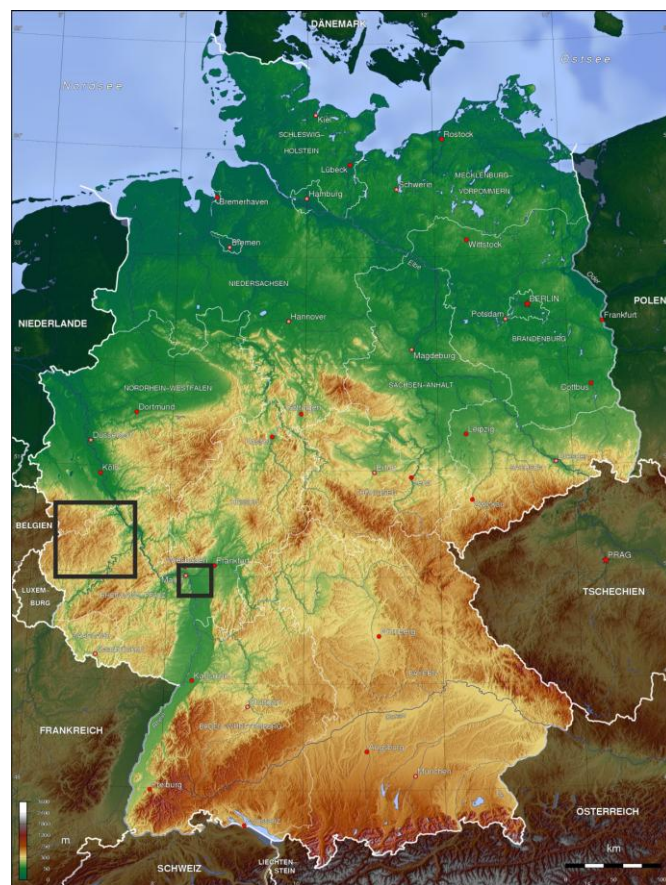


**Figure 1.5: Map showing the locations of the Eifel region and the southern foreland of the Taunus mountains (modified after [www.mygeo.info/landkarten\\_deutschland.html](http://www.mygeo.info/landkarten_deutschland.html))**

The Middle Rhine area provides many loess sections. Loess/palaeosol sequences are often overlain the Rhine terraces or represent crater fillings of volcanoes of the East Eifel volcanic field. Many loess deposits are intercalated by volcanic layers originating from the Eifel volcanism. The volcanism of the East Eifel Volcanic Field in Germany was according to Boenigk and Frechen (2001) reactivated between 500 and 600 ka. The loess/palaeosol sequences of late Middle Pleistocene scoria cones in the East Eifel Volcanic field are generally well preserved (Boenigk and Frechen, 2001). The well age controlled sites Tönchesberg, Dachsbusch and Wannenköpfe are investigated using the post-IR IRSL approach. At the Tönchesberg scoria cone, loess sediments with intercalated weak soils, which cover the volcanic debris, are exposed. The penultimate glacial loess is intercalated by tephra layers and weak tundra gleys. A red-brown forest soil is superimposed on this loess. Above this last Interglacial (Eemian) soil there are about 11 m of loess and loess-like sediments exposed including weak soils, pellet sands, reworked pedosediments, two marker loess and the pumice layer from the Laacher See eruption. The Dachsbusch scoria cone is located in the central part of the Neuwied basin. There are volcanic deposits (with fragments of the Hüttenberg tephra) exposed and an about 1m thick loess solifluction layer is overlain by pumice of the Gleys tephra. The Wannenköpfe scoria complex is located in the East Eifel Volcanic Field. A thick succession of aeolian sediments seems to have been preserved especially for the early penultimate glaciation (Frechen, 1995). The loess/palaeosol sequence is intercalated by tephra and weak soil horizons. The Kärlich section which is regarded as one of the key sections for the Middle Pleistocene stratigraphy of northwestern Europe (Boenigk and Frechen, 2001) provides an excellent archive of climate and environmental change. Pleistocene fluvial deposits as well as loess and loess derivatives exposed, intercalated by tephra horizons are exposed. At the Ariendorf section gravels from the Rhine Middle Terrasse are covered by loess deposits intercalated by tephra layers and palaeosols.

The West Eifel volcanic field contains dry maar lakes, maar lakes, scoria cones and small stratovolcanoes. Volcanism in the West Eifel Area started ca. 700 ka ago producing 250 eruptive centers with more than 50 maars, of which eight are filled with water (Büchel, 1984, Negendank and Zolitschka, 1993). In this thesis the sediments of the Jungfernweiher, a dry maar lake were investigated by luminescence dating. With a diameter of 1500 m it is the largest maar of the Eifel area (Schaber and Sirocko, 2005). Sediment cores have been drilled by the ELSA project (Eifel Laminated Sediment Archive) in Eifel dry maar lakes to reconstruct the palaeoclimatic and palaeoenvironmental conditions as well as the history of the volcanism in the Eifel/Central Europe during the last glacial cycles. Another

loess/palaeosol sequence at the gravel quarry Gaul in Weilbach belonging to the southern foreland of the Taunus Mountains was investigated in this thesis. The record consists mainly of Pleistocene terraces of the river Main covered by thick loess/palaeosol sequences.

#### **1.4. Outline of the thesis**

This thesis is composed of eight chapters. Chapters 2, 3, 4, 5, 6 and 7 have been written as articles to peer-reviewed journals. Two of them, chapters 2 and 4 are published in *Quaternary Geochronology* and *Quaternary International*, respectively. Chapter 6 and 7 are published in *Quaternary Science Journal (Eiszeitalter und Gegenwart)*. Chapter 3 and 8 are submitted to *Quaternary Geochronology* and *Quaternary International*, respectively. Chapter 8 provides a conclusion of all the obtained results.

##### CHAPTER 2: LUMINESCENCE CHRONOLOGY OF THE UPPER PART OF THE STARI SLANKAMEN LOESS SEQUENCE (VOJVODINA, SERBIA) (SCHMIDT ET AL. 2010)

This chapter represents a study about the upper part of the Middle and Late Pleistocene loess/palaeosol sequence exposed at the Stari Slankamen section in the Vojvodina region/Serbia. Ten samples were dated by luminescence methods using a modified single aliquot regenerative dose (SAR) protocol for polymineral fine-grains and for quartz extracts from the upper part of the Stari Slankamen loess sequence. The different luminescence age estimates are compared and the results are tried to fit in the Vojvodinan loess chronostratigraphy.

##### CHAPTER 3: ELEVATED TEMPERATURE IRSL DATING OF THE LOWER PART OF THE STARI SLANKAMEN LOESS SEQUENCE (VOJVODINA, SERBIA) – INVESTIGATING THE SATURATION BEHAVIOUR OF THE pIRIR<sub>290</sub> SIGNAL (SCHMIDT ET AL. SUBMITTED).

This work is the continuation of the study presented in chapter 2. In this chapter the lower part of the Stari Slankamen section is investigated with the aim of studying the behaviour of both the IR<sub>50</sub> and the pIRIR<sub>290</sub> signals in material close to or in saturation with a focus on the relationship between field and laboratory saturation. Furthermore, the bleachability of the signal for young samples is tested. The results are discussed and interpreted in the context of establishing a more reliable chronostratigraphical framework for the lower part of this section.

CHAPTER 4: LUMINESCENCE CHRONOLOGY OF THE LOESS RECORD FROM THE TÖNCHESBERG SECTION: A COMPARISON OF USING QUARTZ AND FELDSPAR AS DOSIMETER TO EXTEND THE AGE RANGE BEYOND THE EEMIAN (SCHMIDT ET AL. 2011).

In this chapter the loess/palaeosol sequences of the Tönchesberg section is investigated using optically stimulated luminescence (OSL), a modified thermally transferred optically stimulated luminescence (TT-OSL) protocol and a new approach for dating feldspar: the pulsed post-IR IRSL. The results are compared concerning the applicability of luminescence dating on loess sediments which were accumulated beyond the Eemian.

CHAPTER 5: ELEVATED TEMPERATURE IRSL DATING OF LOESS SECTIONS IN THE EIFEL REGION OF GERMANY (SCHMIDT ET AL. SUBMITTED).

In this chapter a geochronological framework for the loess sections Kärlich and Ariendorf is presented. The aim is to test the reliability of the post-IR IRSL approach on polymineral fine grains from the Eifel area based on the well age controlled sections Wannenköpfe and Dachbusch. Samples from these sites give pIRIR<sub>290</sub> ages consistent with age control, supporting the apparent reliability of the protocol and in particular the absence of significant fading. Furthermore the saturation behaviour of Rheinisch loess is compared with the results from the Danube loess (chapter 3).

CHAPTER 6: IRSL SIGNALS FROM MAAR LAKE SEDIMENTS STIMULATED AT VARIOUS TEMPERATURES (SCHMIDT ET AL. 2011).

In this chapter the applicability of luminescence dating using maar lake sediments from the dry maar lake Jungfernweiher (West Eifel area/Germany) is investigated to determine the accumulation rate and temporal succession of dust storms. The results show that the Jungfernweiher was effectively filled up with sediments ~250 ka ago, and there either been very little deposition since then, or younger sediments have been stripped by erosion.

CHAPTER 7: LUMINESCENCE DATING OF THE LOESS/PALAEOSOL SEQUENCE AT THE GRAVEL QUARRY GAUL/WEILBACH, SOUTHERN HESSE (GERMANY) (SCHMIDT ET AL. 2011).

This chapter presents the first optically stimulated luminescence (OSL) dating results from the loess/palaeosol sequence at the gravel quarry Gaul located east of Weilbach based on the post-IR IRSL measurement sequence to set up a more reliable chronological framework for this loess/palaeosol sequence.

## References

- Adamiec, M., Aitken, M.J., 1998. Dose-rate conversion factors: update. *Ancient TL* 16, 37-50.
- Aitken, M.J. 1985. *Thermoluminescence Dating*, London.
- Aitken, 1998. *An Introduction to Optical Dating*, Oxford.
- Banerjee, D., Murray, A.S., Bøtter-Jensen, L., Lang, A., 2001. Equivalent dose estimation using a single aliquot of polymineral fine grains. *Radiation Measurements* 33, 73–94.
- Boenigk, W., Frechen, M., 2001. Zur Geologie der Kärlich Hauptwand. *Mainzer geowiss. Mitteilungen*, 30, 123-194.
- Buylaert, J.P., Murray, A.S., Thomson, K.J., Jain, M., 2009. Testing the potential of an elevated temperature IRSL signal from K-feldspar. *Radiation Measurements*, 44, 560-565.
- Büchel, G., 1984. Die Maare im Vulkanfeld der Westeifel, ihr geophysikalischer Nachweis, ihr Alter und ihre Beziehung zur Tektonik der Erdkruste. PhD-Thesis, Universität Mainz.
- Denby, P.M., Bøtter-Jensen, L.; Murray, A.S.; Thomsen, K.J.; Moska, P. 2006. Application of pulsed OSL to the separation of the luminescence components from a mixed quartz/feldspar sample. *Radiation Measurements*, 41, 774-779.
- Duller, G.A.T., 2003. Distinguishing quartz and feldspar in single grain luminescence measurements. *Radiation Measurement*, 37, 161-165.
- Frechen, M., Oches, E. A., Kohfeld, K. E., 2003. Loess in Europe - Mass accumulation rates during OIS 2. *Quaternary Science Reviews*, 22, 1835-1857.

- Frechen, M., 1995. Eruptionsgeschichte und Deckschichtenfolge der Wannenköpfe Vulkangruppe in der Osteifel. *Eiszeitalter und Gegenwart*, 45, 109–129.
- Frechen, M., 1991. Systematic thermoluminescence dating of two loess profiles from the middle Rhine area (F.R.G.). *Quaternary Science Reviews*, 11, 93–101.
- Godfrey-Smith, D.I., Huntley, D.J., Chen, W.-H., 1988. Optical dating of quartz and feldspar extracts. *Quaternary Science Reviews*, 7, 373–380.
- Huntley, D.J., Lamothe, M., 2001. Ubiquity of anomalous fading in K-feldspars and the measurement and correction for it in optical dating. *Canadian Journal of Earth Sciences* 38, 1093-1106.
- Krbetschek M. R.; Götze J.; Dietrich A.; Trautmann T. 1997. Spectral information from Minerals. In: Wintle, A.G. (Ed.) *A Review on Luminescence and Electron Spin Resonance Dating and Allied Research.- Radiation Measurements*, 27, 695-748.
- Lamothe M., Auclair M., Hamzaoui C., Huot S. 2003. Towards a prediction of long-term anomalous fading of feldspar IRSL. *Radiation Measurements*, 37, 493-498.
- Marković, S.B., Hambach, U., Catto, N., Jovanović, M., Buggle, B., Machalett, B., Zöller, L., Glaser, B. Frechen, M. 2009. The middle and late Pleistocene loess/palaeosol sequences at Batajanica, Vojvodina, Serbia. *Quaternary International* 198, 255-266.
- Marković, S.B., Bokhorst, M.P., Vandenberghe, J., McCoy, W.D., Oches, E.A., Hambach, U., Gaudenyi, T., Jovanović, M., Stevens, T., Zöller, L., Machalett, B., 2008. Late Pleistocene loess–palaeosol sequences in the Vojvodina region, North Serbia. *Journal of Quaternary Science* 23, 73-84.
- Marković, S.B., Oches, E.A., McCoy, W.D., Frechen, M., Gaudenyi, T., 2007. Malacological and sedimentological evidence for “warm” glacial climate from the Irig loess sequence, Vojvodina, Serbia. *Geochemistry Geophysics Geosystems* 8, Q09008. doi:10.1029/2006GC001565.

- Marković, S.B., Oches, E., Sümegi, P., Jovanović, M., Gaudenyi, T., 2006. An introduction to the Middle and Upper Pleistocene loess–palaeosol sequence at Ruma brickyard, Vojvodina, Serbia. *Quaternary International* 149, 80-86.
- Marković, S.B., Oches, E.A., Gaudenyi, T., Jovanović, M., Hambach, U., Zöller, L., Sümegi, P., 2004. Paleoclimate record in the Late Pleistocene loess–palesol sequence at Miseluk (Vojvodina, Serbia). *Quaternaire* 15, 361–368.
- Murray, A.S., Wintle, A.G., 2003. The single aliquot regenerative dose protocol: potential for improvements in reliability. *Radiation Measurements* 37, 377-381.
- Murray, A.S., Olley, J.M., 2002. Precision and accuracy in the optically stimulated luminescence dating of sedimentary quartz: a status review. *Geochronometria*, 21, 1-16.
- Murray, A.S., Wintle, A.G., 2000. Luminescence dating of quartz using an improved single-aliquot regenerative-dose protocol. *Radiation Measurements* 32, 57-73.
- Negendank, J.F.W., Zolitschka, B., 1993. Maars and maar lakes of the Westeifel volcanic field. In: J.F.W. Negendank and B. Zolitschka (Editors), *Paleolimnology of European Maarlakes*. Lecture Notes in Earth Sciences. Springer-Verlag, 61-80.
- Pécsi, M., 1968. Loess. In: Fairbridge, R.W. (Ed). *Encyclopedia of Geomorphology*, 674–678.
- Porat, N, Duller, G.A.T., Roberts, H.M., Wintle, A.G., 2009. A simplified SAR protocol for TT-OSL. *Radiation Measurements*, 44, 538-542.
- Prescott, J.R., Hutton, J.T., 1994. Cosmic ray contribution to dose rates for luminescence and ESR dating: large depths and long-term time variations. *Radiation Measurements*, 23, 497–500.
- Prescott, J.R., Stephan, L.G. 1982. The contribution of cosmic radiation to the environmental dose for thermoluminescence dating. *PACT*, 6, 17–25.

- Roberts, H.M., 2008. The development and application of luminescence dating to loess deposits: a perspective on the past, present and future. *Boreas*, 37, 483-507.
- Roberts, H.M., Duller, G.A.T., 2004. Standardised growth curves for optical dating of sediment using multiple-grain aliquots. *Radiation Measurements* 38, 241-252.
- Schaber, K., Sirocko, F. 2005. Lithologie und Stratigraphie der spätpleistozänen Trockenmaare der Eifel, *Mainzer geowiss.Mitt.*, 33, 295-340.
- Schmidt, E.D., Frechen, M., Murray, A.S., Tsukamoto, S., Bittmann, F., 2011. Luminescence chronology of the loess record from the Tönchesberg section – a comparison of using quartz and feldspar as dosimeter to extend the age range beyond the Eemian. *Quaternary International*, 234, 10-22.
- Schmidt, E.D., Machalett, B., Marković, S. B., Tsukamoto, S., Frechen, M., 2010. Luminescence chronology of the upper part of the Stari Slankamen loess sequence (Vojvodina, Serbia). *Quaternary Geochronology*, 5, 137-142.
- Schmidt, E.D., Murray, A.S., Jain, M., Tsukamoto, S., Frechen, M., 2009. Testing recuperated OSL dating on quartz and polymineral fine-grains. Poster, UK Meeting on Luminescence And Electron Spin Resonance Dating, Royal Holloway, 26.-28.08.2009.
- Thiel, C., Buylaert, J.P., Murray, A.S., Terhorst, B., Hofer, I., Tsukamoto, S., Frechen, M. 2011. Luminescence dating of the Stratzing loess profile (Austria) – Testing the potential of an elevated temperature post-IR IRSL protocol. *Quaternary International*, 234, 23-31.
- Thomsen, K.J., Murray, A.S., Jain, M., Bøtter-Jensen, L., 2008. Laboratory fading rates of various luminescence signals from feldspar-rich sediment extracts. *Radiation Measurements*, 43, 1474-1486.



- Tsukamoto, S., Denby, P. M., Murray, A. S., and Bøtter-Jensen, L. 2006. Time-resolved pulsed luminescence from feldspars: new insight into fading. *Radiation Measurements*, 41, 790-795.
- Tsukamoto, S., Duller, G.A.T. and Wintle, A.G., 2008. Characteristics of thermally transferred optically stimulated luminescence (TT-OSL) in quartz and its potential for dating sediments. *Radiation Measurements*, 43, 1204-1218.
- Visocekas, R., 1985. Tunnelling radiative recombination in labradorite: Its association with anomalous fading of thermoluminescence. *Nuclear Tracks and Radiation Measurements*, 10, 521-529.
- Wang, X.L., Wintle, A.G., Lu, Y.C., 2006. Thermally transferred luminescence in fine-grained quartz from Chinese loess: Basic observations. *Radiation Measurement*, 41, 649-658.
- Wang, X.L., Wintle, A.G., Lu, Y.C., 2007. Testing a single-aliquot protocol for recuperated OSL dating. *Radiation Measurements*, 42, 380-391.
- Wintle, A.G., 1973. Anomalous fading of thermoluminescence in mineral samples. *Nature*, 245, 143-144.
- Wintle, A.G, Murray, A.S. 2006. A review of quartz optically stimulated luminescence characteristics and their relevance in single-aliquot regeneration dating protocols. *Radiation Measurements*, 41, 369-391.
- Zimmerman, D.W., 1971. Thermoluminescence dating using fine grains from pottery. *Archaeometry* 13, 29–52.

# Chapter 2

Quaternary Geochronology, 2010 (5): 137-142.

## **Luminescence chronology of the upper part of the Stari Slankamen loess sequence (Vojvodina, Serbia)**

**E.D. Schmidt<sup>1\*</sup>, B. Machalett<sup>1,2</sup>, S.B. Marković<sup>3</sup>, S. Tsukamoto<sup>1</sup>, M. Frechen<sup>1</sup>**

<sup>1</sup>*Leibniz Institute for Applied Geophysics (LIAG), Geochronology and Isotope Hydrology, Stilleweg 2, D-30655 Hannover, Germany*

<sup>2</sup>*Chair of Geomorphology, University of Bayreuth, D-95440 Bayreuth, Germany*

<sup>3</sup>*Chair of Physical Geography, University of Novi Sad, 21000 Novi Sad, Serbia*

### **Abstract**

A thick Middle and Late Pleistocene loess-palaeosol sequence is exposed at the Stari Slankamen section in the Vojvodina region situated in the south-eastern part of the Pannonian basin, Serbia. The profile exposes an about 45 m thick series of loess intercalated by at least eight pedocomplexes. Ten samples were dated by luminescence methods using a modified single aliquot regenerative dose (SAR) protocol for polymineral fine grains and for quartz extracts from the upper part of the Stari Slankamen loess sequence. The infrared stimulated luminescence (IRSL) and post-IR optically stimulated luminescence (OSL) signals from all polymineral samples showed anomalous fading, suggesting that the post-IR OSL signal is still dominated by feldspar OSL. The ages ranging from 4.6 to 193 ka were obtained after fading correction. These ages indicate that the loess unit V-L1L1, the weakly developed soil complex V-L1S1 and the loess unit V-L1L2 were deposited during marine isotope stage (MIS) 2, 3, and 4, respectively, and also indicate that the loess unit V-L2 is of the penultimate glacial age.

*Key words: luminescence dating, IRSL, OSL, fading, fine grain, loess, Vojvodina, chronostratigraphy*

## **2.1. Introduction**

Loess-palaeosol sequences record palaeoclimatic conditions and represent a potential archive to understand glacial-interglacial variability. The sediment successions at Stari Slakamen in the Vojvodina, Serbia are among the oldest and most complete loess sequences in Europe and provide important information of local and regional environmental processes and conditions during the Middle and Late Pleistocene (Marković et al., 2003, 2006, 2009). A detailed description of the Stari Slankamen loess section and a stratigraphic correlation between other loess profiles in Europe and in Asia was made by Bronger (1976, 2003). The current chronostratigraphic model of the Serbian loess was introduced by Marković et al. (2004a,b, 2005, 2006, 2007, 2008, 2009) using lithologic and pedogenic criteria, magnetic susceptibility (MS) variations, amino-acid racemization (AAR) and luminescence dating. However, reliable numeric age estimates are still lacking for most of the loess successions. This makes it still difficult to interpret the terrestrial climate archives as well as to correlate the loess-palaeosol sequences with other European loess records. This study presents the first optically stimulated luminescence (OSL) dating results from the Stari Slankamen loess section and aims to establish a reliable chronology for the upper part of the profile. The results will be discussed by correlating to other sections of the Vojvodina.

## **2.2. Geological setting**

The Vojvodina region (Northern Serbia) is situated in the south-eastern part of the Pannonian basin (Fig. 1) and is covered by loess and loess-like sediments reaching a thickness up to 55 m.

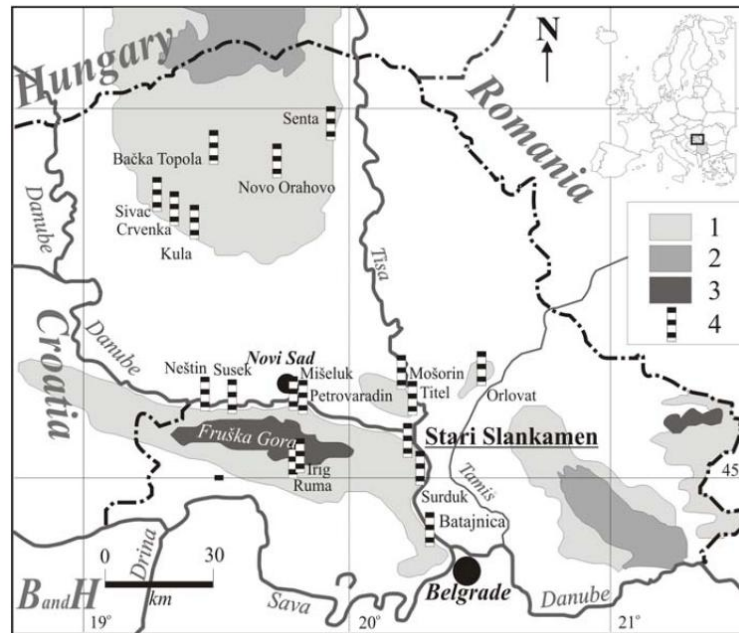


**Figure 2.1: Map of loess distribution in the Vojvodina and adjacent regions showing locations of the investigated section and other main loess sites (modified from Marković et al., 2004). 1. Loess plateau; 2. Sandy area; 3. Mountain; 4. Investigated exposures.**

The loess sequences in the Vojvodina are regarded as a key for understanding and reconstructing the palaeoclimatic and -environmental conditions in South-Eastern Europe (Marković et al., 2008). After the current chronostratigraphic model of the Serbian loess (Marković et al., 2004a; 2004b; 2005; 2006; 2007; 2008; 2009) the Vojvodinian loess (L) and (S) palaeosol units are numbered in the order of increasing age. To refer to the standard Pleistocene loess stratigraphy in the Vojvodina region the prefix “V” is used. The loess V-L2 is correlated with marine isotope stage (MIS) 6. The first strongly developed soil, V-S1 is correlated with the Last Interglacial in MIS 5. Above this palaeosol the loess unit V-L1 was accumulated. The lower part of this loess unit is represented as V-L1L2. The weakly developed soil complex (V-L1S1) is correlated with the Middle Pleniglacial. Above this zone of incipient soil formation, the youngest loess layer V-L1L1 accumulated presumably during the Late Pleniglacial period.

The Stari Slankamen section is located in the Vojvodina region in the north-eastern part of the Srem Loess Plateau. The altitude is 140 m above sea level and the coordinates of the profile under study are 45°07'33,86" N and 20°15'57,15" E. The profile exposes an about 45 m thick series of loess intercalated by at least eight pedocomplexes. In this study, we focus on the upper part of the section which comprises about 14 m. Figure 2 shows the stratigraphy of the loess-palaeosol sequence and the positions of the samples for luminescence dating.

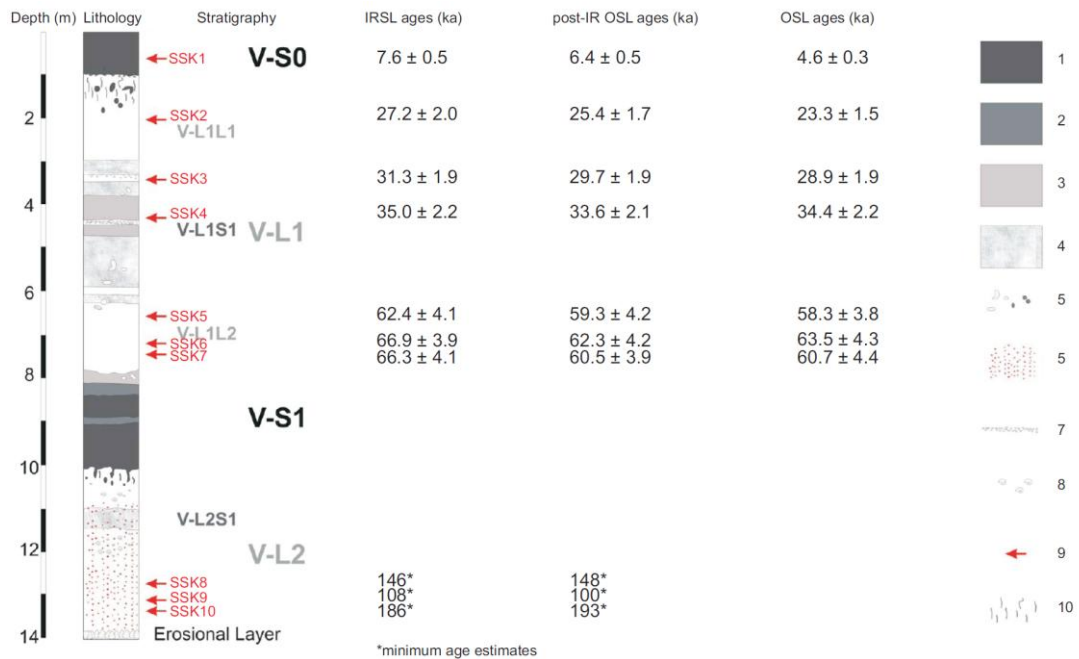


**Figure 2.2: Lithology and luminescence ages of the Stari Slankamen loess site. 1. Ah horizons; 2. Lighter Ah horizons; 3. A horizon; 4. weak humic horizons; 5. krotovinas; 6. hydromorphic features; 7. carbonate concretions; 8. many snail shells; 9. position of the luminescence samples; 10. former root chanel with humic infiltrations**

The loess in this part is intercalated by a weakly developed humic-rich pedocomplex and two brown palaeosols. The loess unit V-L2 is affected by hydromorphic features including a fluvial erosion layer with small gravels at the basis. Above this loess layer, the reddish-brown pedocomplex V-S1 is developed. The loess unit V-L1 consists of V-L1L2 and V-L1L1 separated by the weakly developed humic-rich chernozem-like pedocomplex. The Holocene soil (V-S0) is slightly melanised chernozem. During the fieldwork, 4 samples between the V-S0 and the first weakly developed pedocomplex V-L1S1 (SSK 1, 2, 3,4), 3 samples above the first strongly developed palaeosol V-S1 (SSK 5, 6,7) and 3 samples from loess unit V-L2 (SSK 8, 9, 10) were collected.

### 2.3. Experimental details

The samples were extracted under subdued red light and were pretreated with 10% hydrochloric acid to remove the carbonates, with sodium oxalate to dissolve the aggregates and with 30% hydrogen peroxide to remove organic material. The samples were then refined to a fine silt (4-11  $\mu\text{m}$ ) fraction. The fine grain fraction was subsequently divided into two parts. A polymineral fraction which was used for polymineral infrared stimulated

luminescence (IRSL) and post-IR OSL measurement, and the other for the extraction of quartz grains. The fine-grained quartz was obtained either by treating the polymineral fraction with 20 % hydrofluoric acid (HF) for 20 minutes (Mauz and Lang, 2004) or with fluorosilicic acid ( $\text{H}_2\text{SiF}_6$ ) for 6 days. The purity of the etched samples was checked by IR depletion ratio (Duller, 2003). The discs for the measurements were prepared by settling the polymineral and the quartz fine grains (4-11  $\mu\text{m}$ ) in acetone. All measurements were performed using an automated Risø TL/OSL-DA15 equipped with a  $^{90}\text{Sr}/^{90}\text{Y}$  beta source (Bøtter-Jensen et al., 2000). All measurements were carried out for 100s at 125°C and the luminescence signals were detected through 7.5 mm of Hoya U-340 filter.

The  $D_e$  values were calculated using a modified single aliquot regenerative dose (SAR) protocol (Banerjee et al., 2001; Roberts and Wintle, 2001) for polymineral fine-grains, the so called double SAR protocol. This modified SAR protocol involves stimulations with IR-diodes to bleach the luminescence from feldspar and then stimulate with blue LEDs (post-IR OSL) to measure the OSL signal which is more dominated by OSL from quartz. Two sets of  $D_e$  values can be obtained; the IRSL signal from feldspar and the post-IR OSL signal which is supposed to be dominated by the signal from quartz (Roberts and Duller, 2004). The double SAR protocol was also applied for the fine-grained quartz.

The  $D_e$  values for polymineral IRSL and post-IR OSL were calculated using the initial 2 s of the stimulation curves subtracted by the last 10 s as a background. For fine-grained quartz, the initial 0.8 s of the signal was used after subtracted by the last 4 s of the stimulation curves. All dose response curves were fitted using a saturating exponential function. Twelve aliquots per sample were used for the  $D_e$  measurements for polymineral fine grains, and 8-10 aliquots were measured for quartz fine grains. The arithmetic mean was used to calculate  $D_e$  values, the uncertainty of the  $D_e$  values was given by a standard error ( $\pm 1\text{s.e}$ ). The degree of inter-aliquot scatter for the  $D_e$  is very low (5.7% for polymineral IRSL, 7.1% for polymineral post-IR OSL and 7.7% for quartz OSL).

Fading tests were carried out using the same aliquots of polymineral samples, which were previously used for the  $D_e$  measurement. Repeated  $L_x/T_x$  measurements, with a given dose close to the  $D_e$  value followed by a 260°C preheat for 60s, were made with various delays after the irradiation (Auclair et al., 2003). The fading rates (g-values) were calculated according to Huntley and Lamothe (2001) using the same integrals as for the  $D_e$  calculation, and the g-values were used to correct the ages. The results are summarized in Table 2. All polymineral IRSL and all polymineral post-IR OSL signals show anomalous fading. Mean fading rates of 3.24 % for polymineral IRSL and 1.36 % for polymineral post-IR OSL were

observed, indicating that the post-IR OSL signal shows on average ~60% less fading than the IRSL signal.

Radionuclide concentrations for all samples were obtained by high resolution gamma spectrometry on sediment collected from the immediate surrounding of the samples. According to field observations, a water content of  $12.5 \pm 2.5$  % was assumed. According to Rees-Jones (1995), mean a-values of  $0.08 \pm 0.02$  and  $0.04 \pm 0.02$  for polymineral IRSL and quartz OSL were used, respectively. For polymineral post-IR OSL, an a-value of  $0.06 \pm 0.02$  was used, as the signal is thought to be a mixture of quartz and feldspar but the fraction of the feldspar contribution cannot be clearly defined. The uranium, thorium, potassium contents and the dose rate of the samples are shown in Table 1.

The concentrations of uranium, thorium and potassium were converted into effective dose rate using the dose-rate conversion factors of Adamiec and Aitken (1998) and water-content attenuation factors (Aitken, 1985). Estimation of the cosmic-ray dose rate is based on Prescott and Stephan (1982) and Prescott and Hutton (1994) using depth, altitude, density, latitude and longitude for each sample.

Sample	Uranium (ppm)	Thorium (ppm)	Potassium (%)	IRSL dose rate (Gy/ka)	post IR-OSL dose rate (Gy/ka)	OSL dose rate (Gy/ka)
SSK 1	$2.96 \pm 0.06$	$9.66 \pm 0.20$	$1.32 \pm 0.03$	$3.52 \pm 0.18$	$3.30 \pm 0.18$	$3.09 \pm 0.18$
SSK 2	$3.08 \pm 0.07$	$10.25 \pm 0.21$	$1.35 \pm 0.03$	$3.67 \pm 0.18$	$3.45 \pm 0.18$	$3.22 \pm 0.18$
SSK 3	$3.42 \pm 0.07$	$11.27 \pm 0.27$	$1.59 \pm 0.03$	$4.12 \pm 0.20$	$3.87 \pm 0.20$	$3.62 \pm 0.20$
SSK 4	$3.42 \pm 0.07$	$12.05 \pm 0.25$	$1.57 \pm 0.03$	$4.19 \pm 0.20$	$3.93 \pm 0.20$	$3.67 \pm 0.20$
SSK 5	$3.30 \pm 0.07$	$11.38 \pm 0.24$	$1.48 \pm 0.03$	$3.99 \pm 0.20$	$3.74 \pm 0.20$	$3.50 \pm 0.20$
SSK 6	$3.37 \pm 0.08$	$11.56 \pm 0.24$	$1.58 \pm 0.03$	$4.12 \pm 0.20$	$3.87 \pm 0.20$	$3.62 \pm 0.20$
SSK 7	$3.55 \pm 0.07$	$12.58 \pm 0.26$	$1.70 \pm 0.04$	$4.41 \pm 0.21$	$4.14 \pm 0.21$	$3.87 \pm 0.21$
SSK 8	$3.16 \pm 0.07$	$12.48 \pm 0.26$	$1.63 \pm 0.03$	$4.18 \pm 0.20$	$3.93 \pm 0.20$	
SSK 9	$3.08 \pm 0.07$	$11.01 \pm 0.23$	$1.45 \pm 0.03$	$3.84 \pm 0.19$	$3.60 \pm 0.19$	
SSK 10	$2.55 \pm 0.05$	$9.19 \pm 0.19$	$1.08 \pm 0.02$	$3.11 \pm 0.15$	$2.92 \pm 0.15$	

**Table 2.1: Dose rate data from potassium, uranium and thorium content, as measured by gamma spectrometry. Moisture was estimated to  $12.5 \pm 2.5$ % for all samples.**

## 2.4. Performance tests for luminescence dating

To find an appropriate heating condition for the double SAR protocol for polymineral samples, dose recovery tests at different preheat temperatures (Murray and Wintle, 2003)

were carried out for SSK 3 and SSK 5. The aliquots were bleached twice with 1000s IR stimulation at 125°C and 1000s blue stimulation at 125°C separated by a 5000s pause before giving a dose of 92 Gy (SSK 3) or 173 Gy (SSK 5) approximately equal to the natural dose. This dose was then measured in the same manner as if measuring the equivalent dose to provide confirmation that the protocol is able to recover a known dose successfully. The identical heat treatment was given both before OSL and test dose OSL measurements (Blair et al., 2005). Figure 3 (a, c) shows the results of the dose recovery test for the samples SSK 3 and SSK 5. The recovered dose/given dose is close to unity at preheat of 180° - 260°C for 10s. At temperatures higher than 260°C, the recovered doses overestimated the given dose for IRSL signals and underestimated for the post-IR OSL signals. A preheat plateau test using natural aliquots of the same samples were also conducted (Fig. 3b and d). The  $D_e$  values increased with increasing preheat temperature between 180 and 260°C. Between 260°C and 300°C, the  $D_e$  values are relatively stable but the same tendency (slight increase in IRSL  $D_e$  and decrease in post-IR OSL  $D_e$ ) can be seen as in the dose recovery test. A preheat at 260°C for 10s was selected for all the  $D_e$  measurements for polymineral samples, as it recovers the given dose and the temperature is within the plateau region.

To check the ability of the SAR protocol for quartz, a dose recovery test at different preheat temperatures was also carried out for sample SSK 2. The recovered dose/given dose is close to unity at a preheat of 260°C for 10s ( $1.00 \pm 0.01$ ). A preheat temperature of 260°C for



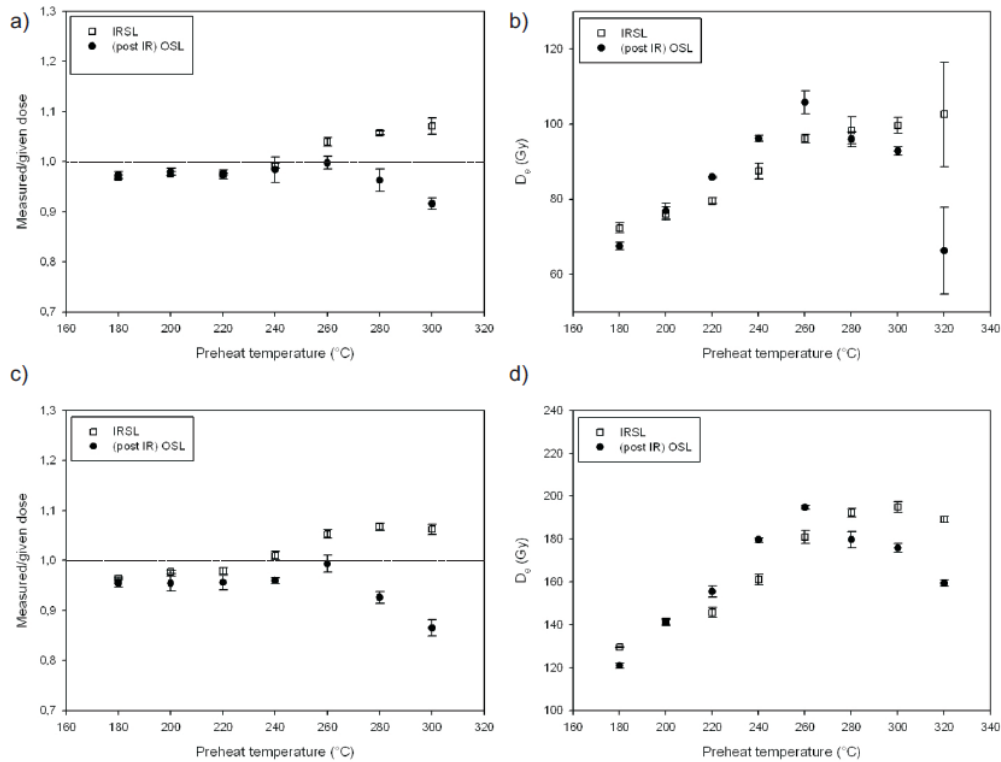


**Figure 2.3: Results of dose recovery and preheat plateau test for sample SSK 3 (a,b) and SSK 5 (c,d).**

10s and a cut heat at 200°C were adopted for all quartz measurements except for sample SSK 1 and SSK 4 which were measured with a preheat temperature of 240°C.

## 2.5. Chronology of the Stari Slankamen loess sequence

The equivalent dose ( $D_e$ ), recycling ratio, dose recovery ratio, fading rate (g-value) and corrected age (obtained by correction for the observed fading) are summarized in Table 2. All polymineral IRSL and post-IR OSL signals showed laboratory fading. The shape of the decay curve of post-IR OSL signal is also clearly different from quartz OSL (Fig. 4). Therefore we conclude that the double SAR protocol was not capable of isolating a quartz signal and also suffer from an underestimation, when no fading correction is applied. The fading corrected polymineral IR and post-IR OSL and the quartz OSL ages agreed within the error range for

Sample	Depth	Measurement	D <sub>e</sub> (Gy)	Recycling	Measured/given dose	g-value (%)	uncorrected Age (ka)	corrected Age (ka)
SSK 1	0.51	P-IR	22.3 ± 0.8	1.01 ± 0.01		2.2 ± 0.09	6.4 ± 0.4	7.6 ± 0.5
		P-blue	18.0 ± 0.6	1.06 ± 0.01		1.04 ± 0.56	5.5 ± 0.3	6.4 ± 0.5
		Q-blue	14.4 ± 0.5	1.01 ± 0.01	0.89 ± 0.02		4.6 ± 0.3	
SSK 2	2.0	P-IR	76.5 ± 2.3	0.99 ± 0.01		3.28 ± 0.11	20.8 ± 1.1	27.2 ± 2.0
		P-blue	77.8 ± 2.4	1.03 ± 0.01		1.4 ± 0.32	22.6 ± 1.4	25.4 ± 1.7
		Q-blue	74.5 ± 2.3	1.03 ± 0.01	1.00 ± 0.01		23.3 ± 1.5	
SSK 3	3.32	P-IR	98.8 ± 3.0	0.99 ± 0.00	0.98 ± 0.01	3.23 ± 0.17	24.0 ± 1.3	31.3 ± 1.9
		P-blue	103 ± 3	1.03 ± 0.01	1.03 ± 0.03	1.47 ± 0.22	26.6 ± 1.6	29.7 ± 1.9
		Q-blue	105 ± 4	1.04 ± 0.01			28.9 ± 1.9	
SSK 4	4.24	P-IR	114 ± 4	0.99 ± 0.01		3.18 ± 0.19	27.2 ± 1.5	35.0 ± 2.2
		P-blue	117 ± 4	1.02 ± 0.01		1.4 ± 0.16	29.8 ± 1.8	33.6 ± 2.1
		Q-blue	126 ± 4	0.98 ± 0.01	0.92 ± 0.02		34.4 ± 2.2	
SSK 5	6.54	P-IR	189 ± 6	0.97 ± 0.01	1.05 ± 0.02	3.41 ± 0.34	47.4 ± 2.6	62.4 ± 4.1
		P-blue	191 ± 8	1.02 ± 0.01	0.99 ± 0.02	1.81 ± 0.3	51.0 ± 3.4	59.3 ± 4.2
		Q-blue	204 ± 7	0.99 ± 0.01			58.3 ± 3.8	
SSK 6	7.18	P-IR	208 ± 6	0.97 ± 0.00		3.38 ± 0.11	50.5 ± 2.7	66.9 ± 3.9
		P-blue	226 ± 9	1.01 ± 0.00		0.93 ± 0.29	58.4 ± 3.8	62.3 ± 4.2
		Q-blue	230 ± 9	0.98 ± 0.01			63.5 ± 4.3	
SSK 7	7.48	P-IR	213 ± 8	0.97 ± 0.01		3.77 ± 0.07	48.3 ± 2.7	66.3 ± 4.1
		P-blue	223 ± 8	1.01 ± 0.00		1.4 ± 0.19	53.9 ± 3.4	60.5 ± 3.9
		Q-blue	235 ± 11	0.98 ± 0.01			60.7 ± 4.4	
SSK 8	12.74	P-IR	459 ± 15	0.96 ± 0.01			110 ± 6	146 ± 9*
		P-blue	517 ± 18	1.00 ± 0.02			131 ± 8	148 ± 9*
SSK 9	13.14	P-IR	306 ± 10	0.95 ± 0.01			79.8 ± 4.4	108 ± 7*
		P-blue	322 ± 15	0.97 ± 0.01			89.4 ± 6.2	100 ± 7*
SSK 10	13.54	P-IR	430 ± 14	0.96 ± 0.01		3.5 ± 0.17	138 ± 8	186 ± 11
		P-blue	502 ± 16	1.03 ± 0.01		1.45 ± 0.12	172 ± 11	193 ± 12

P-IR: polymineral IR-OSL

P-blue: polymineral (post-IR) OSL

Q-blue: quartz blue OSL

\* g-value of SSK 10 was used

**Table 2.2: Equivalent dose (De), recycling ratio, dose recovery, fading and luminescence ages.**

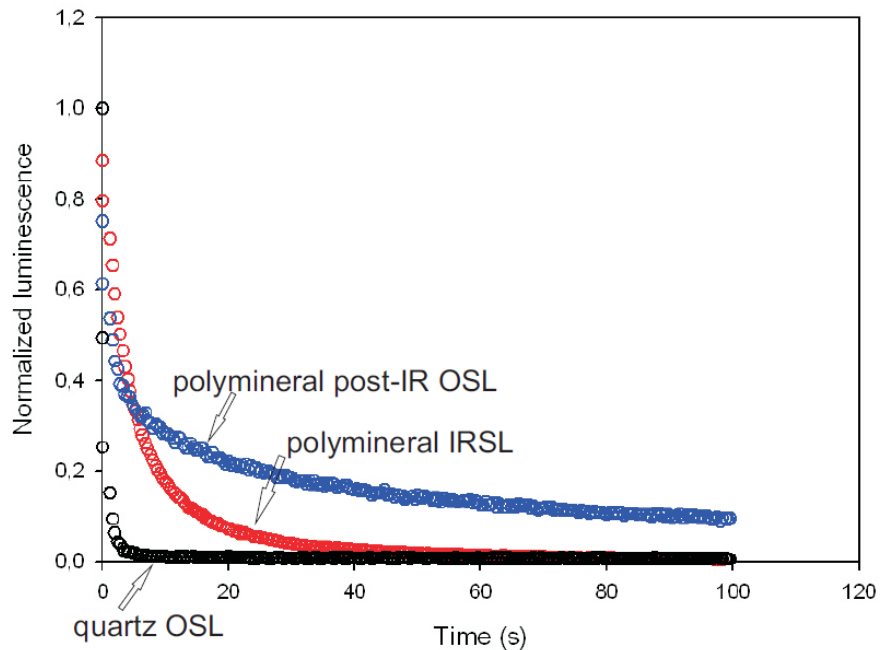


**Figure 2.4: Decay curves of quartz OSL, polymineral IRSL and post-IR OSL for SSK 4.**

most of the samples, which proves that the fading correction was applied successfully for these samples. The quartz OSL and the polymineral post-IR OSL ages are in excellent agreement and are regarded as more reliable age estimates. Only the quartz OSL age for SSK1 seems to be underestimated, which can be related to the slight underestimation of the dose recovery test. On the other hand, the IRSL ages after fading correction tend to overestimate post-IR OSL and quartz OSL ages. This might be due to thermal transfer of charge as there was slight overestimation of dose recovery ratio using the preheat at 260°C (Davids et al., in press) (Fig. 3). However, the fading correction may not be appropriate for the three oldest samples (SSK 8, 9, 10), because the correction method is only valid for the ‘linear part’ of the dose response curve (Huntley and Lamothe, 2001). Therefore the ages should be regarded as minimum ages. The dose response curves for the IRSL and post-IR OSL signals for SSK 8 are shown in Fig. 5.

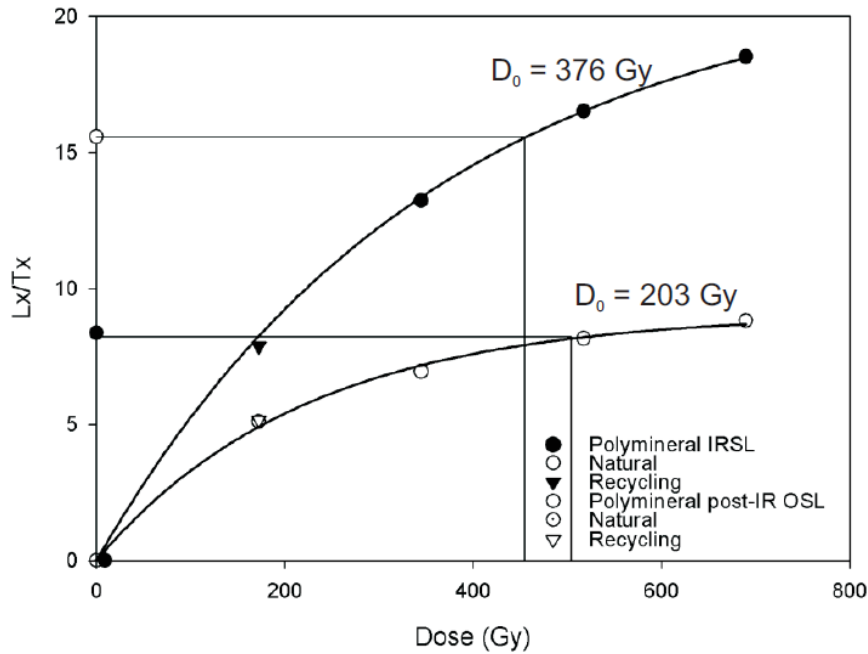


**Figure 2.5: Dose response curves of polymineral IRSL and post-IR OSL for SSK 8. Recycling points are shown as triangles, and zero dose points as reverse triangles.**

It should be noted that the post-IR OSL signal is very close to the saturation level for these old samples. The characteristic saturation dose ( $D_0$ ) of 203 Gy obtained for the post-IR OSL signals suggests that the upper dose limit for this signal is about 400 Gy.

Figure 2 shows the luminescence ages along with the lithology of the Stari Slankamen loess sequence. The corrected polymineral IRSL and post-IR OSL ages as well as the quartz OSL ages are increasing with depths except SSK 6, but this samples was collected only 30 cm above SSK 7 and therefore the ages should be very close. The calculated ages range from  $4.6 \pm 0.3$  ka in the very upper part of the section to 193 ka above the fluvial erosion layer. Since we consider the quartz OSL ages and the polymineral post-IR OSL ages are more reliable than the IRSL ages, the chronology of the Stari Slankamen loess sequence is discussed based on the OSL and the post-IR OSL ages. SSK 1 indicates that V-S0 represents the Holocene soil, taken into account a potential bioturbation at this stratigraphic position. For the uppermost loess layer V-L1L1 yielded ages between 23-30 ka, which suggests that the loess was accumulated during MIS2. The ages about 34 ka were obtained from the weakly developed pedocomplex, indicating that the soil is correlated with MIS3. The lower unit of V-L1 was dated between 58 and 64 ka, corresponding to MIS4. The ages between 100 and 193 ka were obtained for the lowermost part of the loess V-L2.

## 2.6. Discussion and conclusions

Our study presents the first optically stimulated luminescence (OSL) age estimates using a SAR protocol for the Stari Slankamen loess-palaeosol sequence. Our results are in good agreement with the geological situation and support the chronostratigraphic model proposed by Marković et al. (2004a, 2004b, 2005, 2006, 2007, 2008, 2009). The luminescence ages for the last glacial loess unit V-L1 (23-64 ka) obtained in this study are generally similar to previous results of Butrym et al. (1991) and consistent with recent studies for other loess-palaeosol sequences in the Vojvodina region. IRSL ages are provided for the V-L1 from the Irig loess section (19-42 ka; Marković et al., 2007) and Titel loess exposure (15-69 ka; Marković et al., 2008; Bokhorst et al., 2009). Fuchs et al. (2008) provided more detailed IRSL ages from the Surduk loess section, 16-36 ka from V-L1L1, 32-40 ka from V-L1S1, 53-83 ka from V-L1L2. These IRSL ages are generally in agreement with our results for the upper part of the Stari Slankamen section. Singhvi et al. (1989) presented thermoluminescence ages from 63-85 ka for the palaeosol F2 (this palaeosol corresponds to the pedocomplex V-S1 in the current stratigraphic model of Marković et al., 2008) at the Stari Slankamen section. These age estimates are similar to the results of Butrym et al. (1991). Following these results Bronger (2003) correlated palaeosol F2 with MIS 5a. However, Marković et al. (2004a, 2004b, 2006, 2005, 2007, 2008, 2009) correlated the equivalent pedocomplex V-S1 with the complete MIS 5 period. The proposed stratigraphic model is also in agreement with recent results of amino acid racemization (AAR) chronologies for different loess sections in the Vojvodina region (Marković et al., 2004a, 2004b, 2005, 2006, 2006, 2007, 2008, 2009). This stratigraphic interpretation is supported by the recently published IRSL age of  $120.7 \pm 12.7$  ka for the uppermost part of the penultimate loess V-L2 at the Surduk section, located on the right bank of the Danube River 10 km upstream to Stari Slankamen (Fuchs et al., 2008). Our luminescence dating results for the loess V-L2 (samples SSK 8-10), although we regard them as minimum ages, support the chronostratigraphic model proposed by Marković et al. (2004a, 2004b, 2005, 2006, 2007, 2008, 2009) and provides a much older age estimation than the results of Butrym et al. (1991) who indicated an age around 90 ka above the erosion layer for the penultimate loess unit at the Stari Slankamen section. However, for the penultimate loess unit, further studies applying new approaches for example, IRSL measurements at elevated temperatures, which is considered to show less fading (Buylaert et al., in press) are required to verify the age estimation and to get more insights into the deposits of the Middle Pleistocene.

## Acknowledgments

This study was supported by the “Leibniz-Pakt für Innovation und Forschung”. We also thank to Nebojša Milojković and Tin Lukić for their help during the field work. This research was partly supported by Project 146019 of the Serbian Ministry of Science. BM was funded by the *German Federal Environmental Foundation (DBU)* and acknowledges receipt of additional valuable funding from the *von Humboldt-Ritter-Penck* foundation for fieldwork in Serbia from 2006-2007.

## References

- Adamic, M., Aitken, M.J., 1998. Dose-rate conversion factors: update. *Ancient TL* 16, 37-50.
- Aitken, M.J. 1985. *Thermoluminescence Dating*, London.
- Auclair, M., Lamothe, M., Huot, S., 2003. Measurement of anomalous fading for feldspar IRSL using SAR. *Radiation Measurements* 37, 487–492.
- Banerjee, D., Murray, A.S., Bøtter-Jensen, L., Lang, A., 2001. Equivalent dose estimation using a single aliquot of polymineral fine grains. *Radiation Measurements* 33, 73–94.
- Blair, M.W., Yuhikara, E.G., McKeever, S.W.S., 2005. Experiences with single-aliquot OSL procedures using coarse-grain feldspars. *Radiation Measurements* 39, 361–374.
- Bokhorst, M.P., Beets, C.J., Marković, S.B., Gerasimenko, N.P., Matviishina, Z.N., Frechen, M., 2009.pedo-chemical climate proxies in Late Pleistocene Serbian-Ukrainian loess sequences. *Quaternary International* 198, 113-123.
- Bøtter-Jensen, L., Bulur, E., Duller, G.A.T., Murray A.S., 2000. Advances in luminescence instrument systems. *Radiation Measurements* 32, 523-528.

- Bronger, A., 1976. Zur quartären Klima- und Landschaftsentwicklung des Karpatenbeckens auf (Paläo-)pedologischer und bodengeographischer Grundlage. Kiel 1976.
- Bronger, A., 2003. Correlation of loess-palaeosol sequences in East and Central Asia with SE Central Europe: towards a continental Quaternary pedostratigraphy and paleoclimatic history. *Quaternary International* 106-107, 11-31.
- Butrym, J., Maruszczak, H., Zeremski, M., 1991. Thermoluminescence stratigraphy of Danubian loess in Belgrade environs. *Annales, Université Marie-Curie Skłodowska, B* 46, 53–64.
- Buylaert, J.P., Murray, A.S., Thomson, K.J., Jain, M. (in press): Testing the potential of an elevated temperature IRSL signal from K-feldspar, *Rad. Meas.*, doi: 10.1016/j.readmeas.2009.02.007.
- Davids, F., Duller, G.A.T., Roberts, H.M. (in press): Testing the use of feldspars for optical dating of hurricane overwash deposits. *Quaternary Geochronology*.
- Duller, G.A.T., Bøtter-Jensen, L., Murray, A.S., 2003. Combining infrared- and green-laser stimulation sources in single-grain luminescence measurements of feldspar and quartz. *Radiation Measurements* 37, 543-550.
- Fuchs, M., Rousseau, D.-D., Antoine, P., Hatté, C., Gauthier, C., Marković, S., Zoeller, L. 2008. Chronology of the Last Climatic Cycle (Upper Pleistocene) of the Surduk loess sequence, Vojvodina, Serbia. *Boreas*, 37, 66-73.
- Huntley, D.J., Lamothe, M., 2001. Ubiquity of anomalous fading in K-feldspars and the measurement and correction for it in optical dating. *Canadian Journal of Earth Sciences* 38, 1093-1106.
- Marković, S.B., Heller, F., Kukla, G., Gaudenyi, T., Jovanović, M., Miljković, Lj., 2003. Magnetostratigrafija lesnog profila Čot u Starom Slankamenu. *Zbornik radova Instituta za geografiju* 32, 20–28.

- Marković, S.B., Kostić, N.S., Oches, E.A., 2004a. Palaeosols in the Ruma loess section (Vojvodina, Serbia). *Revista Mexicana de Ciencias Geológicas* 21, 79-87.
- Marković, S.B., Oches, E.A., Gaudenyi, T., Jovanović, M., Hambach, U., Zöller, L., Sümeği, P., 2004b. Paleoclimate record in the Late Pleistocene loess–palesol sequence at Miseluk (Vojvodina, Serbia). *Quaternaire* 15, 361–368.
- Marković, S.B., McCoy, W.D., Oches, E.A., Savić, S., Gaudenyi, T., Jovanović, M., Stevens, T., Walther, R., Ivanisević, P., Galić, Z., 2005. Paleoclimate record in the Upper Pleistocene loess–palaeosol sequence at Petrovaradin brickyard (Vojvodina, Serbia). *Geologica Carpathica* 56, 545-552.
- Marković, S.B., Oches, E., Sümeği, P., Jovanović, M., Gaudenyi, T., 2006. An introduction to the Middle and Upper Pleistocene loess–palaeosol sequence at Ruma brickyard, Vojvodina, Serbia. *Quaternary International* 149, 80-86.
- Marković, S.B., Oches, E.A., McCoy, W.D., Frechen, M., Gaudenyi, T., 2007. Malacological and sedimentological evidence for “warm” glacial climate from the Irig loess sequence, Vojvodina, Serbia. *Geochemistry Geophys Geosystems* 8, Q09008. doi:10.1029/2006GC001565.
- Marković, S.B., Bokhorst, M.P., Vandenberghe, J., McCoy, W.D., Oches, E.A., Hambach, U., Gaudenyi, T., Jovanović, M., Stevens, T., Zöller, L., Machalett, B., 2008. Late Pleistocene loess–palaeosol sequences in the Vojvodina region, North Serbia. *Journal of Quaternary Science* 23 (1), 73-84.
- Marković, S.B., Hambach, U., Catto, N., Jovanović, M., Buggle, B., Machalett, B., Zöller, L., Glaser, B., Frechen, M. 2009. The middle and late Pleistocene loess-palaeosol sequences at Batajanica, Vojvodina, Serbia. *Quaternary International* 198, 255-266.
- Mauz, B., Lang, A., 2004. Removal of the feldspar-derived luminescence component from polymineral fine silt samples for optical dating applications: evaluation of chemical treatment protocols and quality control procedures. *Ancient TL* 22, 1-8.



- Murray, A.S., Wintle, A.G., 2003. The single aliquot regenerative dose protocol: potential for improvements in reliability. *Radiation Measurements* 37, 377-381.
- Prasad, S., 2000. HF treatment for the isolation of fine grain quartz for luminescence dating. *Ancient TL* 18, 15-17.
- Prescott, J.R., Hutton, J.T., 1994. Cosmic ray contribution to dose rates for luminescence and ESR dating: large depths and long-term time variations. *Radiation Measurements* 23, 497-500.
- Prescott, J.R., Stephan, L.G. 1982. The contribution of cosmic radiation to the environmental dose for thermoluminescence dating, *PACT* 6, 17-25.
- Rees-Jones, J., 1995. Optical dating of young sediments using fine-grain quartz. *Ancient TL* 13, 9-14.
- Roberts, H.M., Wintle, A.G., 2001. Equivalent dose determination for polymineral fine-grains using the SAR protocol: application to a Holocene sequence of the Chinese Loess Plateau. *Quaternary Science Reviews* 20, 859-863.
- Roberts, H.M., Duller, G.A.T., 2004. Standardised growth curves for optical dating of sediment using multiple-grain aliquots. *Radiation Measurements* 38, 241-252.
- Singhvi, A.K., Bronger, A., Sauer, W., Pant, R.K., 1989. Thermoluminescence dating of loess-palaeosol sequences in the Carpathian basin (east-central Europe): a suggestion for a revised chronology. *Chemical Geology* 73, 307-317.

# Chapter 3

Quaternary Geochronology, submitted.

## **Elevated temperature IRSL dating of the lower part of the Stari Slankamen loess sequence (Vojvodina, Serbia) – investigating the saturation behaviour of the pIRIR<sub>290</sub> signal**

**E.D. Schmidt<sup>1,2\*</sup>, A.S. Murray<sup>2</sup>, T. Stevens<sup>3</sup>, J.P. Buylaert<sup>2,4</sup>, S.B. Marković<sup>5</sup>,  
S. Tsukamoto<sup>1</sup>, M. Frechen<sup>1</sup>**

<sup>1</sup>*Leibniz Institute for Applied Geophysics (LIAG), Geochronology and Isotope Hydrology,  
Stilleweg 2, D-30655 Hannover, Germany*

<sup>2</sup>*Nordic Laboratory for Luminescence Dating, Department of Earth Sciences, Aarhus University,  
Risø DTU, DK-4000 Roskilde, Denmark*

<sup>3</sup>*Centre for Quaternary Research, Department of Geography, Royal Holloway, University of  
London, Egham, Surrey, TW20 0EX, UK.*

<sup>4</sup>*Radiation Research Division, Risø National Laboratory for Sustainable Energy, Technical  
University of Denmark, DK-4000 Roskilde, Denmark*

<sup>5</sup>*Chair of Physical Geography, University of Novi Sad, Trg Dositeja Obradovića 3, 21000 Novi  
Sad, Serbia*

*\* corresponding author: Esther.Schmidt@liag-hannover.de,  
estherdorothe.schmidt@googlemail.com*

### **Abstract**

An elevated temperature post-IR IR protocol (blue [320-460 nm] detection) using a second IR stimulation temperature of 290°C was applied to eleven polymineral fine grain (4-11 µm) samples from the lower part of the Stari Slankamen loess-palaeosol sequence with the aim of investigating the behaviour of both the IR<sub>50</sub> and the pIRIR<sub>290</sub> signals in material close

to or in saturation. Both signals of the lower 8 samples were found to be in saturation. The average ratio of the sensitivity-corrected natural signal to the laboratory saturation level for the pIRIR<sub>290</sub> is  $1.00 \pm 0.03$  (n=8); indicating that field saturation is equal to laboratory saturation for the signal. Minimum equivalent dose estimates were calculated from 2D<sub>0</sub> values, giving minimum age estimates of ~230-390 ka. This result indicates an upper limit for dating these loess deposits of ~300 ka. The age estimate of the younger sample SSK2 is in good agreement with the quartz OSL age showing that the pIRIR<sub>290</sub> signal is bleachable in nature and can be used to date material of ~20 ka. Our data suggest that the loess unit V-L2 accumulated during marine isotope stage (MIS) 6 and that an erosional event marked out by an unconformity and gravel layer has a minimum age of ~170 ka. Pedocomplex V-S1 can be correlated with the complete MIS 5 period. Furthermore we suggest minimum ages of ~230-390 ka for the formation of palaeosols V-S3, V-S4 and V-S5; considerably older than proposed by many previous studies.

**This manuscript is submitted to Quaternary Geochronology and will be online available at**  
***<http://www.sciencedirect.com/science/journal/18711014>***  
**after the successful reviewing process.**





















































# Chapter 4

Quaternary International, 2011 (234): 10-22.

## **Luminescence chronology of the loess record from the Tönchesberg section – a comparison of using quartz and feldspar as dosimeter to extend the age range beyond the Eemian**

**E.D. Schmidt<sup>1,2,3\*</sup>, M. Frechen<sup>1</sup>, A.S. Murray<sup>2</sup>, S. Tsukamoto<sup>1</sup>, F. Bittmann<sup>4</sup>**

<sup>1</sup>*Leibniz Institute for Applied Geophysics, S3: Geochronology and Isotope Hydrology, Stilleweg 2,  
30655 Hannover, Germany*

<sup>2</sup>*Nordic Laboratory for Luminescence Dating, Department of Earth Sciences, Aarhus University,  
Risø DTU, DK-4000 Roskilde, Denmark*

<sup>3</sup>*Radiation Research Division, Risø National Laboratory for Sustainable Energy, Technical  
University of Denmark, DK-4000 Roskilde, Denmark*

<sup>4</sup>*Lower Saxony Institute for Historical Coastal Research, Viktoriastrasse 26/28, 26382  
Wilhelmshaven, Germany*

*\* Corresponding author: Esther.Schmidt@liag-hannover.de*

*Key words: luminescence dating, IRSL, OSL, TT-OSL, loess, Eifel*

### **Abstract**

The loess-palaeosol sequences of the Tönchesberg section, located in the East Eifel Volcanic field (Germany) provide an excellent climate archive of the late Middle and the Upper Pleistocene in the Middle Rhine area. Loess deposits from the last Glacial (Weichselian) and the penultimate Glacial (Saalian) are up to 12 m and 15 m thick, respectively, and intercalated by palaeosols. Optically stimulated luminescence (OSL),

thermally transferred optically stimulated luminescence (TT-OSL) and infrared stimulated luminescence (IRSL) measurements were carried out on 14 samples from the Tönchesberg section to determine the deposition age and to set up a more reliable chronological framework for the penultimate and last interglacial-glacial cycle. The fine-grained quartz OSL and polymineral IRSL ages are in good agreement with each other and also with the geologically estimated age, but the quartz TT-OSL ages are overestimated. The OSL and IRSL ages range from  $16.8 \pm 1.2$  to  $189 \pm 16$  ka indicating that the youngest loess and the weakly developed soils were deposited during marine isotope stage (MIS) 2 and 3 and that the two marker loess were most likely accumulated in the transition MIS 4/5. Loess and reworked loess postdating the Eemian soil yield ages of 110-115 ka indicating that these deposits very likely correlate to MIS 5d. Loess deposits taken below the Eemian soil are attributed to the transition MIS 6/7. A weakly developed soil above the Tönchesberg scoria yield an age of  $189 \pm 16$  ka indicating an interstadial soil formation during MIS 7. This is in good agreement with preliminary  $^{40}\text{Ar}/^{39}\text{Ar}$ -ages for the Tönchesberg scoria and the intercalated tephra layers. Reliable age estimates up to  $\sim 70$  ka could be obtained using quartz OSL and up to  $\sim 190$  ka using the pulsed post-IR IR signal from feldspar. Hence the infrared stimulated luminescence (IRSL) is considered as the best approach to date the loess from the Middle Rhine area  $> 70$  ka.

#### **4.1. Introduction**

Loess records are sensitive archives of climate and environment change and provide important information on local and regional environmental processes and conditions for the Middle and Late Pleistocene period in Europe. Volcanic depressions and crater such as those of the Tönchesberg form excellent sediment traps, and so record the climate and environment changes of the past. The loess-palaeosol sequences of late Middle Pleistocene scoria cones in the East Eifel Volcanic field are generally well preserved (Boenigk and Frechen, 2001). At the Tönchesberg section, loess and reworked loess-like sediments as well as intercalated palaeosols of the last glacial-interglacial cycle and the penultimate glaciation are well exposed and provide an accessible high-resolution archive. Independent age control is provided by  $^{40}\text{Ar}/^{39}\text{Ar}$  dating of (a) the widely distributed Lacher See pumice layer, (b) two intercalated air-fall tephra from the nearby Korrettsberg and Plaidter Hummerich volcano and (c) the Tönchesberg scoria. A reversed magnetization, interpreted as the Blake event ( $\sim 117$  ka) has also been identified in the Tönchesberg deposits (Becker et al. 1989, Reinders and Hambach,

1995). According to Becker et al. (1989) the Tönchesberg loess deposits were first investigated by Windheuser (1977) and have been described in detail by Becker et al. (1989) and Hentzsch (1990). Thermoluminescence (TL) age estimates for the deposits of the Tönchesberg have been presented by Zöller et al. (1991) and Frechen (1991, 1994), and infrared stimulated luminescence (IRSL) ages by Boenigk and Frechen (1999). These previous studies provided apparently reliable TL and IRSL ages up to about 100 ka. Because of this, the loess and loess derivatives of the Tönchesberg seem to be appropriate sediment on which to test the accuracy of new approaches to luminescence dating.

Recently, new methods to extend the age range of luminescence dating using both quartz and feldspar minerals have been proposed. The luminescence signals from feldspars continue to grow at much higher doses than those from quartz; this offers the possibility of dating significantly older material. However luminescence dating of feldspars has a tendency to underestimate the age, because of anomalous fading (Wintle, 1973). Based on the work of Thomsen et al (2008a), Buylaert et al. (2009) proposed a new SAR IRSL protocol, with detection in the blue (320-460 nm). This protocol involves elevated temperature stimulation with IR for 100 s at 225°C (following stimulation with IR for 100 s at 50°C) a so-called post-IR IR measurement sequence. They have shown that the observed fading rates for the post-IR IR signal are significantly lower than those from the conventional IRSL at 50°C, and that this signal is bleachable in nature. A different approach to deal with fading problems was presented by Tsukamoto et al. (2006). They reported that the long-lifetime luminescence component, observed from feldspars when the stimulation light source is pulsed (stimulation is delivered by discrete light pulses) is significantly more stable than shorter lifetime components. A study carried out by Thomsen et al. (2008b) also revealed that the fading rate of the pulsed signal is ~60% of the value of continuous wave (CW) stimulation. In our study, we combined these two suggestions, by included pulsed IR stimulation in a post-IR IR protocol.

The optically stimulated luminescence (OSL) of quartz has also been widely used to estimate the deposition age of sediments and is usually regarded as an accurate and precise dating method (e.g. Murray and Olley, 2000). However, the fast component of the quartz OSL signal (the component normally used for dating) saturates following doses of 200-400 Gy (Wintle and Murray, 2006). Thermally transferred OSL (TT-OSL; Wang, et al. 2006, 2007; Tsukamoto et al., 2008) attempts to overcome this problem by using a different signal, one that saturates at doses more than 10 times higher than the standard OSL signal. This OSL signal is measured after optically removing the standard OSL and heating the sample to some

temperature around 280°C. This study tests the use of the TT-OSL signal from Tönchesberg sediments, using a protocol based on the work of Porat et al. (2009), but with modifications intended to maximise the TT-OSL signal strength.

The aim of our study is to determine luminescence ages for the loess from Tönchesberg using optically stimulated luminescence (OSL), thermally transferred optically stimulated luminescence (TT-OSL) and infrared stimulated luminescence (IRSL), in order (i) to compare the different methods, (ii) to test the suitability and reliability of luminescence dating over the last 200 ka and (iii) to establish a reliable chronostratigraphical framework for the penultimate and last interglacial-glacial sediments from the Tönchesberg section.

#### 4.2. Geological setting

The Tönchesberg is located in the East Eifel Volcanic Field in Germany and consists of a complex of scoria cones (Fig. 1). This volcanism appears to have been reactivated between 500 and 600 ka (oxygen isotope stage 15). Loess and loess derivatives have accumulated in the study area since the Middle Pleistocene, as evidenced by the loess-palaeosol sequences at the Kärlich clay pit (Boenigk and Frechen, 1998). The site is 243 m above sea level and the coordinates of the profile under study are 50° 22' 4" N and 7° 21' 41" E.

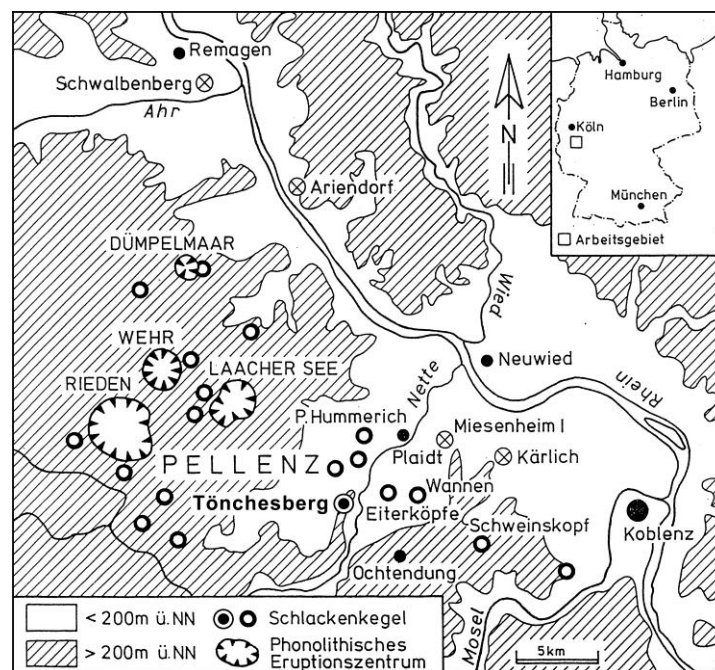


Figure 4.1: Map showing the location of the Tönchesberg section in the East Eifel area.

The Tönchesberg scoria complex belongs to a group of volcanoes erupted after the cataclysmic eruption of the “Wehr phonolithic eruption centre” (“Hüttenberg tephra”) (Boenigk and Frechen, 2001). A phreatomagmatic eruption with initial maar-like deposits was followed by Strombolian volcanism which built up most of the scoria cones.  $^{40}\text{Ar}/^{39}\text{Ar}$ -laser-single grain dating of the basanitic Tönchesberg scoria (Bogaard and Schmincke, 1990) yielded a preliminary age of 188-216 ka (MIS 7). Volcanic debris accumulated at the crater base, followed by two air-fall tephra from the nearby Korrettsberg (preliminary  $^{40}\text{Ar}/^{39}\text{Ar}$ -laser-single grain dating gave an eruption age of  $243 \pm 65$  ka; van den Boogard and Schmincke, 1990) and Plaidter Hummerich volcano ( $^{40}\text{Ar}/^{39}\text{Ar}$ -laser-single grain dating of  $238 \pm 20$  ka, but this age estimate is overestimated according to Bogaard and Schmincke (in Kröger, 1995)). According to Boenigk and Frechen (1999) the eruption of the Tönchesberg volcano post-dated the eruption of the “Hüttenberg tephra” ( $215 \pm 4$  ka, van den Boogard and Schmincke, 1990) as indicated by the presence of the Hüttenberg tephra below the initial maar-like deposits at the base of several scoria complexes in the vicinity of Tönchesberg volcano. However this marker horizon has not yet been found below the pyroclastic deposits of Tönchesberg. A rather cold climatic environment during the eruption is assumed because of reworked sediments showing solifluction (Boenigk and Frechen, 2001). Loess with intercalated weak soils and reworked loess cover the volcanic debris. The craters and the depression between the different scoria cones at the Tönchesberg scoria complex make excellent sediment traps – hence a relatively continuous succession of aeolian sediments seems to have been preserved. The penultimate glacial loess beneath the Eemian soil is intercalated by tephra layers from the Korrettsberg and Plaidter Hummerich volcanoes as well as by a “tephritic tephra” of unknown age. Weak tundra or frost gleys have developed in the loess, typical of the upper part of the Saalian loess in Middle Europe (Bibus, 1974). A red-brown forest soil (“parabraunerde”, clay rich B horizon) is superimposed on the penultimate glacial loess. Above the Eemian soil there are about 11 m of loess and reworked loess exposed. The lower Weichselian is represented by interstadial humic soils, pellet sands, reworked pedosediments and two marker loess. The deposits of the Middle Weichselian are reworked loess with two weakly developed brown interstadial soils. The Upper Weichselian sediments consist of loess with an intercalated weak gleyed horizon and strong dark-brown soil (Allerød soil), which is covered by the pumice horizon of the eruption of the Laacher See volcano. There are several profiles exposed at the Tönchesberg section due to exploitation of the scoria. Fig. 2 shows the lithology of the profiles.

#### **4.2.1. Profile A and B**

Profile A is located at the edge of a depression on the crater rim and Profile B shows the succession at the center of this depression. Both profiles were described in detail by Becker et al. (1989). At the top of the profile there is about 30 cm of thick strong dark-brown soil (“pararendzina”) correlating to the Allerød interstadial, covered by pumice of the Laacher See eruption ( $^{40}\text{Ar}/^{39}\text{Ar}$  dated to 12.9 ka; Schmincke et al., 2000). Beneath this soil ~100 cm homogenous loess was deposited. Two samples (Toe1 and Toe2) were taken from the homogeneous loess unit below this loess, and one sample (Toe3) was taken in the reworked loess between the two weakly developed brown soils. Sample Toe4 was collected from the reworked loess below the lower part of the weak soil. Reworked humic-rich sediments with intercalated weak humic soils and pellet sands were deposited underneath this reworked loess. The reworked humic-rich sediments differ from the intercalated weak soils in their carbonate content, structure and colour. The humic rich sediments contain only carbonate concretions, they exhibit stratification have no real structure and are of brown colour; in contrast the weak soils are calcareous, have a prismatic structure and are of greyish brown colour (Becker et al., 1989). On the top of the pellet sands and below the humic-rich sediments there is a thin (~5 cm thick) band of loess. Below these pellet sands, ~20 cm of loess with many soil veins indicating deep seasonal frost conditions. The two loess bands have a different grain size distribution compared to the homogeneous loess of the upper part of the profile: the clay concentration is much higher while the silt fraction is significantly lower. The marker loess were only found in profile B. Sample Toe7 and Toe8 were taken from these bands. Sample Toe5 came from the reworked humic rich sediments under the reworked loess deposits. In profile A the truncated humic-rich A horizon developed directly underneath the reworked humic-rich sediment, and loess and reworked loess were deposited on top of the last interglacial soil. Samples Toe 12 and Toe 6 were taken from this reworked loess. In total nine samples for luminescence dating were collected from profiles A and B (Fig. 2).



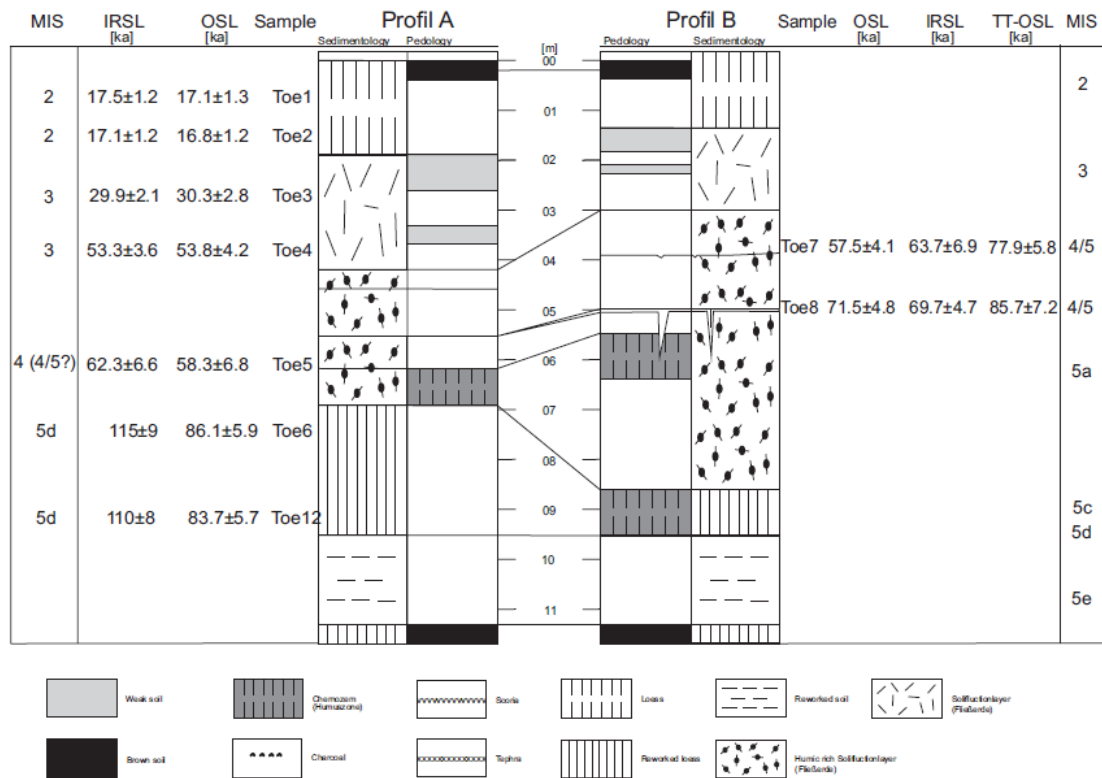


Figure 4.2a: Lithology and luminescence ages of the Tönchesberg section (Weichsel, Profile A and B).

#### 4.2.2. Profile C

Profile C is situated in the northwestern part of the pit. It consists of a succession of about 14 m of penultimate glacial loess superimposed by the last interglacial (Eemian) soil and intercalated by tephra layers. The succession begins underneath the Eemian soil with about 6 m of reworked layered loess. Below these sediments, the “tephritic tephra” is intercalated; in some parts of this profile it is separated by about 2.5 m of reworked loess. It is not clear whether the upper and/or lower part of this tephra is reworked. Sample Toe15 was collected from the reworked loess deposits between the “tephritic tephra” layers. Underneath the lower “tephritic tephra” layer there is ~1.5 m of loess and reworked loess intercalated/deposited. Underneath this loess, the Tönchesberg volcano scoria is exposed.

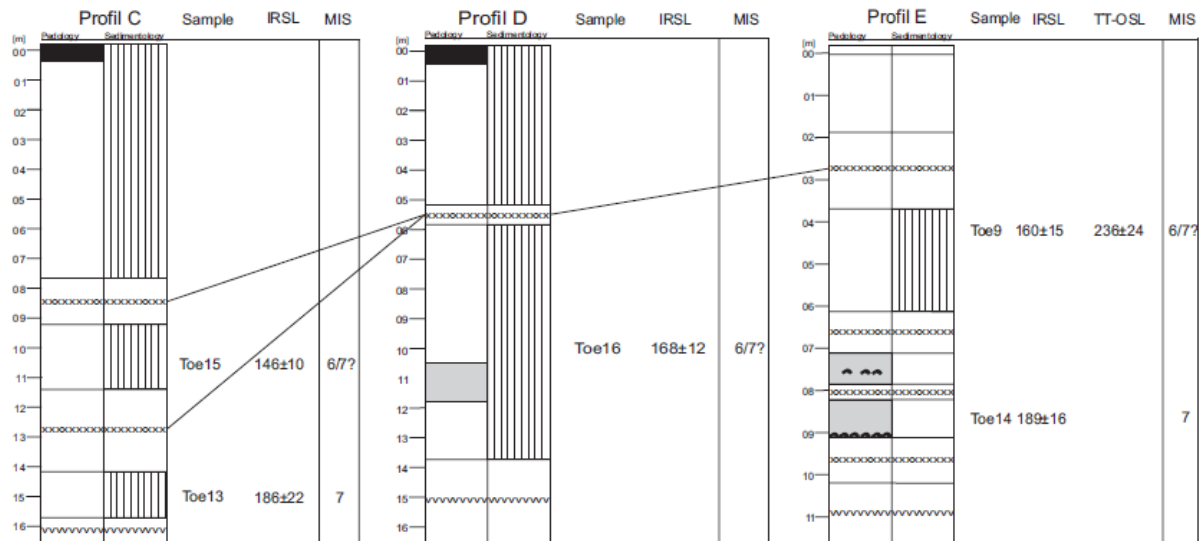


Figure 4.2b: Lithology and luminescence ages of the Tönchesberg section (Saale, Profile C, D and E).

#### 4.2.3. Profile D

Profile D is located in the western part of the pit and consists of a succession of about 14 m of penultimate glacial loess superimposed by the last interglacial (Eemian) soil. These mostly-layered reworked loess sediments are intercalated by several weak-gleyed horizons (“Nassböden”), which are characteristic of loess deposits from the younger part of the penultimate glaciation in Central Europe. The laminated facies can hint at either reworking of loess by water, niveo-eolian processes or purely aeolian processes. From the geomorphological position, it is most likely the result of running water. The “tephritic tephra” is intercalated in this loess. The tephra ranges in thickness from ~1 m to ~5 m. A weak soil has formed at around 10.50 m below surface. It is regarded as *in situ*; it developed in a local depression and is taken as equivalent to the development of recent gley formations. At the base of the profile the Tönchesberg scoria is exposed. Sample Toe9 was collected above the weak palaeosol.

#### 4.2.4. Profile E

Profile E is located in the northwestern part of the section. In the upper part of profile E loess covers the “tephritic tephra”. Underneath the tephra, loess is exposed, and sample Toe9 was collected from this loess unit. Underneath the loess, tephra from the Plaitder Hummerich

and Korrettsberg volcanoes were deposited, intercalated by soil formation. Charcoal was collected (sample Toe9a) from this palaeosol. Below the tephra of the Korreltsberg volcano about 90 cm of reworked loess were deposited, now containing a weakly developed soil with charcoal. Sample Toe14 and charcoal (sample Toe14a) were collected from here. At the base of the profile the Tönchesberg volcano scoria is exposed.

### 4.3. Experimental details

The samples were extracted under subdued red light and pretreated with 10% hydrochloric acid to remove carbonates, sodium oxalate to separate aggregates and 30% hydrogen peroxide to remove organic matter. The 4-11  $\mu\text{m}$  silt fraction was then separated using Stokes Law, with settling in a water column. This fine grain fraction was divided into two parts: (i) an untreated fraction used for polymineral infrared stimulated luminescence (IRSL) measurements, and (ii) a fraction from which quartz grains were extracted. The latter polymineral fraction was treated with 34% fluorosilicic acid ( $\text{H}_2\text{SiF}_6$ ) for 6 days, preferentially dissolving feldspar grains, and leaving behind a quartz-rich extract. Finally, samples were prepared for measurement by settling either the polymineral or the quartz grains (4-11  $\mu\text{m}$ ) from acetone onto aluminium discs. The purity of the quartz extract was checked using the IR depletion ratio (Duller, 2003). All OSL/IRSL measurements were performed using an automated Risø TL/OSL-DA20 equipped with a  $^{90}\text{Sr}/^{90}\text{Y}$  beta source (Bøtter-Jensen et al., 2000). Quartz blue-stimulated OSL was measured for 40 s at 125°C and the signals were detected through 7.5 mm of Hoya U-340 filter (passing 260 to 390 nm, i.e. UV). Feldspar IRSL signal was detected through Schott BG-39 and Corning 7-59 filters (passing 320 to 460 nm; i.e. blue). For calculation of the equivalent dose ( $D_e$ ) of quartz fine-grains a conventional SAR protocol (Murray and Wintle, 2000) was applied. The signal was integrated over the initial 1 s of stimulation, and a background based on the last 5 s of simulation subtracted. All dose response curves were fitted using an exponential function.  $D_e$  estimates from quartz fine-grains from five samples were also calculated using the thermal transferred optically stimulated luminescence (TT-OSL) signal (Wang et al., 2006). The equivalent doses were obtained by integrating the initial 0.8 s of the OSL decay curve after subtracting the last 4 s of the decay curves. An exponential growth curve was fitted to determine the equivalent dose.  $D_e$  estimates from polymineral fine-grains were determined using a pulsed elevated-temperature IRSL (SAR) protocol. This SAR protocol employs pulsed IR stimulation for 400

s with the sample held at at 150°C, preceded by stimulation with IR for 100 s at 50°C; this is referred to here as a pulsed post-IR IR measurement sequence. The initial 1.6 s of the pulsed post-IR IR signal is used for calculating the  $D_e$  values, with a background based on the signal observed in the last 10 s of the decay curve. All dose response curves were fitted using an exponential function

Radionuclide concentrations for all samples were obtained using high resolution gamma spectrometry of sediment collected from the immediate surrounding of the samples. Present day water contents of 10-18% were measured directly on several samples; an average value of  $15 \pm 5 \%$  was used for all samples down to the depth of 12 m. For samples taken below 12 m (i.e. below the former estimated surface) a water content of  $20 \pm 5 \%$  was used for age calculation. Mean  $a$ -values of  $0.04 \pm 0.02$  for quartz OSL and of  $0.08 \pm 0.02$  for polymineral IRSL were used to derive the effective alpha dose rate (Rees-Jones, 1995). The uranium, thorium, potassium contents and the dose rate of the samples are summarised in Table 1. The concentrations of uranium, thorium and potassium were converted into infinite-matrix dose rates using the conversion factors of Adamiec and Aitken (1998) and water-content attenuation factors (Aitken, 1985). Estimation of the cosmic-ray dose rate was based on Prescott and Stephan (1982) and Prescott and Hutton (1994) from a knowledge of burial depth, altitude, matrix density, latitude and longitude for each sample.

Sample	Uranium (Bq/kg)	Thorium (Bq/kg)	Potassium (Bq/kg)	OSL dose rate (Gy/ka)	IRSL dose rate (Gy/ka)
Toe1	34.21 $\pm$ 0.12	40.23 $\pm$ 0.12	460.41 $\pm$ 3.09	2.72 $\pm$ 0.17	2.99 $\pm$ 0.2
Toe2	34.46 $\pm$ 0.12	42.14 $\pm$ 0.24	460.41 $\pm$ 3.09	2.82 $\pm$ 0.18	3.09 $\pm$ 0.21
Toe3	39.40 $\pm$ 0.12	48.07 $\pm$ 0.16	482.04 $\pm$ 3.09	2.97 $\pm$ 0.19	3.29 $\pm$ 0.19
Toe4	31.74 $\pm$ 0.12	44.09 $\pm$ 0.12	463.50 $\pm$ 3.09	2.71 $\pm$ 0.17	2.98 $\pm$ 0.2
Toe5	32.60 $\pm$ 0.12	43.81 $\pm$ 0.20	451.14 $\pm$ 3.09	2.71 $\pm$ 0.17	2.99 $\pm$ 0.2
Toe6	36.43 $\pm$ 0.12	44.54 $\pm$ 0.24	441.87 $\pm$ 3.09	2.76 $\pm$ 0.17	3.11 $\pm$ 0.21
Toe7	32.60 $\pm$ 0.12	50.38 $\pm$ 0.16	451.14 $\pm$ 3.09	2.73 $\pm$ 0.16	3.17 $\pm$ 0.21
Toe8	33.47 $\pm$ 0.12	49.78 $\pm$ 0.08	417.15 $\pm$ 3.09	2.62 $\pm$ 0.16	3.05 $\pm$ 0.21
Toe9	32.48 $\pm$ 0.12	45.96 $\pm$ 0.24	528.39 $\pm$ 3.09	2.83 $\pm$ 0.17	3.26 $\pm$ 0.21
Toe12	37.91 $\pm$ 0.12	43.89 $\pm$ 0.24	448.05 $\pm$ 3.09	2.68 $\pm$ 0.17	3.12 $\pm$ 0.22
Toe13	35.82 $\pm$ 0.49	50.71 $\pm$ 0.45	605.64 $\pm$ 9.27	3.18 $\pm$ 0.19	3.66 $\pm$ 0.24
Toe14	18.65 $\pm$ 0.25	35.44 $\pm$ 0.20	444.96 $\pm$ 3.09	2.16 $\pm$ 0.14	2.46 $\pm$ 0.17
Toe15	35.07 $\pm$ 0.25	45.88 $\pm$ 0.24	460.41 $\pm$ 3.09	2.69 $\pm$ 0.17	3.13 $\pm$ 0.21
Toe16	27.54 $\pm$ 0.49	58.50 $\pm$ 0.49	618.00 $\pm$ 9.27	3.19 $\pm$ 0.18	3.66 $\pm$ 0.23

**Table 4.1: Dose rate data from potassium, uranium and thorium content, as measured by gamma spectrometry.**

#### 4.4. Performance tests

To test the reliability of the OSL and IRSL dose measurement protocols adopted, various laboratory parameters such as recycling ratio, recuperation and dose recovery ratio were investigated. Any laboratory bleaching was carried out in a Hönle SOL2 solar simulator.

##### 4.4.1. OSL

###### *Thermal transfer*

To check for thermal transfer (Wintle and Murray, 2006) the aliquots were bleached twice at 125°C with 1000s blue stimulation separated by a 5000s pause. The aliquots were measured with increasing temperatures ranging from 200°C to 300°C in steps of 20°C. After bleaching,  $D_e$  estimates should be close to zero; a significant  $D_e$  value with increasing preheat temperature indicates thermal transfer of charge from thermally-shallow optically insensitive traps to the deeper OSL trap. The results of this experiment for samples Toe1 and Toe5 are shown in Fig. 3. Equivalent doses are close to zero for preheats up to ~240°C, from 240°C up the values increase indicating the presence of detectable thermal transfer. From these data, it appears that the preheat temperature should be kept below 240°C.

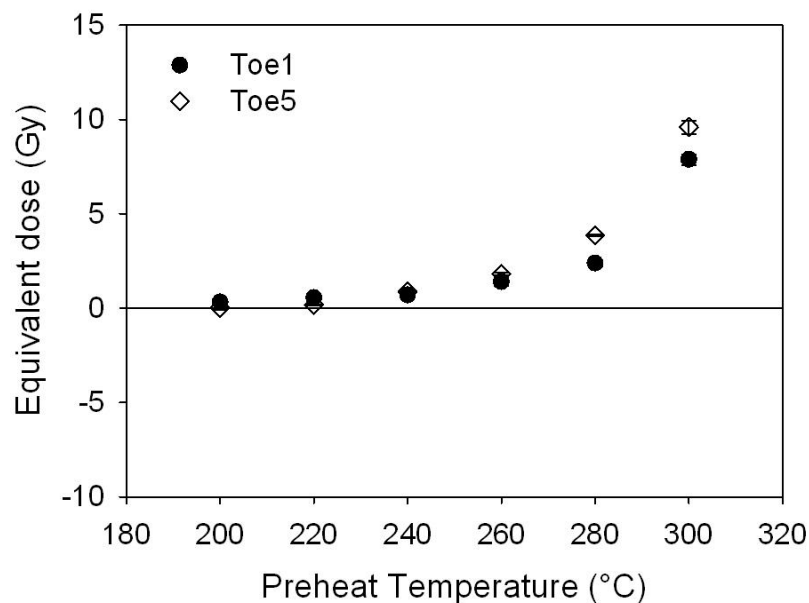
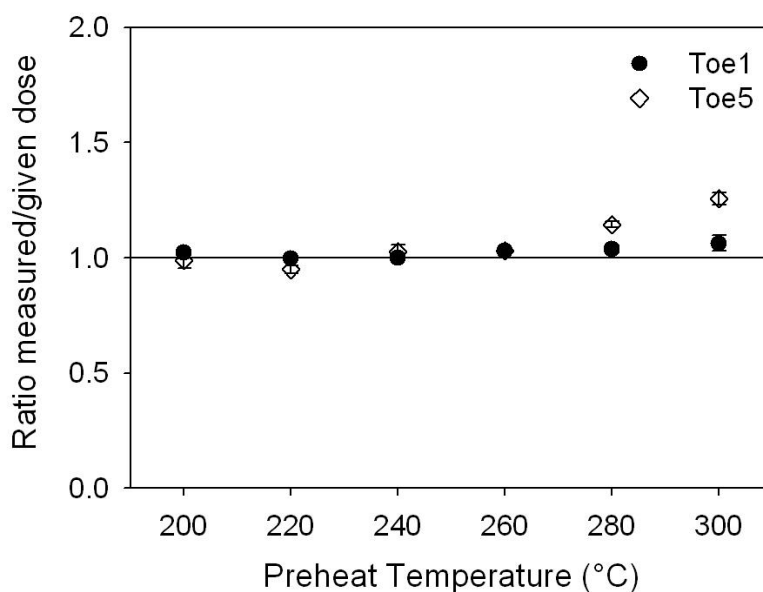


Figure 4.3: Thermal transfer test for Sample Toe1 and Toe5.

### *Dose recovery*

To test the suitability of the SAR protocol to these samples, and to confirm the most appropriate preheat temperature, the dose recovery ratio (Murray and Wintle, 2003) was determined for different preheat temperatures, using samples Toe1 and Toe5.



**Figure 4.4:** Dose recovery test with different preheat temperatures for Sample Toe1 and Toe5.

In addition, dose recovery ratios were measured for all samples using a preheat temperature of 240°C for 10 s following all natural and regeneration doses, and 200°C for 1 s following all test doses. All aliquots were first bleached twice with 1000s blue stimulation at room temperature separated by a 5000s pause to allow the decay of any charge transferred to the 110°C TL trap, before giving a dose approximately equal to the natural dose. This dose was then measured as if it were a natural dose. Fig. 4 shows the ratio of the measured dose to the known (given) dose as a function of preheat temperature for sample Toe1 and Toe5 (using a fixed thermal treatment following the test dose of 200°C for 1 s). The measured dose/given dose ratio is close to unity between 200° and 260°C preheat temperature. At preheat temperatures higher than 260°C, the measured dose is systematically greater than the given dose; this is most likely caused by thermal transfer (e.g. Fig. 3). Fig. 5 shows the dose recovery ratio for all aliquots of all samples as a histogram, for a fixed preheat temperature of 240°C for 10s; the mean ratio of measured to given dose is  $0.994 \pm 0.011$  ( $n = 33$ ), demonstrating that we are able to accurately measure a known dose given in the laboratory prior to any heating of the sample.

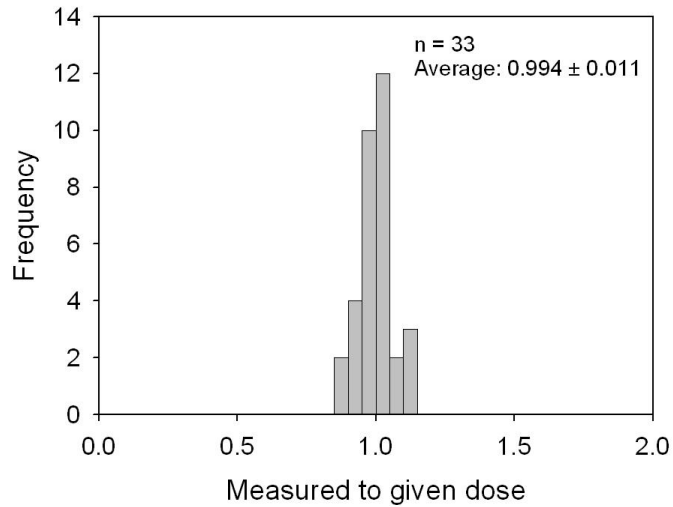


**Figure 4.5: Ratio of the measured to given dose for the routine dose recovery test for the OSL SAR protocol for all samples.**

#### **4.4.2. TT-OSL**

##### *Dose recovery / Residuals*

To test the applicability of the TT-OSL SAR protocol, the dose recovery ratio was measured for sample Toe8. In our experiment three aliquots were bleached for four hours in a Hönle SOL2 solar simulator. The aliquots were then given a dose of 240 Gy. This dose was then measured as if it were a natural dose. The same procedure was carried out using additional bleached but undosed aliquots, to measure the residual dose remaining after bleaching. The mean value of the measured dose for the dosed aliquots is  $424 \pm 14$  Gy ( $n = 3$ ) and  $180 \pm 19$  Gy ( $n = 3$ ) for the undosed aliquots. After subtracting the residual doses from the doses measured from the dosed aliquots, the mean ratio of the measured to given dose is  $1.08 \pm 0.06$  ( $n = 3$ ).

#### **4.4.3. Pulsed post-IR IR luminescence signal**

##### *Preheat plateau*

To confirm the thermal stability of the pulsed post-IR IR signal, the dependence of equivalent dose ( $D_e$ ) on preheat temperature was investigated using the same thermal

treatment following the natural/regeneration doses and the test doses (Blair et al., 2005). Fig. 6 shows the results of this experiment for sample Toe8.

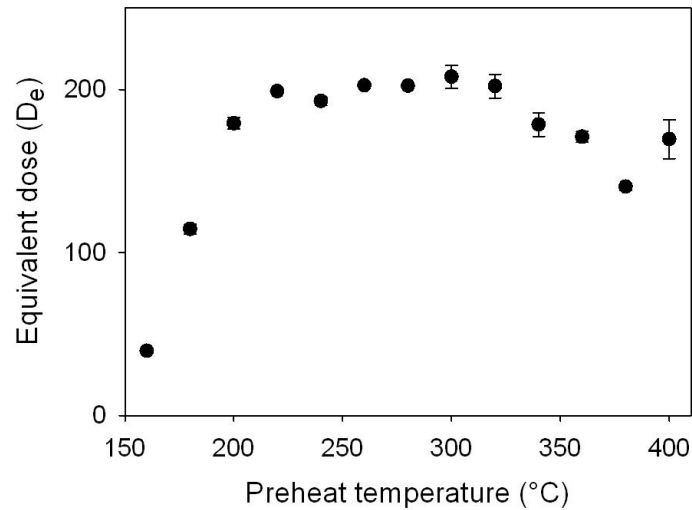


**Figure 4.6: De preheat plateau test for sample Toe8.**

A stable signal is reached at a preheat temperature of 220°C and above, at temperatures lower than 200°C the  $D_e$  estimates decrease rapidly. These results are similar to those presented by Schmidt, et al. (2010) for polymineral fine-grained loess from Serbia. It seems that the blue IRSL signal from polymineral loess grains has a component which is significantly thermally unstable, in contrast to the IRSL signal from sand sized grains of separated K-feldspar (e.g. Murray et al., 2009).

### *Residuals*

To confirm that this pulsed post-IR IR signal is bleachable by natural daylight we exposed three aliquots per sample for four hours to a Hönle SOL2 solar simulator and then measured the apparent dose in the usual manner; this residual dose ranged from  $3.04 \pm 0.3$  Gy to  $8.11 \pm 0.096$  Gy, with a mean of  $5.4 \pm 0.2$  Gy ( $n = 39$ ).

### *Dose recovery*

Dose recovery ratios were measured for all samples using the pulsed post-IR IR SAR protocol. Aliquots were first bleached for 4h in a Hönle SOL2 solar simulator, and then given a dose approximately equal to the natural dose. Fig. 7 shows the individual dose recovery ratios for all aliquots as a histogram; the mean ratio of the measured to given dose is  $0.9701 \pm 0.007$ ,  $n = 42$ .



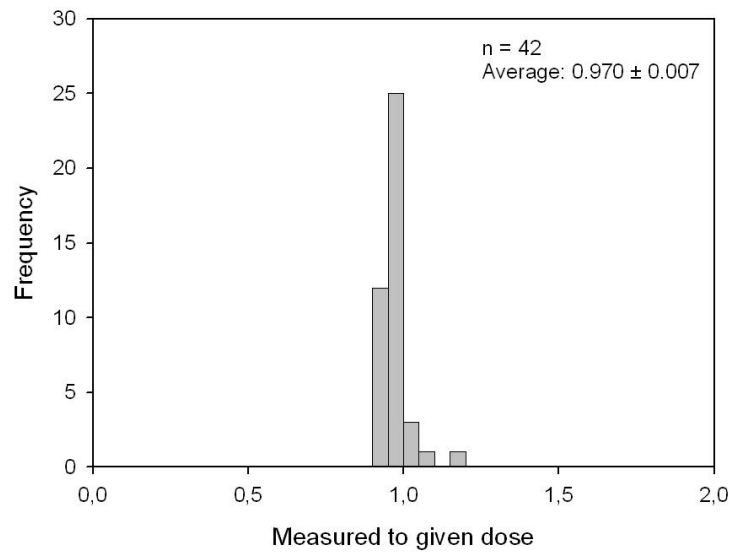


**Figure 4.7: Ratio of the measured to given dose for the routine dose recovery test for the pulsed post-IR IR protocol for all samples.**

#### *Laboratory fading*

Previous studies have shown that the IRSL signals from polymineral grains can suffer from anomalous fading, an unwanted loss of signal, resulting in age underestimation (Wintle, 1973). To test for anomalous fading, those aliquots which had been used for  $D_e$  measurement, were then used to test for fading, by dosing and preheating the aliquots and then storing for various periods of time up to ~16 hours before measurement. This sequence was repeated several times on each aliquot. The fading rates are expressed in terms of the percentage decrease of intensity per decade of time (g-value; Aitken, 1985; Auclair et al., 2003), referred to the period of irradiation. The g-values range from  $-1.95 \pm 0.83\%/decade$  to  $0.58 \pm 0.15\%/decade$ , with an average of  $-0.52 \pm 0.39\%/decade$ ,  $n = 28$  (Fig. 8) indicating that we can not detect significant fading. Fig. 9 shows the results of fading tests for sample Toe7 and Toe8.

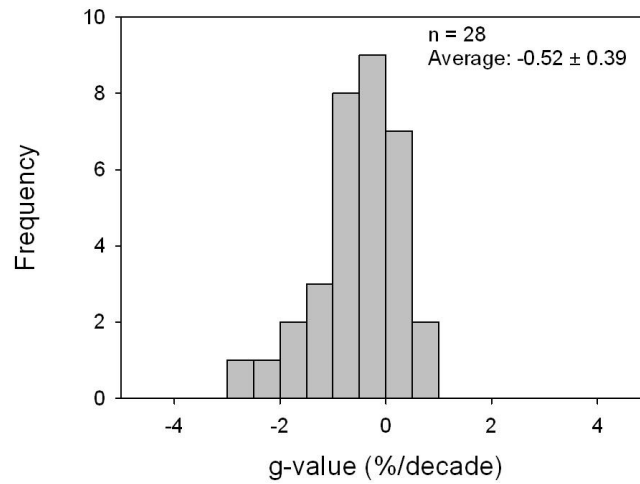


Figure 4.8: G-values for all samples.

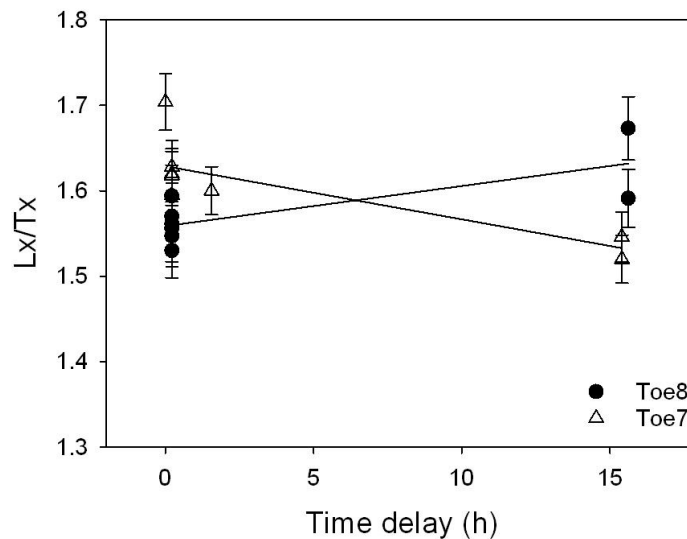


Figure 4.9: Fading test for sample Toe7 and Toe8.

## 4.5. Results & Discussion

### 4.5.1. Dosimetry, Equivalent doses and Luminescence ages

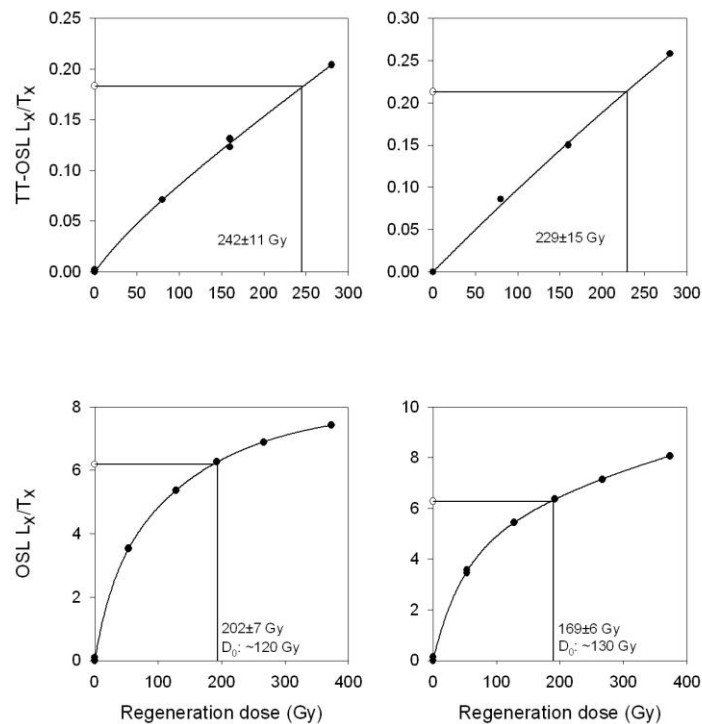
The uranium, thorium, potassium content and total dose rates are shown in Table 1. The mean dose rate is  $2.77 \pm 0.07$  Gy/ka for quartz and  $3.14 \pm 0.08$  Gy/ka for polymineral feldspar, similar to those obtained earlier for the Tönchesberg site (Frechen, 1991; Zöller et al., 1991).

Table 2 summarises the equivalent doses, recycling ratios, dose recovery results and the resulting luminescence ages for all samples.

Sample	Depth	Measurement	D <sub>e</sub> (Gy)	Recycling	Measured/given dose	Residual doses	g-value (%)	uncorrected Age (ka)
Toe 1	1.00	OSL	49.9 ± 2.5	1.00 ± 0.01	0.999 ± 0.013			17.1 ± 1.3
		IRSL	52.2 ± 1.2	0.99 ± 0.01	0.955 ± 0.001	3.04 ± 0.3	-0.48 ± 0.23	17.5 ± 1.2
Toe 2	1.80	OSL	50.7 ± 1.8	1.02 ± 0.01	0.964 ± 0.075			16.8 ± 1.2
		IRSL	52.9 ± 2.03	0.98 ± 0.01	0.955 ± 0.019	3.54 ± 0.2	0.15 ± 0.11	17.1 ± 1.1
Toe 3	2.60	OSL	96.3 ± 7.1	0.99 ± 0.01	0.963 ± 0.058			30.3 ± 2.8
		IRSL	98.3 ± 4.8	0.97 ± 0.01	0.955 ± 0.075	4.01 ± 0.01	-0.65 ± 0.33	29.9 ± 2.1
Toe 4	3.50	OSL	157.38 ± 6	0.98 ± 0.01	1.004 ± 0.014			53.8 ± 4.2
		IRSL	159.5 ± 1.6	0.99 ± 0.01	0.923 ± 0.003	4.9 ± 0.1	-1.67 ± 0.98	53.3 ± 3.6
Toe 5	4.50	OSL	170 ± 17	0.99 ± 0.01	1.005 ± 0.049			58.3 ± 6.8
		TT-OSL	316 ± 40	1.21 ± 0.05				123 ± 9
		IRSL	186 ± 15	0.97 ± 0.01	0.989 ± 0.005	5.26 ± 0.37	-0.59 ± 0.42	62.3 ± 6.6
Toe 6	4.00	OSL	248 ± 9	0.99 ± 0.01	0.985 ± 0.027			86.1 ± 5.9
		IRSL	343 ± 11	1.02 ± 0.01	0.968 ± 0.012	8.11 ± 0.096	0.24 ± 0.17	115 ± 9
Toe 7	3.80	OSL	169 ± 6	0.97 ± 0.01	0.972 ± 0.045			57.5 ± 4.1
		TT-OSL	229 ± 15	1.08 ± 0.03				77.9 ± 5.8
		IRSL	192 ± 5	1.01 ± 0.01	0.969 ± 0.004	5.08 ± 0.7	0.58 ± 0.15	63.7 ± 4.5
Toe 8	5.00	OSL	202 ± 7	0.97 ± 0.01	0.987 ± 0.012			71.5 ± 4.8
		TT-OSL	242 ± 11	1.02 ± 0.01	1.048 ± 0.086			85.7 ± 7.2
		IRSL	203 ± 5	0.99 ± 0.01	0.928 ± 0.003	5.31 ± 0.21	-0.74 ± 0.29	69.7 ± 6.9
Toe 9	4.20	TT-OSL	716 ± 62	0.71 ± 0.03				236 ± 24
		IRSL	496 ± 31	1.02 ± 0.01	0.978 ± 0.012	5.99 ± 0.74	-0.16 ± 0.13	160 ± 15
Toe 12	5.50	OSL	242 ± 8	0.97 ± 0.01	1.042 ± 0.036			83.7 ± 5.7

**Table 4.2: Equivalent dose (D<sub>e</sub>), recycling ratio, dose recovery, fading and luminescence ages.**

The results of the dose recovery tests prove that our SAR protocols are able to measure equivalent doses in our samples accurately. OSL dose response curves using the SAR protocol for one aliquot each from sample Toe7 and Toe8 are shown in Fig.10 (c,d). The curves are fitted with a saturating exponential function including a linear term. The equivalent doses from quartz OSL range from  $49.9 \pm 2.5$  Gy to  $248 \pm 9$  Gy. The  $D_0$ -values for all samples are about 120-130 Gy, except for sample Toe6 where the  $D_0$ -value is about 150 Gy. These values are very similar to those reported by Wintle and Murray (2006) suggesting that it should be possible to measure doses up to about 250 Gy for this material, and perhaps somewhat higher for Toe6. For this sample the observed dose is 248 Gy, and the growth curve does not yet saturate in this dose range. Buylaert et al. (2007) made similar observation for Chinese loess but concluded that equivalent doses larger than  $D_0$  ( $\sim 120$  Gy) were not very reliable. The quartz OSL ages range from  $16.8 \pm 1.2$  to  $86.1 \pm 5.9$  ka. All quartz OSL ages are in stratigraphic order.



**Figure 4.10: OSL and TT-OSL dose response curves for representative aliquots of sample Toe7 and Toe8.**

Using the TT-OSL signal  $D_e$  values could only be determined for samples Toe5, Toe7, Toe8, Toe9 and Toe13 – for all other samples the signal was too weak to be useful. Equivalent doses range from  $229 \pm 15$  Gy to  $987 \pm 125$  Gy, giving ages ranging from  $80 \pm 6$  ka to  $291 \pm 40$  ka. In our study we compared the OSL signal to the recuperated OSL signal. The dose response curve for quartz OSL has a characteristic dose level of  $D_0 \sim 120$ -130 Gy, so laboratory saturation is  $\sim 250$  Gy. The TT-OSL grows to much higher doses with predicted saturation  $>1000$  Gy. Comparing TT-OSL signals between samples, we found significant differences in characteristics. Samples Toe7 and Toe8 yield much lower residuals and emit a much brighter signal than the other samples (Fig. 11).

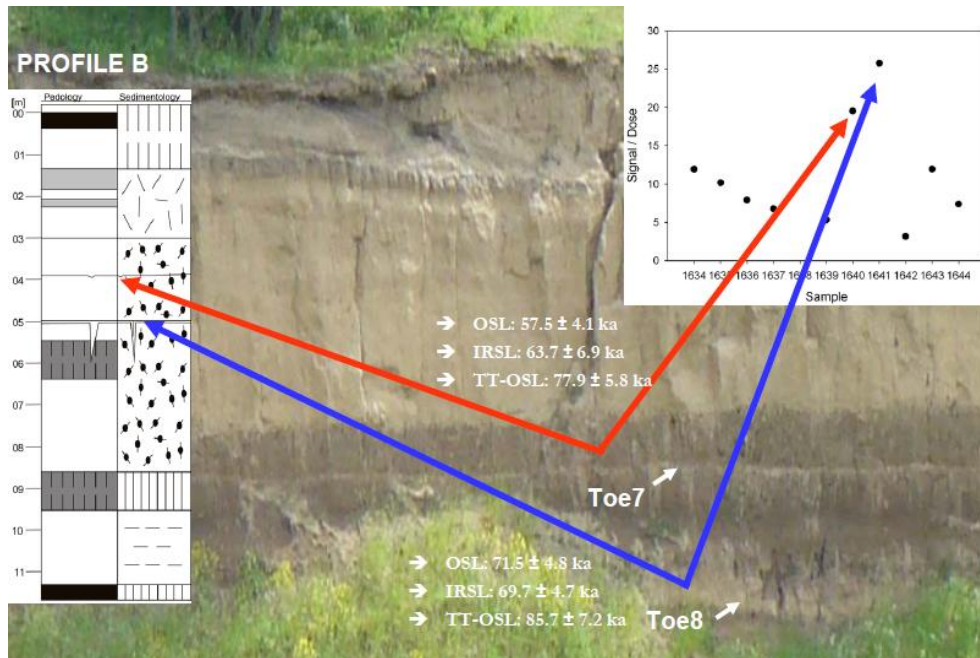


**Figure 4.11: Profile B.**

The equivalent doses  $D_e$  obtained using the pulsed post-IR IR signal from feldspar range from  $52.2 \pm 1.2$  Gy to  $645 \pm 63$  Gy, giving ages between  $17.1 \pm 1.1$  and  $189 \pm 16$  ka. For all samples the IRSL  $D_e$  values and ages increase with depths. The OSL ages obtained from fine-grain quartz are in good agreement back to  $\sim 70$  ka with the ages obtained from polymineral fine-grains using a pulsed post-IR IR measurement sequence. Sample Toe6 and Toe12 yield significantly lower  $D_e$  ( $\sim 250$  Gy) for the quartz OSL signal than for the pulsed post-IR IR signal ( $\sim 320$ -340 Gy), most likely owing to the lower saturation level of quartz. Many studies report systematically younger ages using the IRSL from feldspar (presumably because of anomalous fading). As discussed above, we cannot detect fading in these samples using the

pulsed post-IR IR signal from polymineral fine-grains. All TT-OSL ages are significantly larger than the OSL and IRSL ages, as well as the expected age. For sample Toe7 and Toe8 the difference between the methods is not so large as for the other samples – the TT-OSL age overestimates the OSL and IRSL age by about 20% whereas sample Toe5, Toe9 and Toe13 overestimate by almost twice the amount obtained from OSL/IRSL. This overestimation may be caused by significant residuals arising from insufficient bleaching during transport. The OSL and IRSL ages are in good agreement with each other, and are consistent with the stratigraphy – we regard these results as reliable age estimates.

#### ***4.5.2. Weichselian deposits***

The loess-palaesol sequence at the Tönchesberg section provides a relatively detailed terrestrial record of climate and environmental change for the penultimate and last glacial cycle. Previous studies presented detailed sedimentological, pedological, archeological, palaeomagnetic, mineralogical and chronological investigations on the loess deposits from this section (Becker et. al., 1989, Bogaard and Schmincke, 1990, Conard, 1992, Frechen 1991, 1994, Reinders and Hambach, 1995, Boenigk and Frechen, 1999, 2001). The geochronological framework has been based on paleomagnetic measurements, preliminary  $^{40}\text{Ar}/^{39}\text{Ar}$ -laser-single grain dating (of the basanitic Tönchesberg scoria and two air-fall tephra from the nearby Korrettsberg and Plaidter Hummerich volcano), and thermoluminescence (TL) and infrared stimulated luminescence (IRSL) dating. Our study presents the first optically stimulated luminescence (OSL) dating results from fine-grained quartz and thermally transferred optically stimulated luminescence (TT-OSL); it also presents ages based on a new infrared stimulated luminescence (IRSL) signal which has been shown to fade at a very much lower rate than the conventional IRSL signal. In all cases, the TT-OSL ages overestimate the OSL and IRSL ages; the latter are in good agreement back to ~70 ka and since OSL ages from quartz are generally regarded as precise and accurate, our interpretation is based on the latter two methods.

A strong brown soil was developed above the Upper Weichselian loess – indicating a rather warm climate during the Allerød interstadial (age deduced from the presence of the pumice of the Laacher See eruption;  $^{40}\text{Ar}/^{39}\text{Ar}$  age estimated as 12.9 ka; Bogaard and Schmincke, 1985). The luminescence ages from the homogenous loess deposits of the Upper Weichselian are all about 17 to 18 ka, indicating deposition during marine isotope stage 2

(MIS) and suggesting that this loess unit is not complete; an erosion event at ~17 ka is implied, as the ages do not increase with depth – according to Boenigk and Frechen (2001) a major erosion interval around 17 ka is typical for many loess sections in the Middle Rhine area. Frechen (1994) and Boenigk and Frechen (1999) provide IRSL estimates of ~13 ka and TL age estimates of ~15-18 ka. Their IRSL ages underestimate both their TL ages and our OSL and IRSL ages, most likely as a result of anomalous fading. Below the Upper Weichselian loess unit, reworked loess sediments with two intercalated weakly developed brown soils are observed. The loess between the soils yield age estimates of  $29.9 \pm 2.1$  and  $30.3 \pm 2.8$  ka; the loess unit below the lower soil gave age estimates of  $53.8 \pm 4.2$  and  $53.3 \pm 3.6$  ka indicating that the lower soil is younger than ~53 ka and that these soils represent warm intervals during MIS 3. This soil is correlated to the Lohne soil (Lohner Boden), which corresponds to the Stillfried-B complex in Austria. The early Middle glacial exhibits a number of warm intervals during MIS 3 in the north-west European pollen record (Behre, 1989), at La Grande Pile (Woillard & Mook, 1982) and Moershoft in the Netherlands (Zagwijn, 1996). Frechen (1991, 1994); Boenigk and Frechen (1999) provide IRSL and TL ages ranging from 50 to 33 ka for these deposits and correlated the two palaeosols with the Hengelo (39-36 ka) and Denekamp (32-28 ka) interstadials of the Middle Weichselian (Ran and van Huisteden, 1990).

Reworked humic-rich sediments with intercalated weak humic soils and pellet sands are deposited underneath the reworked loess. Above the pellet sands and below the humic-rich sediments a thin loess band of about 5 cm gives luminescence ages ranging from  $57.5 \pm 4.1$  to  $63.7 \pm 4.5$  ka. Below this reworked humic-rich sediment, there is ~20 cm of loess with many soil veins. Luminescence ages of  $69.7 \pm 4.7$  and  $71.5 \pm 4.8$  ka indicate a deposition during the end of MIS 5a / beginning of MIS 4. TT-OSL ages are similar to these OSL and IRSL ages, this agreement was only observed for the loess of the two marker horizons (sample Toe 7 and Toe 8). These samples show different luminescence characteristics compared to the other samples which could suggest that the loess originated from different sources. While the loess deposits from the nearby Rhine area showed a weak TT-OSL signal combined with high residuals suggesting insufficient bleaching during the short transport, the loess from the marker horizons (samples Toe7 and 8) yields a signal up to 10 times stronger with much smaller residuals, suggesting well bleached mineral grains after a long transport (Fig. 11), i.e. a distal source, different from the other loess horizons. These loess bands were designated as marker loess by Becker et al. (1989); they correlated them with the Czech loess stratigraphy. Kukla and Koci (1972) described these marker loess layers in Bohemia and Moravia where

they were found as thin bands of silt separating humus-rich steppe soils from pellet sands (pedocomplex PKII - Kukla and Koci, 1972). These markers were thought to have been deposited around 72 ka at the MIS 5/4 boundary (consistent with our chronology). Kukla and Koci (1972) interpreted them as deposits from long-distance dust storms indicating the abrupt end of the interstadial and the first strong cold event of this glacial cycle. Rousseau et al. (1998) also described a thin loess band in Achenheim (France) and assumed that this marker loess originated from a dust storm of a continental-scale which was deposited at the time of strong dust peaks observed in the GRIP ice-core at around 72 ka. A marker loess has also been described from the loess section at Koblenz-Metternich (Middle Rhine valley) (Boenigk and Frechen, 2001). Our results support the assumption that these deposits origin from a European wide duststorm with a long distance transport and hence more complete bleaching of the TT-OSL signal. The luminescence ages are in good agreement with the TL age estimates of 60-70 ka of Boenigk and Frechen (2001) for this horizon. A truncated humic-rich A horizon is present underneath the reworked humic-rich sediment. A reverse magnetisation, correlated with the Blake event (~117 ka) was recognized in this pedosediment (Becker et al., 1989, Reinders and Hambach, 1995) indicating the two A-horizons formed during MIS 5c. This A horizon is underlain by reworked loess and loess. This layer of reworked loess (Schwemmloess) is deposited on top of the last interglacial soil and yields age estimates ranging from  $83.7 \pm 5.7$  to  $115 \pm 9$ . The OSL age estimates tend to underestimate the post-IR IRSL ages, probably because quartz OSL is very close to, or in, saturation – hence we base our interpretation only on the IRSL ages ranging from  $110 \pm 8$  to  $115 \pm 9$  indicating accumulation during MIS 5d. The ages do not increase with depth. This most likely suggests that the loess accumulated in a relatively short period which cannot be resolved by luminescence dating. Frechen (1994) made the same observation – he presents TL age estimates of ~100-112 ka; in good agreement with our IRSL ages and also with the TL age estimate of  $114 \pm 9$  ka given by Zöller et al. (1991).

#### ***4.5.3. Saalian deposits***

The volcanic debris at the Tönchesberg section is covered by more than 15 m of penultimate glacial loess and reworked loess. This penultimate glacial loess beneath the Eemian soil is intercalated by tephra layers from the nearby Korrettsberg and Plaidter Hummerich volcanoes, as well as by a “tephritic tephra”. Weak tundra or frost gleys are



intercalated in the loess; these are typical of the upper part of the Saalian loess in Middle Europe. So far no reliable numeric dating has been undertaken on the penultimate glacial deposits. The TL ages of Frechen (1991) for the Upper Saalian loess deposits range from  $118 \pm 9$  and  $104 \pm 11$  ka, but do not increase with depth. Frechen (1994) assumed an accumulation during the Upper Saalian for the loess deposits underneath the Eemian soil – but his TL ages do not support this. Zöller et al. (1991) provides TL ages ranging from  $129 \pm 12$  and  $121 \pm 11$  ka. The ages of both studies are probably underestimated – most likely because of anomalous fading. Underneath the Eemian soil there is about 6 m of reworked layered loess sediments. Below these sediments the “tephritic tephra” is intercalated by about 2.5 m of reworked loess in the profile under study. These loess deposits between the “tephritic tephra” yield an IRSL age estimate of  $146 \pm 10$  ka indicating deposition during MIS 6 and an origin for the “tephritic tephra” in a volcano which erupted around ~140-150 ka. Sample Toe9 was taken directly below the tephra from the loess and reworked loess and give an age of  $160 \pm 15$  ka. Approximately 5 m below the tephra, a weakly developed palaeosol is intercalated – sample Toe16 was taken directly above the soil from the loess deposits and yields an IRSL age of  $168 \pm 12$  ka pointing also to accumulation during MIS 6. As the age estimates for these loess and reworked loess sediments do not increase with depth, it is assumed that accumulation occurred over a relatively short period which cannot be resolved by luminescence dating. Underneath this loess the tephras from the Plaitder Hummerich volcano (preliminary  $^{40}\text{Ar}/^{39}\text{Ar}$ -laser-single grain dating of  $238 \pm 20$  ka, but this age estimate is overestimated according to van den Bogaard and Schmincke, in Kröger (1995) and Korrettsberg volcano (preliminary  $^{40}\text{Ar}/^{39}\text{Ar}$ -laser-single grain dating of  $243 \pm 65$  ka (van den Boogard and Schmincke, 1990)) were deposited intercalated by a soil formation (Fig. 12); charcoal was found in this palaeosol. Below the tephra of the Korrettsberg volcano, ~90 cm thick loess-like layer was superimposed by weak soil formation with charcoal; sample Toe14 and charcoal was collected from this palaeosol.

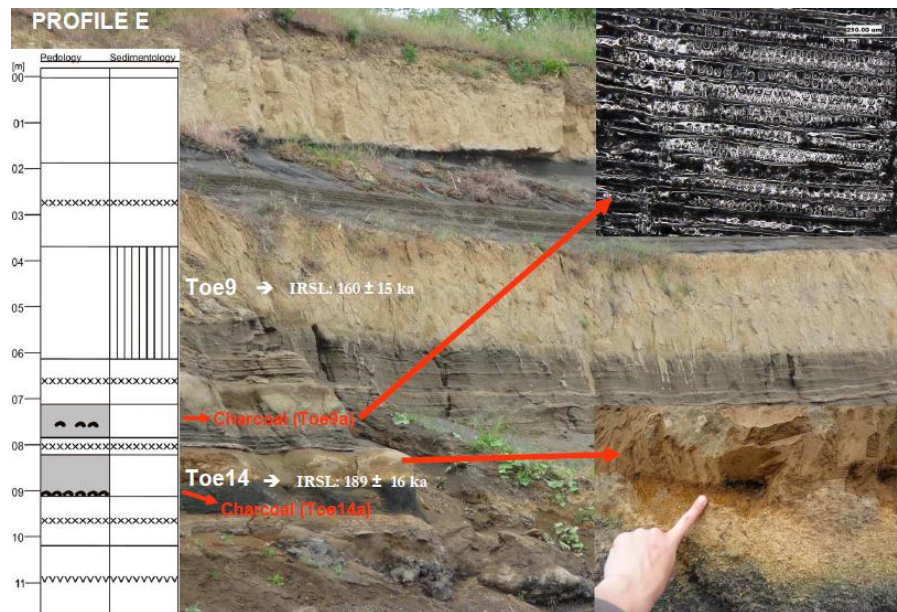


**Figure 4.12: Profile E.**

An IRSL age of  $189 \pm 16$  ka was determined for these deposits indicating soil formation in the late phase of MIS 7. Charcoal collected from the two weak palaeosols developed in Saalian loess, profile E (Figs. 2, 12, 13 and 14), were dendrologically analysed and identified. From the soil between the tephras of the Plaidter Hummerich and Korrettsberg (Toe9, IRSL:  $160 \pm 15$  ka) larger and well preserved pieces up to 2 cm diameter could be picked out. The annual growth rings showed only a slight bend (Fig. 14, a) which gives evidence that the pieces are from a larger tree.

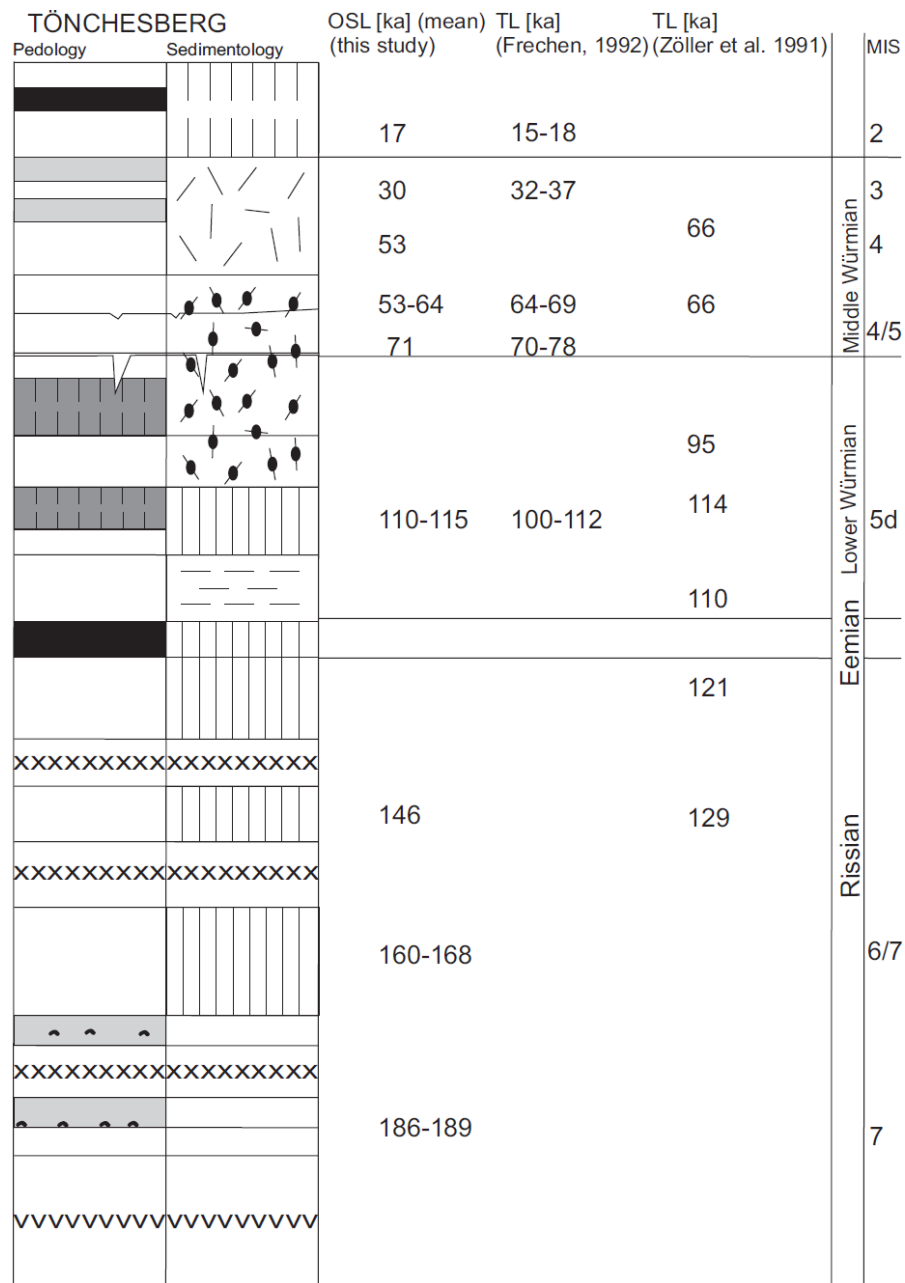
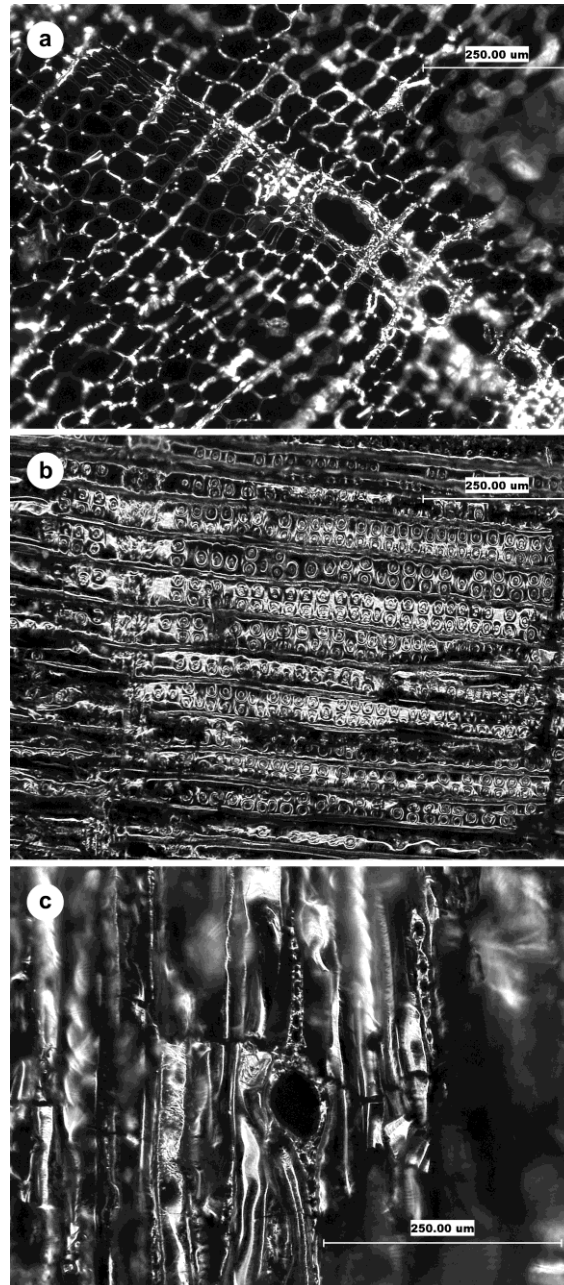


Figure 4.13: Idealized profile of the Tönchesberg section.

The simple structure without vessels (only tracheids) are characteristic for coniferous wood. Vertical and radial resin canals (Fig. 14, a and c) exclude fir (*Abies*) and numerous small pits in the radial rays (Fig. 14, b) pine (*Pinus*). The sharp transition to the latewood (Fig. 14, a) and the regularly present two-rowed bordered pits within the tracheids (Fig. 14, b) allow the distinction from spruce (*Picea*) and identification as larch (*Larix*). Larch is today a typical tree at the alpine and northern treeline and can be found during forested interstadials and sometimes at the end or beginning of interglacials (e.g. Behre, 1989, Bittmann, 1992; Welten, 1982, 1988, re-interpreted in Preusser et al. 2005). Small, badly preserved and fragile charcoal pieces from the soil below the Korretsberg-tephra (Toe14, IRSL:  $189 \pm 16$  ka) could

be also identified as coniferous wood and are from pine (*Pinus* sp., *P. sylvestris*-type). The identifications imply that both palesols were formed at least under interstadial conditions which allowed the growing of trees (if not brought to the site by Palaeolithic people).



**Figure 4.14: Charcoal of larch (*Larix*), a – cross section with vertical resin canals, sharp transition to the latewood and the boundary of an annual growth ring, b – radial section showing two-rowed bordered pits, c – tangential section with a radial resin canal within a ray.**

Whether this taxa could survive stadial conditions at sheltered places (like the crater) is a matter for debate, although soil formation processes also speak in favour of improved climatic conditions. It remains uncertain to which interstadials the palaeosols correlate and if these

were formed before the first ice advance of the Saalian glacial or between the Saalian ice advances (Drenthe/Warthe stages). Currently there are no forested interstadials proven for the latter in northern and middle Europe. In Profile C these weak soil formations are not exposed. Sample Toe13 was taken from the loess-like sediments above the Tönchesberg scoria and yields an IRSL age estimate of  $186 \pm 22$  ka. At the base of the profile, scoria of the Tönchesberg volcano (preliminary  $^{40}\text{Ar}/^{39}\text{Ar}$ -laser-single grain age of  $202 \pm 14$  ka) are exposed. This age is in good agreement with our IRSL age estimates for the deposits directly above the scoria. According to Frechen (1994) this  $^{40}\text{Ar}/^{39}\text{Ar}$  age may be overestimated, because there is no obvious evidence for interglacial or interstadial conditions directly above the Tönchesberg scoria. He assumed an eruption during a cold period. The first sediments we found above the scoria (Profile E) were loessic sediments, also indicating that glacial conditions prevailed during the eruption.

#### **4.6. Conclusion**

In our study we have applied optically stimulated luminescence (OSL), thermally transferred optically stimulated luminescence (TT-OSL) and infrared stimulated luminescence (IRSL) (i) to test the suitability and reliability of different luminescence dating methods on loess and loess derivatives of the past 200 ka and (ii) to establish a reliable chronostratigraphical framework for the penultimate and last interglacial-glacial cycle of the sediment succession at the Tönchesberg section. Performance tests such as preheat-plateau, dose recovery and residual checks were carried out to confirm the suitability of our SAR protocols. The fine-grained quartz OSL and polymineral post-IR IRSL ages are in good agreement with each other, and with the geologically expected ages, back to ~70 ka. In contrast, the TT-OSL ages are overestimated. The TT-OSL luminescence characteristics of the samples are different; the loess deposits from the nearby Rhine area gave a weak signal with large residuals, the loess from the marker horizons yield a signal up to 10 times stronger, with much smaller residuals, indicating that the loess from the Tönchesberg section originates from different sources. OSL and post-IR IRSL ages ranged from  $16.8 \pm 1.2$  to  $189 \pm 16$  ka. These ages indicate that the youngest loess and the weakly developed soils were deposited during marine isotope stage (MIS) 2 and 3, respectively, and that the two marker loess most likely accumulated in the transition of MIS 4/5. This reworked loess yields ages of ~110-115 ka correlating to MIS 5d. The weakly developed soil intercalated in the penultimate glacial

loess deposits is attributed to the transition MIS 6/7. The weakly developed soil above the Tönchesberg scoria yields an age of  $189 \pm 16$  ka indicating an interstadial soil formation during MIS 7. This is in good agreement with the preliminary  $^{40}\text{Ar}/^{39}\text{Ar}$ -age for the Tönchesberg scoria. Our results show that reliable age estimates up to  $\sim 70$  ka could be obtained using quartz OSL and up to  $\sim 200$  ka using the pulsed post-IR IR signal from feldspar.

## Acknowledgements

This research is part of a PhD study in the frame of the “Leibniz Pakt für Forschung und Innovation” at the LIAG-Institute in Hannover. Pierre Antoine is thanked for the useful comments on the manuscript.

## References

- Adamic, M., Aitken, M.J., 1998. Dose-rate conversion factors: update. *Ancient TL* 16, 37-50.
- Aitken, M.J. 1985. *Thermoluminescence Dating*, London.
- Antoine, P., Rousseau, D.D., Kunesch, S., Hatté, C., Lang, A., Zöller, L., Moine, O., 2009. Evidence of rapid and cyclic eolian deposition during the Last Glacial in European loess series (Loess Events): the high-resolution records from Nussloch (Germany). *Quaternary Science Reviews*, 28, 2955-2973.
- Becker, U., Boenigk, W., Hentzsch, B. 1989. Reverse Magnetisierung in den frühWeichselzeitlichen Deckschichten am Tönchesberg/Osteifel. *Mainzer Naturw. Archiv*, 27, 1-22.
- Behre, K.-E., 1989. Biostratigraphy of the last glacial period in Europe. *Quaternary Science Reviews*, 8, 25-44.
- Bibus, E., 1974. Abtragungs- und Bodenbildungsphasen im Rißlöß. *Eiszeitalter und Gegenwart*, 25, 166-182.

- Bittmann, F., 1992. The Kärlich Interglacial, Middle Rhine region, Germany: vegetation history and stratigraphic position. *Vegetation History and Archaeobotany*, 1, 243-258.
- Blair, M.W., Yuhikara, E.G., McKeever, S.W.S., 2005. Experiences with single-aliquot OSL procedures using coarse-grain feldspars. *Radiation Measurements*, 39, 361–374.
- Boenigk, W., Frechen, M., 1998. Zur Geologie der Deckschichten von Kärlich/Mittelrhein. *Eiszeitalter und Gegenwart*, 48, 38-49.
- Boenigk, W., Frechen, M., 1999. Klimaschwankungen im Frühweichsel der Lößabfolgen des Mittelrheingebietes. *Eiszeitalter und Gegenwart*, 49, 124-131.
- Boenigk, W., Frechen, M., 2001. The loess record in sections at Koblenz-Metternich and Tönchesberg in the Middle Rhine area. *Quaternary International*, 76/77, 201-209.
- Bøtter-Jensen, L., Bulur, E., Duller, G.A.T., Murray A.S., 2000. Advances in luminescence instrument systems. *Radiation Measurements*, 32, 523-528.
- Buylaert, J.P., Vandenberghe, D., Murray, A.S., Huot, S., De Corte, F., Van den haute, P., 2007. Luminescence dating of old (>70 ka) Chinese loess: a comparison of single-aliquot OSL and IRSL techniques. *Quaternary Geochronology*, 2, 9-14.
- Buylaert, J.P., Murray, A.S., Thomson, K.J., Jain, M., 2009. Testing the potential of an elevated temperature IRSL signal from K-feldspar. *Radiation Measurements*, 44, 560-565.
- Bogaard, Van den, P., Schmincke, H.U., 1985. Laacher See Tephra: A widespread isochronous late Quaternary tephra layer in central and northern Europe. *Geological Society of American Bulletin*, 96, 1554-1571.
- Bogaard, Van den, P., Schmincke, H.U., 1990. Die Entwicklungsgeschichte des Mittelrheinraumes und die Eruptionsgeschichte des Osteifel-Vulkanfeldes. In: Schirmer, Wolfgang (Hrsg.): *Rheingeschichte zwischen Mosel und Maas. DEUQUA Führer*, 1, 166-190.

- Conard, N. J., 1992. Tönchesberg and its Position in the Paleolithic Prehistory of Northern Europe. *Römisch-Germanisches Zentralmuseum Monographien*, 20, 176p.
- Duller, G.A.T., 2003. Distinguishing quartz and feldspar in single grain luminescence measurements. *Radiation Measurement*, 37, 161-165.
- Frechen, M., 1991. Thermolumineszenz-Datierungen an Lössen des Mittelrheingebietes. *Sonderveröff. Geol. Inst. Univ. Köln*, 79, 1-137.
- Frechen, M., 1994. Thermolumineszenz-Datierungen an Lössen des Tönchesberges aus der Osteifel. *Eiszeitalter und Gegenwart*, 44, 79-93.
- Hentzsch, B., 1990. Die Lößdeckschichten am Tönchesberg (Osteifel). In: *Rheingeschichte zwischen Mosel und Maas*, Hrsg. W. Schirmer, DEUQUA-Führer 1, 42-46.
- Kröger K. 1995. Plaidter Hummerich: Ein Fundplatz aus der Zeit des Neandertalers im Krater eines erloschenen Vulkans. *Inaug.-Diss. Univ. Köln*: 138 p.
- Kukla, G.J., Koci, A., 1972. End of the last interglacial in the loess record. *Quarternary Research*, 2, 374-383.
- Murray, A.S. and Wintle, A.G., 2000. Luminescence dating of quartz using an improved single-aliquot regenerative-dose protocol. *Radiation Measurements*, 32, 57-73.
- Murray, A.S., Olley, J.M., 2002. Precision and accuracy in the optically stimulated luminescence dating of sedimentary quartz: a status review. *Geochronometria*, 21, 1-16.
- Murray, A.S. and Wintle, A.G., 2003. The single regenerative dose protocol: potential for improvements in reliability. *Radiation Measurements*, 37, 377-381.
- Murray, A.S., Buylaert, J.P., Thomson, K.J., Jain, M., 2009. The effect of preheating on the IRSL signal from feldspar. *Radiation Measurements*, 44, 554-559.



- Prescott, J.R., Hutton, J.T., 1994. Cosmic ray contribution to dose rates for luminescence and ESR dating: large depths and long-term time variations. *Radiation Measurements*, 23, 497–500.
- Prescott, J.R., Stephan, L.G. 1982. The contribution of cosmic radiation to the environmental dose for thermoluminescence dating. *PACT*, 6, 17–25.
- Porat, N., Duller, G.A.T., Roberts, H.M. & Wintle, A.G., 2009. A simplified SAR protocol for TT-OSL. *Radiation Measurements*, 44, 538-542.
- Preusser, F., Drescher-Schneider, R., Fiebig, M., Schlüchter, C., 2005. Re-interpretation of the Meikirch pollen record, Swiss Alpine Foreland, and implications for Middle Pleistocene chronostratigraphy. *Journal of Quaternary Science*, 20, 607-620.
- Ran, E.T.H., Huissteden, J. Van, 1990. The Dinkel valley in the Middle Pleniglacial: dynamics of a tundra river system. *Mededelingen Rijks Geologische Dienst*, 44, 209-220.
- Rees-Jones, J., 1995. Optical dating of young sediments using fine-grain quartz. *Ancient TL*, 13, 9-14.
- Reinders, J., Hambach, U., 1995. A geomagnetic event recorded in loess deposits of the Tönchesberg. *Geophysical Journal International*, 122, 407-418.
- Rousseau, D.-D., Kukla, G., Zöller L. & Hradilova, J., 1998. Early Weichselian dust storm layer at Achenheim in Alsace, France. *Boreas*, 27, 200-207.
- Schmidt, E.D., Machalett, B., Marković, S. B., Tsukamoto, S., Frechen, M., 2010. Luminescence chronology of the upper part of the Stari Slankamen loess sequence (Vojvodina, Serbia). *Quaternary Geochronology*, doi:10.1016/j.quageo.2009.09.006.
- Schmincke, H.-U., Park, C., Harms, E., 2000. Evolution and environmental impacts of the eruption of Laacher See Volcano (Germany) 12,900 a BP. *Quaternary International*, 61, 61-72.

- Thomsen, K.J., Murray, A.S., Jain, M., Bøtter-Jensen, L., 2008a. Laboratory fading rates of various luminescence signals from feldspar-rich sediment extracts. *Radiation Measurements*, 43, 1474-1486.
- Thomsen, K.J., Jain, M., Murray, A.S., Denby, P.M., Roy, N., Bøtter-Jensen, L., 2008b. Minimizing feldspar OSL contamination in quartz UV-OSL using pulsed blue stimulation. *Radiation Measurements*, 43, 752-757.
- Tsukamoto, S., Denby, P. M., Murray, A. S., and Bøtter-Jensen, L., 2006. Time-resolved pulsed luminescence from feldspars: new insight into fading. *Radiation Measurements*, 41, 790-795.
- Tsukamoto, S., Duller, G.A.T. and Wintle, A.G., 2008. Characteristics of thermally transferred optically stimulated luminescence (TT-OSL) in quartz and its potential for dating sediments. *Radiation Measurements*, 43, 1204-1218.
- Wang, X.L., Wintle, A.G., Lu, Y.C., 2006. Thermally transferred luminescence in fine-grained quartz from Chinese loess: Basic observations. *Radiation Measurement*, 41, 649-658.
- Wang, X.L., Wintle, A.G., Lu, Y.C., 2007. Testing a single-aliquot protocol for recuperated OSL dating. *Radiation Measurements*, 42, 380-391.
- Welten, M., 1982. Pollenanalytische Untersuchungen im Jüngeren Quartär des nördlichen Alpenvorlandes der Schweiz. *Beiträge zur Geologischen Karte der Schweiz–Neue Folge*, 156, 179 pp.
- Welten, M., 1988. Neue pollenanalytische Ergebnisse über das Jüngere Quartär des nördlichen Alpenvorlandes der Schweiz (Mittel- und Jungpleistozän). *Beiträge zur Geologischen Karte der Schweiz–Neue Folge*, 162, 40 pp.
- Wintle, A.G., 1973. Anomalous fading of thermoluminescence in mineral samples. *Nature*, 245, 143-144.

- Wintle, A.G, Murray, A.S. 2006. A review of quartz optically stimulated luminescence characteristics and their relevance in single-aliquot regeneration dating protocols. *Radiation Measurements*, 41, 369-391.
- Woillard, G.M., Mook, W.G., 1982. Carbon-14 Dates at Grande Pile: Correlation of Land and Sea Chronologies. *Science*, 215, 159-161.
- Zagwijn, W.H., 1996. An analysis of Eemian climate in western and central Europe. *Quaternary Sciences Reviews*, 15, 451–469.
- Zöller, L., Conard, N.J., Hahn, J.,1991. Thermoluminescence dating of Middle Palaeolithic open air sites in the middle Rhine valley/ Germany. *Naturwissenschaften*, 78, 408-410.

# Chapter 5

Submitted to Quaternary International.

## Elevated temperature IRSL dating of loess sections in the Eifel region of Germany

E.D. Schmidt<sup>1,2\*</sup>, A.S. Murray<sup>2</sup>, M. Frechen<sup>1</sup>, S. Tsukamoto<sup>1</sup>

<sup>1</sup>Leibniz Institute for Applied Geophysics (LIAG): Geochronology and Isotope Hydrology,  
Stilleweg 2, 30655 Hannover, Germany

<sup>2</sup>Nordic Laboratory for Luminescence Dating, Department of Earth Sciences, Aarhus University,  
Risø DTU, DK-4000 Roskilde, Denmark

\* Corresponding author: Esther.Schmidt@liag-hannover.de

### Abstract

Several studies showed that the infrared stimulated luminescence signals measured at elevated temperature after an IR stimulation at 50°C (post-IR IRSL) are significantly more stable than the conventional IRSL at 50°C (IR<sub>50</sub>). In this study a post-IR IRSL protocol using a second IR stimulation temperature of 290°C (pIRIR<sub>290</sub>) was applied to 17 polymineral fine grain (4-11 μm) samples from various loess sections in the Eifel region with independent age control to test the reliability of ages using the pIRIR<sub>290</sub> signal. The laboratory-measured fading rates are below 1%/decade on average for pIRIR<sub>290</sub>. Both IR<sub>50</sub> and pIRIR<sub>290</sub> signals of 9 samples were found to be in field saturation. The average ratio of the sensitivity-corrected natural signal to the laboratory saturation level for the pIRIR<sub>290</sub> is  $0.98 \pm 0.02$  (n=9), showing that field saturation is equal to laboratory saturation for the pIRIR<sub>290</sub> signal from polymineral fine grains from the Eifel region. Minimum equivalent dose estimates were calculated from the characteristic saturation dose of the dose response curves, giving minimum age estimates of ~230-420 ka suggesting that the pIRIR<sub>290</sub> signal can be used to date loess back to ~300 ka.

The age estimates of the samples from the Wannenköpfe and Dachsbusch sites are in good agreement with independent age control showing that the IRSL dating using pIRIR<sub>290</sub> signal without fading correction is apparently reliable. Our data suggest that the loess units E, F, G and the lower part of H at the Kärlich site were accumulated before 270 ka and that the palaeosol of the “Kärlich Interglazial” I most likely developed during MIS 9 or earlier. The palaeosol on the top of Loess bed II at the Ariendorf section can be correlated with a warm event of MIS 7.

**This manuscript is submitted to Quaternary International and will be online available at <http://www.sciencedirect.com/science/journal/10406182> after the successful reviewing process.**











































































# Chapter 6

Quaternary Science Journal, 2011 (60).

## IRSL Signals from Maar Lake Sediments Stimulated at Various Temperatures

E. D. Schmidt<sup>1,3\*</sup>, A.S. Murray<sup>2</sup>, F. Sirocko<sup>3</sup>, S. Tsukamoto<sup>1</sup>, M. Frechen<sup>1</sup>

<sup>1</sup>Leibniz Institute for Applied Geophysics (LIAG), Section 3: Geochronology and Isotope Hydrology, Stilleweg 2, 30655 Hannover, Germany

<sup>2</sup>Nordic Laboratory for Luminescence Dating, Department of Earth Sciences, Aarhus University, Risø DTU, DK-4000 Roskilde, Denmark

<sup>3</sup>University of Mainz/Germany, Institute for Geoscience

\* corresponding author: Esther.Schmidt@liag-hannover.de

### Abstract

Optically stimulated luminescence (OSL) and infrared stimulated luminescence (IRSL) have been measured from seven fine-grained samples from core JW3 from the dry maar of Jungfernweiher (West Eifel /Germany). Two different elevated temperature post-IR IRSL protocols in the blue detection were applied to polymineral fine grains (4-11  $\mu\text{m}$ ). These protocols involve stimulation with IR for up to 200s at 50°C prior to elevated temperature stimulation with IR for 100s at 225°C or 200s at 290°C. Quartz OSL saturates at doses of 260-300 Gy, and the  $D_e$  values obtained using IRSL at 50°C ( $IR_{50}$ ) do not increase with depth indicating that this signal is also in field saturation at ~500 Gy. However, the post-IR IRSL signals at 225°C ( $pIRIR_{225}$ ) and 290°C ( $pIRIR_{290}$ ) increase with depth from ~800 Gy to ~1400 Gy, suggesting a minimum (fading uncorrected) age of ~200 ka for the youngest sediments. Mean laboratory fading rates are  $4.09 \pm 0.02\%$ /decade for  $IR_{50}$  and  $2.55 \pm 0.14\%$ /decade for polymineral  $pIRIR_{225}$ . For sample JWS1 a g-value of  $0.52 \pm 1.12\%$ /decade for the  $pIRIR_{290}$  was obtained. Both fading corrected  $pIRIR_{225}$  and uncorrected  $pIRIR_{290}$   $D_e$

values from the youngest sample (~16 m below modern surface) indicate an age estimate of ~250 ka for the uppermost sample increasing up to ~400 ka for the oldest samples taken ~94 m below modern surface.

*Key words: luminescence dating, IRSL, OSL, fading, fine grain, maar lake, Jungfernweiher, ELSA*

## **6.1. Introduction**

Maars are volcanic craters caused by phreatomagmatic eruptions. Volcanic depressions and craters such as those of maar lakes form excellent sediment traps, and so can record past climatic and environmental changes. Sediments accumulating in maar lakes are often thought to have undergone continuous deposition since the eruption of the maar volcanoes, and hence may contain unique continuous local records of climate change. Aeolian dust (loess) can make up a large part of the sediment inventory, because the catchment surrounding the lake often only extends to the rim of the crater. Because of its more or less continuous supply during cold periods, loess is one of the most detailed and wide-spread terrestrial archives of climate and environment change. As a result it often provides information on local and regional environmental processes and conditions for the Middle and Late Pleistocene. The West Eifel volcanic field (Fig.1) contains dry maars, maar lakes, scoria cones and small stratovolcanoes.



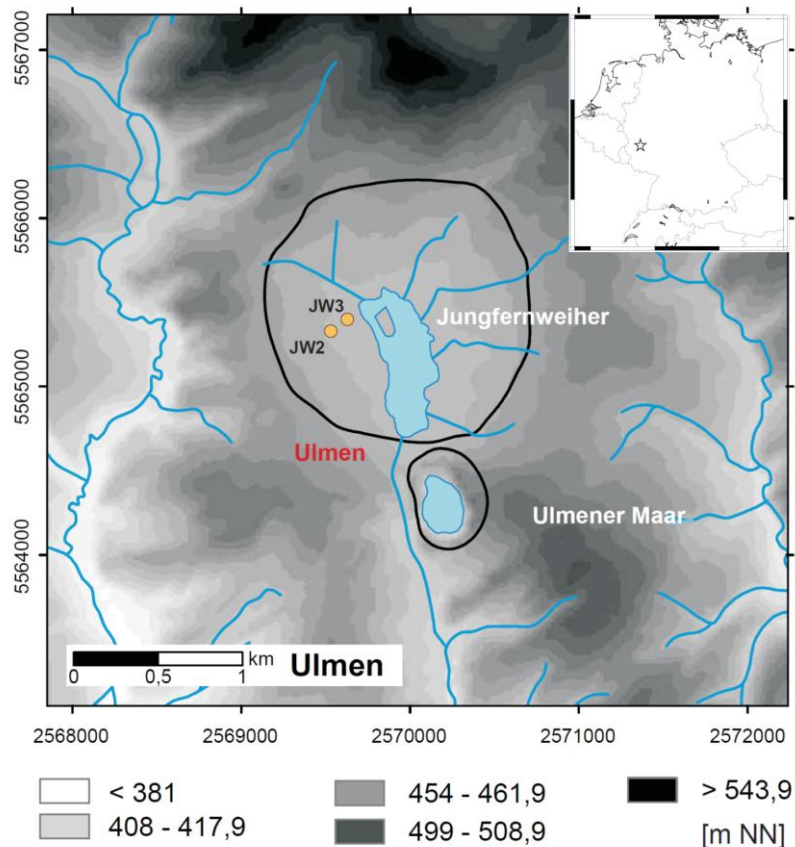


**Figure 6.1:** Map showing coring locations of the dry maar of Jungfernweiher, West Eifel Volcanic Field.

The Jungfernweiher is one of about 60 dry maars; with a diameter of 1500 m it is the biggest maar in the Eifel area. Nowadays there is a pond in the dry maar lake (Schaber & Sirocko, 2005). Sediment cores have been drilled within the framework of the ELSA project (Eifel Laminated Sediment Archive) in Eifel dry maar lakes (Sirocko et al. 2005), and samples for luminescence dating were taken from core JW3 and JW2 from the Jungfernweiher.

Luminescence dating is used to date the time that has passed since the last exposure of minerals (quartz or feldspar) to daylight (Aitken, 1998). Such minerals are able to store energy (as trapped electrons) within their crystal structure; this energy originates from ionising radiation (alpha, beta and gamma) from environmental radioactivity, and from cosmic rays. The trapped electrons can be stored for long periods at lattice defects in the crystal lattice. In the laboratory the grains are stimulated with light and the trapped electrons are released. During recombination they release their stored energy as light (luminescence). A measurement of this luminescence allows an estimation of the radiation dose (palaeodose or equivalent dose,  $D_e$ ) that the crystal has absorbed since the last exposure to daylight. The most important requirement is that the sediments are well bleached or zeroed at the time of

deposition due to a sufficient exposure to daylight. For loess it is expected that any residual trapped charge has been completely removed during the long aeolian transport. The optically stimulated luminescence (OSL) of quartz has been widely used to estimate the deposition age of sediments and is usually regarded as an accurate and precise dating method (e.g. Murray & Olley, 2002). However, the fast component of the quartz OSL signal (the component normally used for dating) saturates at doses of 200-400 Gy (WINTLE & MURRAY, 2006). This implies a quartz upper age limit of ~50-70 ka for loess deposits for a typical dose rate of between 3 and 4 Gy/ka (e.g. Frechen, 1992, Roberts, 2008, Schmidt et al., 2011).

In contrast, the infrared stimulated luminescence (IRSL) signals from feldspars grow to much higher doses than those from quartz, and this offers the possibility of significantly extending the age range. Several studies report the application of luminescence to limnic sediments (e.g. Degering & Krbetschek, 2007b), but infrared stimulated luminescence (IRSL) on maar sediments has only been used in a few studies (e.g. Lang & Zolitschka, 2001, Degering & Krbetschek, 2007a). Lang & Zolitschka (2001) obtained reliable IRSL ages only for clastic-rich horizons; IRSL ages of sediments with high concentrations of biogenic material were inaccurate. Degering & Krbetschek (2007a) provided two IRSL ages (multiple aliquot additive dose protocol, MAAD) from the Jungfernweiher.

Luminescence dating of feldspars tends to underestimate the age, because of anomalous fading (Wintle, 1973) caused by quantum-mechanical tunnelling (Visocekas, 1985). Feldspar dating is normally carried out using a 50° C IR stimulation with detection in the blue (-violet) spectrum. Many studies have shown that the IRSL ages without fading correction consistently underestimate quartz OSL ages (e.g. Schmidt et al., 2010) due to anomalous fading. Hence the fading rate (g-value; Aitken, 1985) has to be determined in the laboratory and the ages corrected for this effect. Several methods of age corrections have been proposed (e.g. Huntley & Lamothe, 2001; Lamothe et al., 2003) and many studies give corrected IRSL ages which are in good agreement with quartz OSL ages. However, there is no general consensus as to which correction method should be used and the most commonly adopted method is only valid for the 'linear part' of the dose response curve (Huntley & Lamothe, 2001). Clearly, if the fading rate could be reduced, feldspar dating would be more reliable. Thomsen et al. (2008) found out that stimulation at elevated temperatures significantly reduces the fading rate. Based on this study Buylaert et al. (2009) tested a SAR protocol with detection in the blue (320-460 nm); this involves a stimulation with IR for 100s at 50°C prior to an elevated temperature stimulation with IR for 100s at 225°C, a so called post-IR IRSL measurement

sequence. They have shown that the observed fading rates for the post-IR IRSL signal are significantly lower than those from the conventional IRSL at 50°C and that the signal is bleachable in nature. Thiel et al. (2011) extended this investigation following the observation of Murray et al. (2009) that the IR dosimetry trap lies above 320°C, and hence preheat temperatures up to this temperature can be used. In their study they chose a preheat of 320°C (60s) and a stimulation temperature of 290°C (200s) for the post-IR IR signal. They found natural signals from a sample below the Brunhes/Matuyama boundary in saturation on a laboratory growth curve and they concluded that they were unable to detect fading in this field sample.

The aim of this study is to investigate the applicability of luminescence dating using maar sediments, and ultimately to determine the accumulation rate of sediments within the archive and temporal succession of dust storms. The different IRSL signals are compared and discussed in regard to their performance in SAR; the equivalent doses ( $D_e$ ) the fading rates are then determined and ages calculated. The IRSL signal measured at 50°C and the subsequent post-IR IRSL signals measured at 225°C and 290°C are hereafter referred to as IR<sub>50</sub>, pIRIR<sub>225</sub> and pIRIR<sub>290</sub> respectively. The results are discussed in terms of continuity of sedimentation and sedimentation rates.

## 6.2. Geological setting

The West Eifel volcanic field/Germany with an aerial extension of 600 km<sup>2</sup> is aligned NW-SE from Ormont to Bad Bertrich in the Rhineland Palatinate, i.e. west of the river Rhine. Volcanism in the West Eifel Area started ca. 700 ka ago producing 250 eruptive centers with more than 50 maars, of which 8 are still filled with water (Büchel, 1984, Negendank & Zolitschka, 1993).

Sediment cores have been drilled by the ELSA project (Eifel Laminated Sediment Archive) in Eifel dry maar lakes to reconstruct the palaeoclimatic and palaeoenvironmental conditions as well as the history of the volcanism in the Eifel/Central Europe during the last glacial cycles. Two drillings (JW2 and JW3) have been carried out at the Jungfernweiher. JW3 was drilled close to center of the maar and exhibits a more undisturbed sedimentation and a better core quality than core JW2 which is located closer to the edge of the maar (Schaber & Sirocko, 2005). Seven samples for luminescence dating were taken from core JW3. According to Schaber & Sirocko (2005) coversand and loess layers were accumulated

during high-glacial conditions and during cold phases rhythmic stratification of clay and silt was dominating. All samples were taken from a glacial cycle with mainly silt lamination. Additionally, one sample was taken from the drill core JW2. The sampled material consists of loessic gyttja with intercalated small bands of coarser silty to sandy material, which is supposed to originate from dust storms. Some independent age control is provided by 16 radiocarbon age estimates. However, the uncalibrated ages range from  $35 \pm 2$  ka to  $56 \pm 4$  ka and do not increase with depth. A study carried out by Lenaz et al. (2010) presents mineralogical data from core JW3 suggesting that the tephra layer at a depth of 107.39 m could be correlated with the Rocourt Tephra which has an age range between 90.3 and 74 ka (Poucllet et al., 2008). Luminescence dating was carried out by Degering & Krbetschek (2007a) on two samples with a depth of 104.5 m and 122.5 m from core JW2. They applied a multiple aliquot additive dose (MAAD) protocol on the polymineral fine-grain fraction and could not detect anomalous fading for their samples. They obtained equivalent doses ( $D_e$ ) of  $441 \pm 49$  Gy and  $517 \pm 62$  Gy and calculated ages of  $98 \pm 15$  ka and  $117 \pm 18$  ka.

### 6.3. Experimental details

Samples were extracted under subdued red light and pretreated with 10% hydrochloric acid to remove carbonates, sodium oxalate to dissolve aggregates and 30% hydrogen peroxide to remove organic matter. The 4-11  $\mu\text{m}$  silt fraction was separated and divided into two parts: (i) an untreated fraction used for polymineral infrared stimulated luminescence (IRSL) measurements, and (ii) a fraction from which quartz grains were extracted. The latter polymineral fraction was treated with 34% fluorosilicic acid ( $\text{H}_2\text{SiF}_6$ ) for 6 days, preferentially dissolving feldspar grains, and leaving behind a quartz-rich extract. Finally, samples were prepared for measurement by settling either the polymineral or the quartz grains (4-11  $\mu\text{m}$ ) from acetone onto aluminium discs. The purity of the quartz extract was checked using the IR depletion ratio (Duller, 2003). All OSL/IRSL measurements were performed using an automated Risø TL/OSL-DA20 equipped with a  $^{90}\text{Sr}/^{90}\text{Y}$  beta source. Quartz blue-stimulated OSL was measured for 40 s at  $125^\circ\text{C}$  and the signals were detected through 7.5 mm of Hoya U-340 filter (passing from 260 to 390 nm, i.e. UV). Feldspar IRSL was detected through Schott BG-39 and Corning 7-59 filters (passing from 320 to 460 nm; i.e. blue). For measurement of the equivalent dose ( $D_e$ ) of quartz fine-grains a conventional SAR protocol (Murray & Wintle, 2000) was applied. The signal was integrated over the initial 1 s of

stimulation, and a background based on the last 5 s of simulation subtracted.  $D_e$  estimates from polymineral fine-grains were determined using a post-IR elevated-temperature IR SAR protocol.

Radionuclide concentrations for all samples were obtained using high-resolution gamma spectrometry of sediment collected from the immediate surrounding of the samples. A water content of  $20 \pm 5$  % was estimated for all samples. To derive the effective alpha dose rate, mean  $a$ -values of  $0.04 \pm 0.02$  for quartz OSL and of  $0.08 \pm 0.02$  for polymineral IRSL were assumed (Rees-Jones, 1995). The uranium, thorium, potassium contents and the dose rate of the samples are summarised in Table 1. The concentrations of uranium, thorium and potassium were converted into infinite-matrix dose rates using the conversion factors of Adamiec & Aitken (1998) and water-content attenuation factors (Aitken, 1985). Estimation of the cosmic-ray dose rate was calculated according to Prescott & Stephan (1982) and Prescott & Hutton (1994) from a knowledge of burial depth, altitude, matrix density, latitude and longitude for each sample. The uranium, thorium, potassium content and total dose rates are shown in Table 1. The mean dose rate is  $3.61 \pm 0.15$  Gy/ka for quartz and  $4.01 \pm 0.15$  Gy/ka for polymineral samples.

Sample	Uranium (ppm)	Thorium (ppm)	Potassium (%)	IRSL dose rate (Gy/ka)	OSL dose rate (Gy/ka)
JWS1	$2.78 \pm 0.04$	$13.33 \pm 0.10$	$2.49 \pm 0.02$	$4.25 \pm 0.21$	$3.85 \pm 0.21$
JWT3	$2.90 \pm 0.04$	$14.22 \pm 0.12$	$2.59 \pm 0.03$	$4.44 \pm 0.21$	$4.02 \pm 0.22$
JWT9	$2.85 \pm 0.04$	$14.56 \pm 0.04$	$2.76 \pm 0.03$	$4.60 \pm 0.23$	$4.18 \pm 0.23$
JWT5	$3.03 \pm 0.04$	$11.85 \pm 0.09$	$1.91 \pm 0.02$	$3.70 \pm 0.19$	$3.31 \pm 0.19$
JWT7	$2.67 \pm 0.04$	$11.59 \pm 0.10$	$1.81 \pm 0.02$	$3.96 \pm 0.20$	$3.65 \pm 0.20$
JWS8	$3.43 \pm 0.05$	$11.81 \pm 0.12$	$1.55 \pm 0.03$	$3.51 \pm 0.18$	$3.09 \pm 0.18$
JWT8	$3.21 \pm 0.04$	$11.55 \pm 0.10$	$1.74 \pm 0.02$	$3.58 \pm 0.18$	$3.18 \pm 0.18$
JWT9	$3.17 \pm 0.05$	$13.27 \pm 0.08$	$2.22 \pm 0.02$	$4.04 \pm 0.21$	$3.67 \pm 0.21$

**Table 6.1:** Dose rate data from potassium, uranium and thorium content, as measured by gamma spectrometry.

## 6.4. Luminescence dating

### 6.4.1. OSL dating of quartz

To test the suitability of the SAR protocol to the samples from the Jungfernweiher, and to confirm the most appropriate preheat temperature, the dose recovery ratio (Murray & Wintle,

2003) was determined for preheat temperatures between 200 and 260°C for 10 s following all natural and regeneration doses, and 200°C for 1 s following all test doses, using sample JWS 1. The aliquots were first bleached twice with 1000s blue stimulation at room temperature separated by a 5000s pause to allow the decay of any charge transferred to the 110°C TL trap, before giving a dose approximately equal to the natural dose. This dose was then measured in the same manner as if measuring the equivalent dose to provide confirmation that the protocol is able to recover a known dose successfully. If the SAR protocol is appropriate for our samples, the measured to given dose ratio should be close to unity. The measured dose/given dose ratio is close to unity for preheat temperatures of 220°C and 240°C ( $0.99 \pm 0.01$ ). We chose a preheat temperature of 240°C for our measurements. Fig. 2 shows the dose response curve for sample JWS1. This curve is representative for all measured samples. Fine-grain equivalent doses ( $D_e$ ) were measured for samples JWS1, JWT3 and JWT7 and range from  $440 \pm 30$  Gy to  $580 \pm 40$  Gy (Table 3); the  $D_0$ -values for all samples are about ~130-150 Gy, when the dose response curve is fitted to a single saturating exponential plus linear function,

$$I = I_{\max} (1 - \exp(-D/D_0)) + kD, \quad (1)$$

where  $I$  is the sensitivity corrected OSL intensity,  $I_{\max}$  is saturation intensity of OSL,  $D$  is dose, and  $D_0$  is the characteristic saturation dose.

Wintle & Murray (2006) suggested equivalent dose ( $D_e$ ) values should only be reported up to  $\sim 2D_0$ . In our case it should therefore be possible to measure doses up to about ~260-300 Gy using our material, although the laboratory-generated dose response curves continue to grow up to  $\sim 1000$  Gy, because of a more slowly saturating component which is expressed by the linear term in equation 1. Buylaert et al. (2007), Timar et al. (2010) and Lowick et al. (2010a,b) made similar observation for their fine-grain quartz samples and concluded that equivalent doses larger than  $2D_0$  (~120-140 Gy) were not very reliable. At doses higher than this value they observed an increasing age underestimation towards the Eemian. The samples described by Lowick et al. (2010b) passed all standard performance criteria and still show an increasing dose response curve at 500 Gy. Taking all these observations into account, we consider our quartz fine-grain equivalent doses to be in or close to saturation, and conclude that they provide a minimum dose estimate of ~450 Gy for the youngest sample.

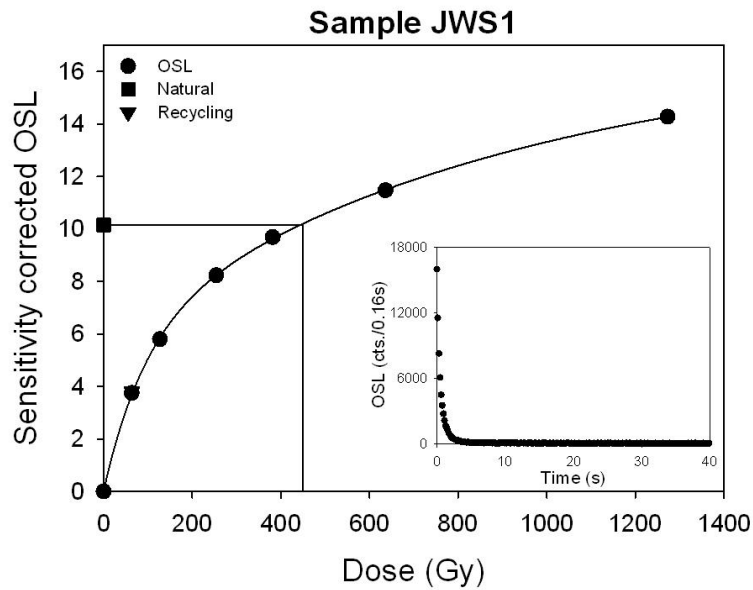


Figure 6.2: Dose response and decay curve for sample JWS1 showing the OSL from fine grain quartz.

## 6.4.2. IRSL dating of polymineral fine-grains

### 6.4.2.1. Post-IR IRSL measurement sequence

Based on the work of Thomsen et al. (2008), Buylaert et al. (2009) proposed a new SAR protocol, with detection in the blue (320–460 nm). This protocol involved elevated temperature stimulation with IR for 100 s at 225°C (pIRIR<sub>225</sub>), following stimulation with IR for 100 s at 50°C, a so-called post-IR IRSL measurement sequence (Table 2), and these authors chose a preheat of 250°C to make their results comparable to other studies. Recently Thiel et al. (2011) used a preheat of 320°C for 60 s for their post-IR IRSL protocol and used a stimulation at 290°C for 200 s after bleaching the aliquots with IR diodes at 50°C for 200 s to date polymineral fine-grains. Buylaert et al. (2009) showed that the observed fading rates for their post-IR IRSL signal (stimulated at 225°C) were significantly lower than from the conventional IR<sub>50</sub> and that the signal is bleachable in nature. Thiel et al. (2011) reported natural signals in saturation on the laboratory growth curve and concluded that fading is negligible for their samples.

Step	Treatment	Observed
1	Dose	
2	Preheat, 60s at 250°C / 60s at 320°C	
3	IR stimulation, 100s at 50°C / 200s at 50°C	Lx
4	IR stimulation, 100s at 225°C / 200s at 290°C	<b>Lx</b>
5	Test dose	
6	Preheat, 60s at 250°C / 60s at 320°C	
7	IR stimulation, 100s at 50°C / 200s at 50°C	Tx
8	IR stimulation, 100s at 225°C / 200s at 290°C	<b>Tx</b>
9	IR stimulation, 40s at 290°C / 40s at 325°C	
10	Return to step 1	

**Table 6.2: Elevated temperature post-IR IRSL measurement sequence.**

In this study, the pIRIR<sub>225</sub> protocol is applied to polymineral fine-grains from the Jungfernweiher, and in addition the pIRIR<sub>290</sub> is measured for two samples. The initial 2 s of the post-IR IR signal are used for calculating the D<sub>e</sub> values, with a background based on the signal observed in the last 10 s of the decay curve. To test for anomalous fading and to compare the fading rates of the IR<sub>50</sub>, the pIRIR<sub>225</sub> and the pIRIR<sub>290</sub>, those aliquots which had been used for D<sub>e</sub> measurement were then used to test for fading, by dosing and preheating the aliquots and then storing for various delays after irradiation and before measurement. This sequence was repeated several times on each aliquot. The fading rates are expressed in terms of the percentage decrease of intensity per decade of time (g-value; Aitken, 1985; Auclair et al., 2003). G-values were calculated according to Huntley & Lamothe (2001) using the signal integration limits as for the D<sub>e</sub> calculation. Fading corrections use the methods proposed in Huntley & Lamothe (2001); it is recognised that this method is strictly applicable only for natural doses in the linear region of the growth curve, although Buylaert et al. (2008; 2009; in press) have shown that the correction can give accurate ages outside of this range.

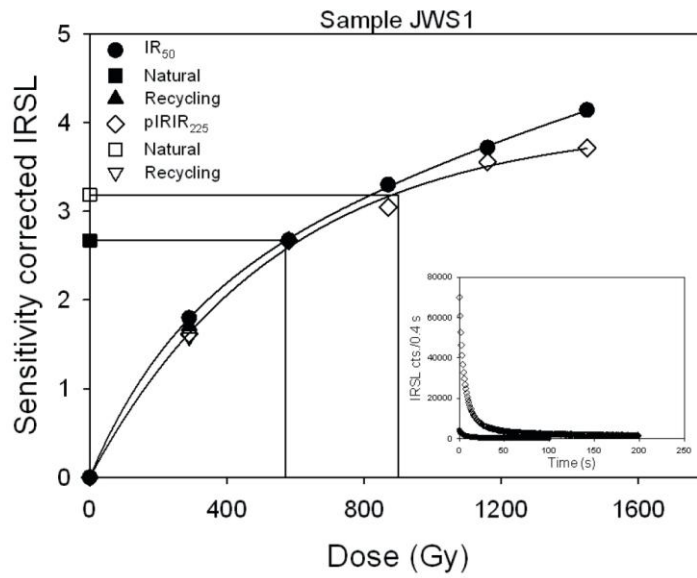
#### **6.4.2.2 Luminescence characteristics and performance in SAR**

The dose response curves and the decay curves for IR<sub>50</sub> and pIRIR<sub>225</sub> for the uppermost sample JWS1 (~17 m) and for the lowermost sample JWT8 (~94 m) is shown in Fig. 3a,b. The curves are representative for all the other samples measured using the pIRIR<sub>225</sub>. The natural IRSL signal clearly lies below the natural post-IR IRSL signal, by about 15-20% on average. The shapes of the growth curves are similar but the growth curve for IR<sub>50</sub> tends to lie



somewhat above the curve for pIRIR<sub>225</sub> for all our samples. Fig.4 a,b shows corresponding dose response and decay curves for IR<sub>50</sub> and pIRIR<sub>290</sub> for the uppermost sample JWS1 (~17 m) and for one of the lowermost samples JWS8 (~94 m). As for pIRIR<sub>225</sub>, the natural pIRIR<sub>290</sub> lies clearly above the natural IRSL signal, and the growth curves for IR<sub>50</sub> lie somewhat above the curves for pIRIR<sub>290</sub> for all samples.

a)



b)

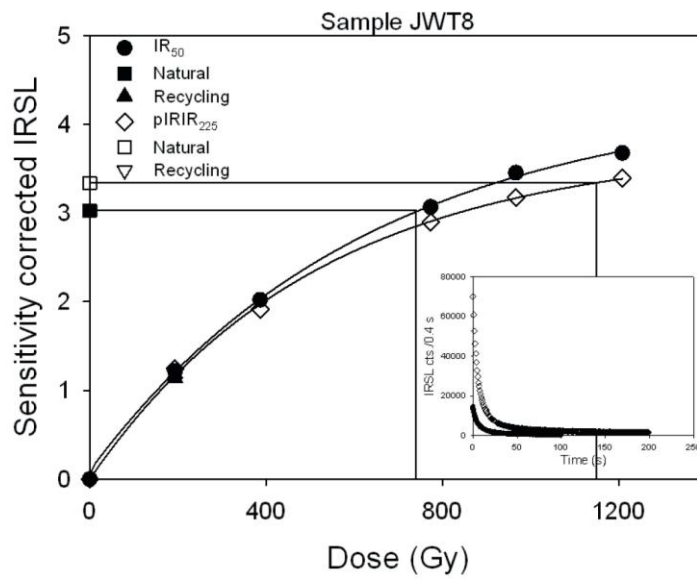


Figure 6.3: Dose response and decay curves for sample a) JWS1 and b) JWS8 showing the IR<sub>50</sub> (filled symbols) and the pIRIR<sub>225</sub> (open symbols).

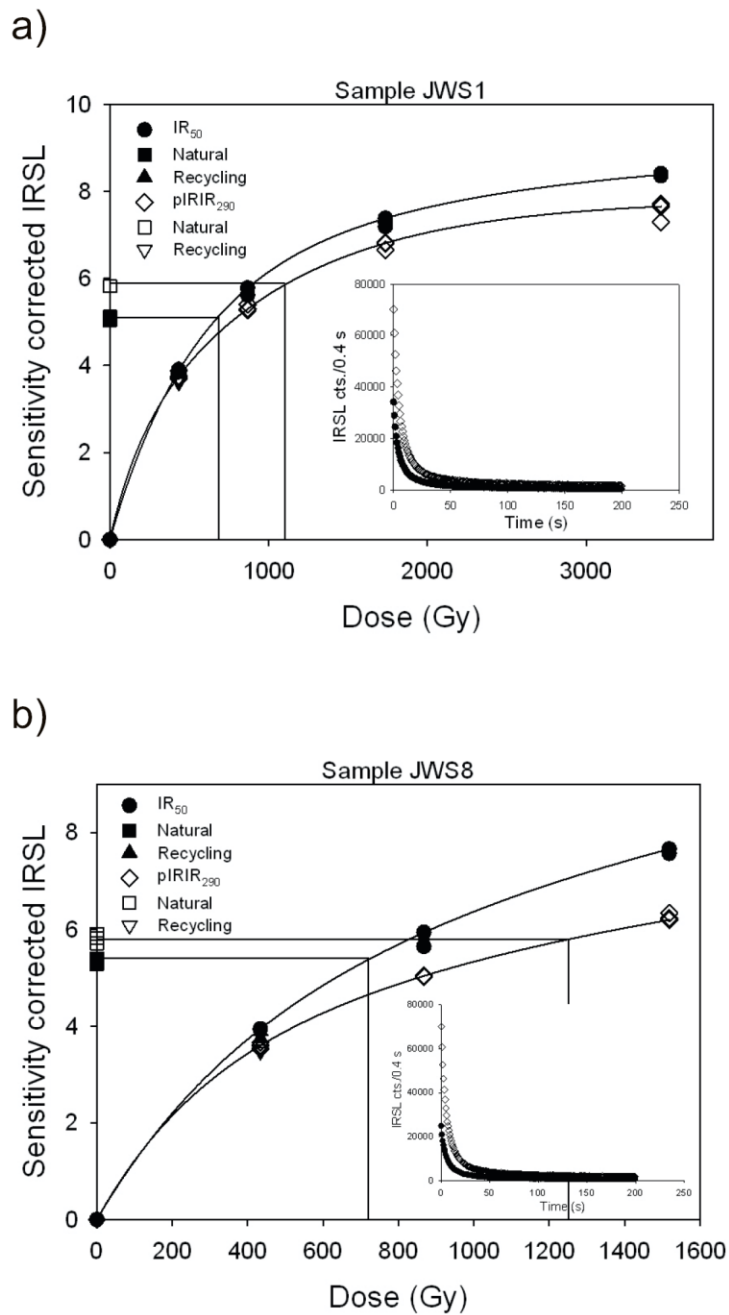
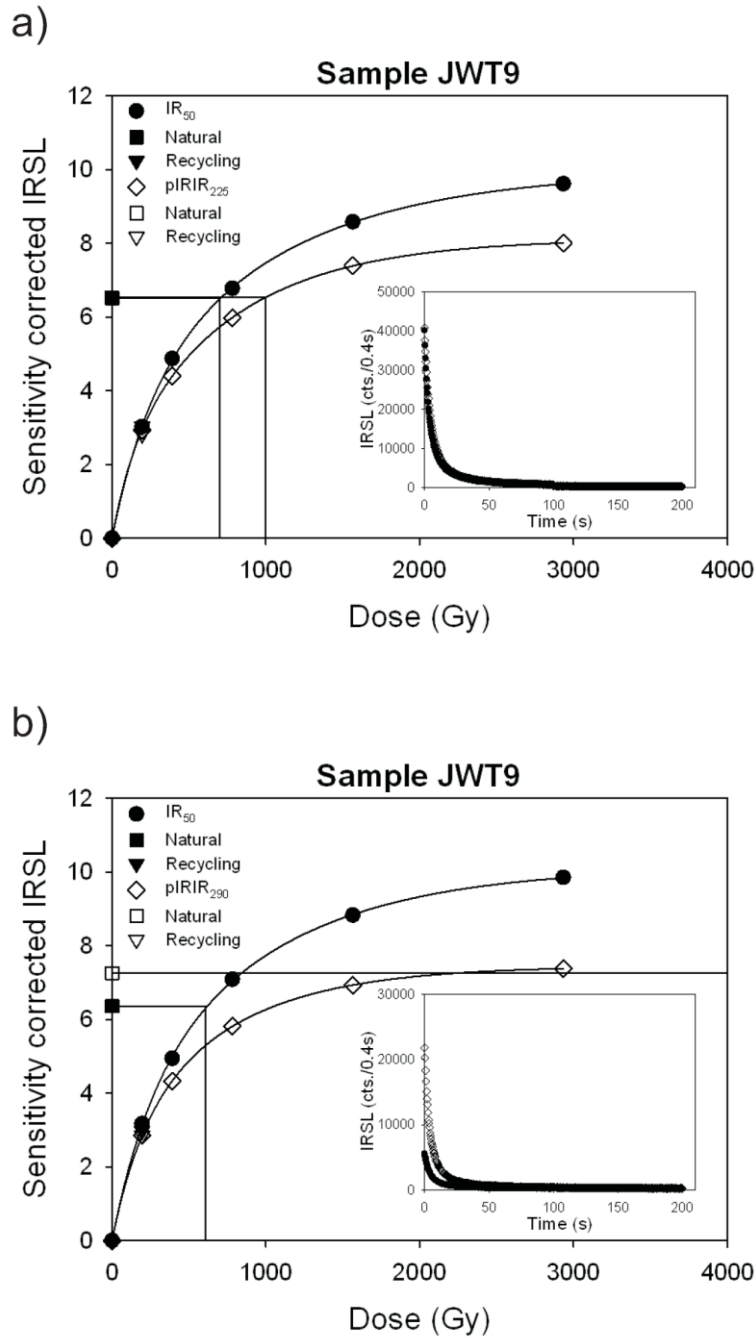


Figure 6.4: Dose response and decay curves for sample a) JWS1 and b) JWS8 showing the  $IR_{50}$  (filled symbols) and the  $pIRIR_{290}$  (open symbols).

Fig. 5 a,b show dose response curves and decay curves for  $IR_{50}$ , the  $pIRIR_{225}$  and  $pIRIR_{290}$  for sample JWS9.

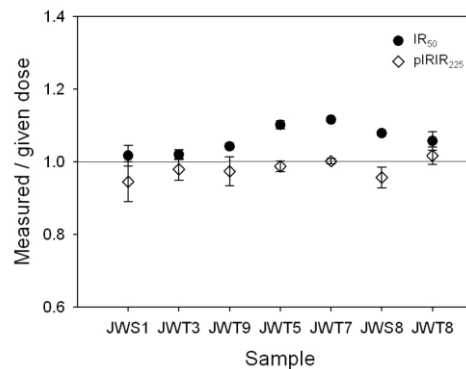


**Figure 6.5: Dose response and decay curves for sample JWT9 showing the IR<sub>50</sub>, pIRIR<sub>225</sub> and the pIRIR<sub>290</sub>.**

This is in contrast to the study of Buylaert et al. (2009) who observed that the shape of the growth curves for IR<sub>50</sub> and pIRIR<sub>225</sub> are indistinguishable. Thiel et al. (2011) also investigated IR<sub>50</sub> and pIRIR<sub>290</sub> growth curves and observed very similar shapes. In our study, the pIRIR<sub>225</sub> from all the samples is brighter (~12-20%) than for the IR<sub>50</sub>. The pIRIR<sub>290</sub> is ~3 times brighter than for the IR<sub>50</sub>. Buylaert et al. (2009) and Thiel et al. (in press) made similar observations. Recycling ratios for our samples range from  $0.96 \pm 0.01$  to  $1.02 \pm 0.02$  for the IR<sub>50</sub> and from  $0.95 \pm 0.02$  to  $0.98 \pm 0.01$  for pIRIR<sub>225</sub>. Recuperation for all the IRSL, pIRIR<sub>225</sub> and pIRIR<sub>290</sub>

signals is below 5% of the natural signal. To test the applicability of the post-IR IRSL protocol using a stimulation temperature of 225°C, the dose recovery ratio was measured for all samples (Murray & Wintle, 2003). The aliquots were bleached for 4 hours in a Hönle SOL2 solar simulator before giving a dose approximately equal to the natural dose. Fig. 6a shows the results of the dose recovery test for all samples for IR<sub>50</sub> and pIRIR<sub>225</sub>.

a) Dose recovery



b) Residual doses

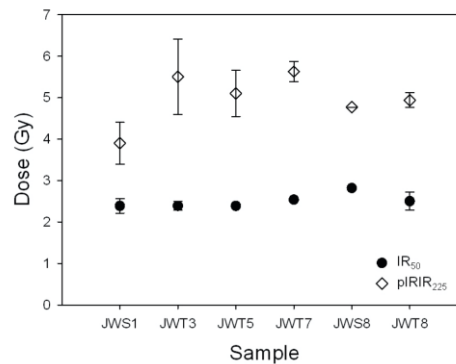


**Figure 6.6: Dose recovery test (a) and the residual doses (b) for the IR<sub>50</sub> and the pIRIR<sub>225</sub> signal for all samples. Three aliquots were measured per sample. Error bars represent 1-sigma standard error.**

The mean ratio of the measured to given dose is  $1.060 \pm 0.011$ ,  $n = 21$  for IR<sub>50</sub> and  $0.98 \pm 0.006$ ,  $n = 21$  for pIRIR<sub>225</sub> confirming the suitability of our post-IR IRSL protocol. To confirm that IRSL and post-IR IRSL signals are bleachable by natural daylight we exposed three aliquots per sample for four hours to a Hönle SOL2 solar simulator and then measured the apparent dose in the usual manner. The results are shown in Fig. 6b. The residual doses range from  $2.21 \pm 0.13$  Gy to  $2.84 \pm 0.01$  Gy, with a mean of  $2.37 \pm 0.15$  Gy ( $n = 18$ ) for IR<sub>50</sub> and from  $3.92 \pm 0.51$  Gy to  $5.54 \pm 0.91$  Gy, with a mean of  $4.88 \pm 0.19$  Gy ( $n = 19$ ) for pIRIR<sub>225</sub>. The residual doses were subtracted from the measured equivalent doses ( $D_e$ ) for age calculation.

#### ***6.4.2.3 Equivalent Dose ( $D_e$ ), fading rates and age estimates***

Equivalent doses ( $D_e$ ) have been measured using IR<sub>50</sub>, pIRIR<sub>225</sub> for all samples, and pIRIR<sub>290</sub> for three samples. Table 3 summarises the equivalent doses, saturation of the signal, recycling ratio, dose recovery results, residual doses, g-values and the resulting luminescence ages for all samples.

Sample	Depth	Measurement	D <sub>e</sub> (Gy)	Saturation	Recycling	Measured/given dose	Residuals (Gy)	g-value (%)	uncorrected Age (ka)	corrected Age (ka)
JWS1	16.60 - 16.62 m	IR <sub>90</sub>	527 ± 29	0.47 ± 0.02	0.96 ± 0.01	1.02 ± 0.003	2.49 ± 0.22	3.64 ± 0.12	124 ± 9	188 ± 19
		pIR <sub>225</sub>	846 ± 52	0.72 ± 0.04	0.98 ± 0.01	0.94 ± 0.05	3.82 ± 0.51	2.63 ± 0.34	199 ± 16	271 ± 35
		pIR <sub>390</sub>	1137 ± 17	0.79 ± 0.004	0.97 ± 0.01	0.97 ± 0.01		0.52 ± 1.12	>270	
JWT3	18.54 - 18.56 m	OSL	441 ± 28		0.99 ± 0.02	0.97 ± 0.01			>100	
		IR <sub>90</sub>	686 ± 66	0.58 ± 0.03	0.99 ± 0.01	1.02 ± 0.13	2.21 ± 0.13	4.79 ± 0.11	154 ± 16	270 ± 31
		pIR <sub>225</sub>	921 ± 63	0.79 ± 0.03	0.97 ± 0.01	0.98 ± 0.03	5.54 ± 0.91	2.31 ± 0.48	207 ± 17	271 ± 44
JWT9	21.58 - 21.70 m	pIR <sub>390</sub>	523 ± 17		0.97 ± 0.01				>100	
		IR <sub>90</sub>	524 ± 30	0.41 ± 0.02	0.97 ± 0.02	1.04 ± 0.007		4.52 ± 0.23	113 ± 9	191 ± 28
		pIR <sub>225</sub>	936 ± 46	0.69 ± 0.03	0.97 ± 0.03	0.97 ± 0.04		3.33 ± 1.02	203 ± 14	297 ± 99
JWT5	44.64 - 44.72 m	OSL	602 ± 26	0.6 ± 0.002	1.01 ± 0.07	1.10 ± 0.11	2.53 ± 0.04	4.35 ± 0.50	162 ± 12	271 ± 42
		IR <sub>90</sub>	928 ± 38	0.79 ± 0.04	0.98 ± 0.01	0.89 ± 0.015	5.14 ± 0.63	2.45 ± 0.19	250 ± 18	336 ± 39
		pIR <sub>225</sub>								
JWT7	65.29 - 65.40 m	pIR <sub>390</sub>	641 ± 37	0.65 ± 0.02	1.02 ± 0.02	1.12 ± 0.001	2.59 ± 0.02	3.98 ± 0.37	161 ± 12	258 ± 44
		IR <sub>90</sub>	927 ± 61	0.87 ± 0.02	0.97 ± 0.01	1.00 ± 0.01	5.65 ± 0.28	2.51 ± 0.24	234 ± 20	316 ± 39
		pIR <sub>225</sub>								
JWS8	93.12 - 93.15 m	OSL	581 ± 54		0.98 ± 0.02				>100	
		IR <sub>90</sub>	588 ± 32	0.57 ± 0.03	0.96 ± 0.02	1.06 ± 0.002	2.84 ± 0.01	4.21 ± 0.43	170 ± 13	279 ± 41
		pIR <sub>225</sub>	1174 ± 64	0.86 ± 0.02	0.98 ± 0.02	0.96 ± 0.03	4.83 ± 0.03	2.48 ± 0.38	334 ± 25	>450
JWT8	93.73 - 93.83 m	pIR <sub>390</sub>	1373 ± 53	0.78 ± 0.03	0.98 ± 0.01				>390	
		OSL				1.04 ± 0.01	2.52 ± 0.26	4.15 ± 0.61	243 ± 22	397 ± 79
		IR <sub>90</sub>	871 ± 63	0.75 ± 0.05	0.98 ± 0.02	1.02 ± 0.02	4.97 ± 0.23	2.11 ± 0.21	319 ± 21	>410
JWT9 (core JW2)	104.5 - 104.6 m	pIR <sub>225</sub>	1143 ± 49	0.86 ± 0.01	0.95 ± 0.01					
		OSL	600 ± 24	0.65 ± 0.01	0.99 ± 0.02				149 ± 10	
		IR <sub>90</sub>	1041 ± 30	0.87 ± 0.01	0.98 ± 0.01				259 ± 15	
			> 930*	0.89 ± 0.01	0.97 ± 0.01			>270		

**Table 3. Summary of equivalent dose (D<sub>e</sub>), saturation level, recycling ratio, dose recovery, residual doses, fading and luminescence ages. Six aliquots were measured per sample for dose determination. For the fading tests three aliquots/sample were measured.**

The equivalent doses ( $D_e$ ) obtained using the  $IR_{50}$  are in the range of ~500-700 Gy for core JW3 except for sample JWT8 which gives a significantly higher dose of  $871 \pm 63$  Gy. These  $D_e$  estimates give minimum (uncorrected for fading) age estimates between  $113 \pm 9$  ka and  $240 \pm 20$  ka.  $D_e$  values obtained for  $IR_{50}$  do not increase systematically with depth, and indicate that this signal is in field saturation (equilibrium between the accumulation of new charge and the loss by anomalous fading) at ~500 Gy. Similar results were obtained by Degering & Krbetschek (2007a) on two samples with a depth of 104.5 m and 122.5 m from core JW2 from Jungfernweiher. They applied a multiple aliquot additive dose (MAAD) protocol to the polymineral fine-grain fraction and obtained equivalent doses ( $D_e$ ) of  $441 \pm 49$  Gy and  $517 \pm 62$  Gy. The  $D_0$ -values of all IRSL and post-IR IRSL signals are about ~500-600 Gy suggesting that doses up to about ~1000-1200 Gy can be measured. The equivalent doses  $D_e$  obtained using  $pIRIR_{225}$  from feldspar range from  $846 \pm 52$  Gy to  $1174 \pm 64$  Gy for core JW3, which is ~25-50% higher than those obtained using  $IR_{50}$ . The  $D_e$  values of  $pIRIR_{225}$  increase with depth, but the values for the lowermost two samples are already in the range of  $2D_0$ . This suggests a minimum uncorrected age of ~200 ka for the youngest sample.  $D_e$  values for  $pIRIR_{290}$  signal are only available for sample JWS 1 ( $1137 \pm 17$  Gy) and for sample JWS 8 ( $1373 \pm 53$  Gy); these values are ~15-25% higher than the equivalent doses ( $D_e$ ) obtained using the  $pIRIR_{225}$  and give minimum age estimates of ~260 ka for the youngest sample and ~390 ka for one of the two oldest samples of JW3. The ages increase with depth but the  $D_e$  values are in the range of or exceed  $2D_0$ . The uncorrected  $pIRIR_{225}$  ages underestimate the uncorrected  $pIRIR_{290}$  age estimates by about 25-30 % on average, presumably because the  $pIRIR_{225}$  signals have to be corrected for fading. The ratio of the sensitivity-corrected natural signal to the laboratory saturation level was calculated for  $IR_{50}$ ,  $pIRIR_{225}$  and for  $pIRIR_{290}$  signals, and average values of  $0.58 \pm 0.04$ ,  $0.79 \pm 0.03$  and  $0.79 \pm 0.01$  for  $IR_{50}$ ,  $pIRIR_{225}$  and  $pIRIR_{290}$  were obtained, respectively. Schmidt et al. (submitted) tested the  $pIRIR_{290}$  protocol on polymineral fine grains from Serbian loess investigating the behavior of both  $IR_{50}$  and  $pIRIR_{290}$  in material close to or in saturation with a focus on the relationship between field and laboratory saturation. They could demonstrate that field saturation is equal to laboratory saturation for  $pIRIR_{290}$ , i.e., the ratio of the natural signal to the laboratory saturation level is close to 1. These findings show that the measured samples are not yet in field saturation for  $pIRIR_{290}$  signal. Sample JWT9 (Fig.5 a,b), which was taken from core JW2 was measured using  $IR_{50}$ ,  $pIRIR_{225}$  and  $pIRIR_{290}$ . The equivalent doses ( $D_e$ ) obtained using  $IR_{50}$  are around 600 Gy, which is in the range of the field saturated results for JW3 using this signal. For



pIRIR<sub>225</sub> an equivalent dose ( $D_e$ ) of  $1041 \pm 30$  Gy was measured, which is in the range of  $2D_0$ . For pIRIR<sub>290</sub> an equivalent dose ( $D_e$ ) could not be calculated as the natural signal lies very close to the saturation level; the ratio of the sensitivity-corrected natural signal to the laboratory saturation level is  $0.99 \pm 0.01$  ( $n=3$ ) indicating that this sample is in saturation. Therefore, only a minimum dose estimate of  $\sim 270$  ka based on the  $2D_0$  value (86% of saturation) can be derived ( $\sim 1100$  Gy).

The measured fading rates for IR<sub>50</sub>, pIRIR<sub>225</sub> and pIRIR<sub>290</sub> are shown in Fig. 7.

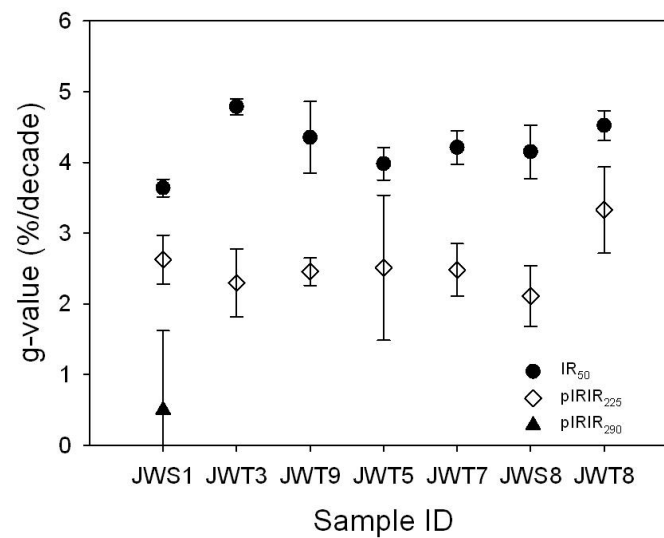


**Figure 6.7: Fading rates for the post the IR<sub>50</sub> and pIRIR<sub>225</sub> signals for all samples. Three aliquots were measured per sample. Error bars represent 1-sigma standard error.**

For IR<sub>50</sub>, the g-values range from  $3.64 \pm 0.12\%$ /decade to  $4.79 \pm 0.11\%$ /decade, with an average of  $4.09 \pm 0.02\%$ /decade,  $n = 21$ , and for the pIRIR<sub>225</sub> signal, from  $2.1 \pm 0.2\%$ /decade to  $3.3 \pm 1.0\%$ /decade, with an average of  $2.55 \pm 0.14\%$ /decade,  $n = 21$  (Fig. 8). These data suggest that pIRIR<sub>225</sub> fades by  $\sim 40\%$  less than IR<sub>50</sub>. For sample JWS1 a g-value of  $0.5 \pm 1.1\%$ /decade for pIRIR<sub>290</sub> was obtained.

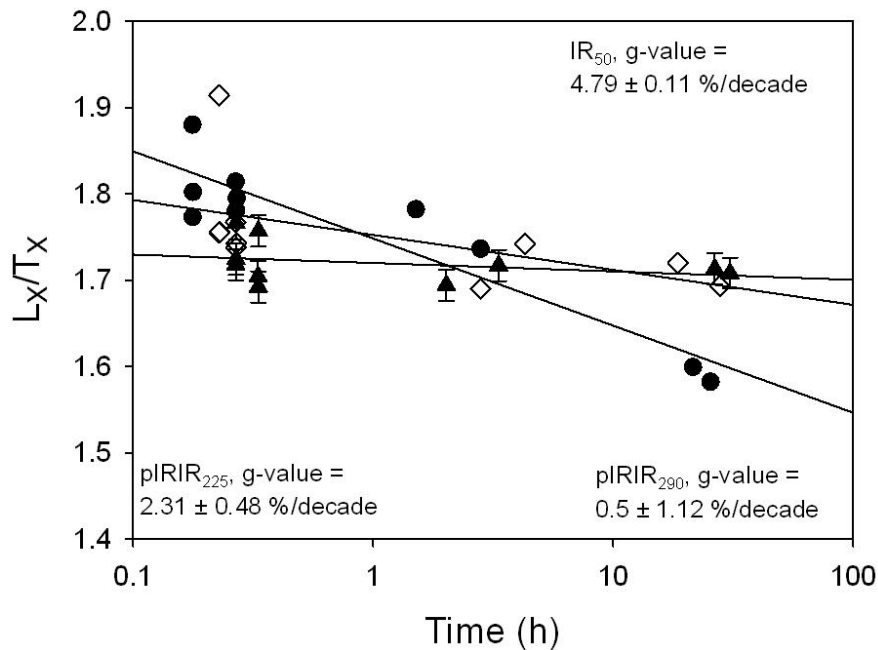


**Figure 6.8: Anomalous fading of IRSL<sub>50</sub>, pIRIR<sub>225</sub> and pIRIR<sub>290</sub> signals.**

Similar fading rates for the pIRIR<sub>225</sub> and pIRIR<sub>290</sub> are reported by Thiel et al. (in press) for their polymineral fine-grain samples, although they measured lower fading rates for IR<sub>50</sub>. The fading corrected age estimates for IR<sub>50</sub> and pIRIR<sub>225</sub> are listed in Table 3. The IR<sub>50</sub> age estimates range from  $188 \pm 19$  ka to  $400 \pm 80$  ka. The age estimates for pIRIR<sub>225</sub> range from  $270 \pm 40$  ka to  $>450$  ka. The age estimates for pIRIR<sub>290</sub> are not fading corrected; Thiel et al. (2011) argue that fading rates below 1%/decade may not be significant, based on their finding of natural signals in saturation on a laboratory growth curve. The age estimates obtained for IR<sub>50</sub> are consistently lower than those from pIRIR<sub>225</sub>, except for sample JWT 3 and JWT 8. In contrast, our fading corrected pIRIR<sub>225</sub> age estimates are consistent with those from the uncorrected pIRIR<sub>290</sub>. The underestimates from IR<sub>50</sub> are consistent with the observation that this signal is in field saturation.

## 6.5. Discussion

Both pIRIR<sub>225</sub> and pIRIR<sub>290</sub>  $D_e$  values from the youngest sample (~16 m below modern surface) indicate a minimum (uncorrected for fading) age of ~200 ka for the deposits from Jungfernweiher. Fading corrected pIRIR<sub>225</sub> and uncorrected pIRIR<sub>290</sub> age estimates increase with depth from ~250 ka for the uppermost sample up to ~400 ka for the oldest samples taken

~94 m below modern surface indicating an accumulation of ~100 m over at least 150 ka. Thus according to post-IR IRSL ages, Jungfernweiher was effectively filled up with sediments ~250 ka ago, and there either has been very little deposition since then, or younger sediments have been eroded. However, there are uncalibrated radiocarbon age estimates ranging from  $34.5 \pm 2.1$  ka BP to  $56 \pm 4$  ka BP (no systematic increase with depth) which might indicate that these deposits are of late Weichselian age. Lenaz et al. (2010) also regard it as possible that the tephra layer at a depth of 107.39 m could be correlated with the Rocourt Tephra which has an age range between 90.3 and 74 ka. One possible explanation for our high  $D_e$ -values can be based on mixing of well-bleached aeolian dust with locally eroded old (field saturated) crater-wall sediment – then the sediment would have been deposited with an average finite residual dose, perhaps close to saturation. However, a simple mixing model indicates that for such a mixture to have been deposited at, say, ~20 ka, one would require >75% of the total lake sediment to be locally-derived old material in order to give a dose indistinguishable from field saturation today. Such a large catchment input to a maar lake seems very unlikely. Overestimated  $D_e$ -values could, of course, also arise because of incomplete bleaching. However it seems most likely that the laminated coarser dust-storm and loess layers were deposited during high-glacial times; if such aeolian dust is making up a very large part of the sediment inventory it is difficult to accept that the IRSL is not well-bleached. There is considerable evidence in the literature that the  $IR_{50}$  from loess and from sediments originating from dust storms is well bleached (Roberts, 2008). It is also known that the fast component of quartz can be depleted in only a few minutes exposure to daylight (Godfrey-Smith et al., 1988) and yet we still obtain an equivalent dose for the fine-grain quartz of  $441 \pm 28$  Gy giving a minimum age estimate of ~100 ka based on the  $2D_0$  value of ~260-300 Gy for the youngest sample. Finally, a study from a nearby East Eifel crater fill (Schmidt et al, 2011) showed that the pulsed  $pIRIR_{150}$  from loess deposits in this area is in fact well bleached. Their luminescence age estimates are in good agreement with stratigraphic evidence and with independent age control provided by  $^{40}Ar/^{39}Ar$  dating of intercalated air-fall tephra and scoria. Thus we appear to have a discrepancy between the established stratigraphy and all IRSL data. Most of the radiocarbon ages are in the range of ~43-55 ka (except for one of ~35 ka) which is at or close to the upper age limit of the method. Luminescence age estimates are provided by Degering & Krbetschek (2007a) on two samples with a depth of 104.5 m and 122.5 m from core JW2 yielding equivalent doses ( $D_e$ ) of  $441 \pm 49$  Gy and  $517 \pm 62$  Gy. Age estimates of  $98 \pm 15$  ka and  $117 \pm 18$  ka were calculated for these samples. To enable comparison of our results for samples from the drill core JW3 and the published age estimates

of Degering & Krbetschek (2007a) we additionally measured one sample (JWT9) from drill core JW2 taken from a depth of 104.5 m. The results show that this sample is in saturation for all the different signals, IR<sub>50</sub>, pIRIR<sub>225</sub> and for pIRIR<sub>290</sub> suggesting a minimum age estimate of ~270 ka for pIRIR<sub>290</sub> signal for this sample. The calculated age estimates of Degering & Krbetschek (2007a) are underestimating our results significantly. One possible reason might be field saturation of their signal, i.e. the trap filling and anomalous fading had reached to the equilibrium state. In addition, the association of the tephra at 107 m with the Rocourt Tephra is not secure. In our view the post-IR IRSL ages represent the most secure ages for this deposit. It has to be mentioned, that one co-author (F.Sirocko) does not agree with this interpretation and proposes an alternative stratigraphy for core JW3 and neighbouring core JW2 (see appendix).

## 6.6. Conclusion

We have investigated the application of luminescence dating to maar lake sediments from the dry maar Jungfernweiher in the West Eifel volcanic field by using quartz OSL and two different protocols for feldspar IRSL. Using OSL, we obtained  $D_e$  values ranging from  $440 \pm 30$  Gy to  $580 \pm 40$  Gy for the fine-grain quartz extracts. All these results exceed the  $2D_0$  value of 260-300 Gy corresponding to minimum ages of ~80-100 ka (although the laboratory growth curve does not fully saturate before ~1000 Gy). For polymineral fine-grains, the  $D_e$  values obtained for IR<sub>50</sub> do not increase with depth, and indicate that this signal is in field saturation at ~500 Gy. The  $D_e$  values for pIRIR<sub>225</sub> and pIRIR<sub>290</sub> are increasing with depth from ~800 Gy to ~1400 Gy, suggesting a minimum age of ~200 ka for the youngest material, although the obtained equivalent doses ( $D_e$ ) are already in the range or exceeding  $2D_0$  for two bottom samples for JW3 and the sample from JW2. Mean laboratory fading rates are  $4.09 \pm 0.02\%$ /decade for IR<sub>50</sub> and  $2.55 \pm 0.14\%$ /decade for pIRIR<sub>225</sub>. Although we observed a  $g$ -value of  $0.52 \pm 1.12\%$ /decade for pIRIR<sub>290</sub> from sample JWS1, we have chosen not to correct the age estimates for pIRIR<sub>290</sub> for fading. Corrected age estimates for pIRIR<sub>225</sub> range from  $270 \pm 40$  ka to  $>450$  ka. These ages are consistent with uncorrected pIRIR<sub>290</sub> age estimates. Not surprisingly, fading corrected age estimates obtained for IR<sub>50</sub> underestimate the fading corrected age estimates for pIRIR<sub>225</sub>. However radiocarbon age estimates and a possible tephra association suggest that these dated deposits should be of late Weichselian age. Based on the results from a simple sediment mixing model and on the results from analyses of well-

bleached aeolian material from the nearby East Eifel, it is not likely that the high  $D_e$ -values observed within this study could originate from mixing or incomplete bleaching. Therefore we regard the results from the luminescence measurements conducted within this study to represent the most reliable age estimates for the sediments from the Jungfernweiher. The discrepancy between the established stratigraphy and the IRSL data from this study remains to be explained.

## **Acknowledgements**

This research is part of the PhD study of EDS in the framework of the “Leibniz Pakt für Forschung und Innovation” at the LIAG-Institute in Hannover. EDS wishes to thank all members of the Sedimentology group of the Institute of Geosciences at the Johannes Gutenberg University in Mainz for their timely help, especially Stephan Dietrich, Klaus Schwibus and Frank Dreher. Christopher Lüthgens and an anonymous reviewer are thanked for the useful comments on the manuscript.

## **References**

- Adamic, M., Aitken, M.J., 1998. Dose-rate conversion factors: update. *Ancient TL* 16, 37-50.
- Aitken, M.J. 1985. *Thermoluminescence Dating*, London.
- Aitken, 1998. *An Introduction to Optical Dating*, Oxford.
- Auclair, M., Lamothe, M., Huot, S., 2003. Measurement of anomalous fading for feldspar IRSL using SAR. *Radiation Measurements*, 37, 487–492.
- Büchel, G., 1984. *Die Maare im Vulkanfeld der Westeifel, ihr geophysikalischer Nachweis, ihr Alter und ihre Beziehung zur Tektonik der Erdkruste*. PhD-Thesis, Univ. Mainz, 385 pp.

- Buylaert J.P., Murray A.S. and Huot S., 2008. Optical dating of an Eemian site in Northern Russia using K-feldspar. *Radiation Measurements*, 43, 715-720.
- Buylaert, J.P., Murray, A.S., Thomson, K.J., Jain, M., 2009. Testing the potential of an elevated temperature IRSL signal from K-feldspar. *Radiation Measurements*, 44, 560-565.
- Buylaert, J.P., Huot, S., Murray, A.S., Van den haute, P., in press. Infrared stimulated luminescence dating of an Eemian (MIS 5e) site in Denmark using K-feldspar, *Boreas*, 10.1111/j.1502-3885.2010.00156.x. ISSN.
- Buylaert, J.P., Vandenberghe, D., Murray, A.S., Huot, S., De Corte, F., Van den haute, P., 2007. Luminescence dating of old (>70 ka) Chinese loess: a comparison of single-aliquot OSL and IRSL techniques. *Quaternary Geochronology*, 2, 9-14.
- Degering, D. and Krbetschek, M. R., 2007a. Dating of Interglacial Deposits by Luminescence Methods.- In: Sirokko et al. (Eds.): *The Climate of Past Interglacials*, Elsevier, 157-172
- Degering, D., Krbetschek, M. R., 2007b. Lumineszenzdatierungen an limnischen Sedimenten von Klinge/Kreis Forst. *Natur und Landschaft*, 120-128.
- Duller, G.A.T., 2003. Distinguishing quartz and feldspar in single grain luminescence measurements. *Radiation Measurement*, 37, 161-165.
- Duller, G.A.T., 2004. Luminescence dating of quaternary sediments: recent advances *Journal of Quaternary Science*, 19(2): 183-192.
- Frechen, M., 1991. Systematic thermoluminescence dating of two loess profiles from the middle Rhine area (F.R.G.). *Quaternary Science Reviews*, 11, 93-101.
- Godfrey-Smith, D.I., Huntley, D.J., Chen, W.-H., 1988. Optical dating of quartz and feldspar extracts. *Quaternary Science Reviews*, 7, 373-380.

- Huntley, D.J., Lamothe, M., 2001. Ubiquity of anomalous fading in K-feldspars and the measurement and correction for it in optical dating. *Canadian Journal of Earth Sciences* 38, 1093-1106.
- Lamothe M., Auclair M., Hamzaoui C., Huot S. 2003. Towards a prediction of long-term anomalous fading of feldspar IRSL. *Radiation Measurements*, 37, 493-498.
- Lang, A., Zolitschka, B., 2001. Optical dating of annually laminated lake sediments A test case from Holzmaar/Germany. *Quaternary Science Reviews*, 20, 5-9, 737-742.
- Lenaz, D., Marciano, R., Veres, D., Dietrich, S., Sirocko, F. 2010. Mineralogy of the Dehner and Jungferweiher maar tephras (Eifel, Germany). *N.Jb.Geol.Palaont.Abh. Fast track* DOI:10.1127/0077-7749/2010/0062.
- Lowick, S., Preusser, F., Wintle, A., 2010a. Investigating quartz optically stimulated luminescence dose-response curves at high doses. *Radiation Measurements*, 45, 975-984
- Lowick, S.E., Preusser, F., Pini, R., Ravazzi, C. 2010b. Underestimation of fine grain quartz OSL dating towards the Eemian: comparison with palynostratigraphy from Azzano Decimo, northeastern Italy, *Quaternary Geochronology*, 5, 583-590.
- Murray, A.S., Buylaert J.P., Thomsen, K.J. and Jain M., 2009. The effect of preheating on the IRSL signal from feldspar. *Radiation Measurements* 44, 554-559.
- Murray, A.S., Wintle, A.G., 2003. The single regenerative dose protocol: potential for improvements in reliability. *Radiation Measurements*, 37, 377-381.
- Murray, A.S., Olley, J.M., 2002. Precision and accuracy in the optically stimulated luminescence dating of sedimentary quartz: a status review. *Geochronometria*, 21, 1-16.

- Negendank, J.F.W., Zolitschka, B., 1993. Maars and maar lakes of the Westeifel volcanic field. In: J.F.W. Negendank and B. Zolitschka (Editors), *Paleolimnology of European Maarlakes*. Lecture Notes in Earth Sciences. Springer-Verlag, 61-80.
- Pouclot, A., Juvigné, E., Pirson, S., 2008. The Rocourt Tephra, a widespread 90-74 ka stratigraphic marker in Belgium. *Quaternary Research*, 70, 105-120.
- Prescott, J.R., Hutton, J.T., 1994. Cosmic ray contribution to dose rates for luminescence and ESR dating: large depths and long-term time variations. *Radiation Measurements*, 23, 497–500.
- Prescott, J.R., Stephan, L.G. 1982. The contribution of cosmic radiation to the environmental dose for thermoluminescence dating. *PACT*, 6, 17–25.
- Rees-Jones, J., 1995. Optical dating of young sediments using fine-grain quartz. *Ancient TL*, 13, 9-14.
- Roberts, H.M., 2008. The development and application of luminescence dating to loess deposits: a perspective on the past, present and future. *Boreas*, 37, 483-507.
- Schaber, K., Sirocko, F. 2005. Lithologie und Stratigraphie der spätpleistozänen Trockenmaare der Eifel, *Mainzer geowiss.Mitt.*, 33, 295-340.
- Sirocko, F., Seelos, K., Schaber K., Rein, B., Dreher, F., Diehl, M., Lehné, R., Jäger, K., Krbetschek, M., Degering, D., 2005. A Late Eemian Aridity Pulse in central Europe during the last glacial inception. *Nature*, 436: 833-836.
- Schmidt, E.D., Murray, A.S., Stevens, T., Buylaert, J.P., Marković, S.B., Tsukamoto, S., Frechen, M., *subm.* Elevated temperature IRSL dating of the lower part of the Stari Slankamen loess sequence (Vojvodina, Serbia) – investigating the saturation behaviour of the pIRIR<sub>290</sub> signal. *Quaternary Geochronology*.
- Schmidt, E.D., Frechen, M., Murray, A.S., Tsukamoto, S., Bittmann, F., 2011. Luminescence chronology of the loess record from the Tönchesberg section – a comparison of using



- quartz and feldspar as dosimeter to extend the age range beyond the Eemian. *Quaternary International*, 234, 10-22.
- Schmidt, E.D., Machalett, B., Marković, S. B., Tsukamoto, S., Frechen, M., 2010. Luminescence chronology of the upper part of the Stari Slankamen loess sequence (Vojvodina, Serbia). *Quaternary Geochronology*, 5, 137-142.
- Thiel, C., Buylaert, J.P., Murray, A.S., Terhorst, B., Hofer, I., Tsukamoto, S., Frechen, M., 2011. Luminescence dating of the Stratzing loess profile (Austria) – Testing the potential of an elevated temperature post-IR IRSL protocol. *Quaternary International*, 234, 23-31.
- Thiel, C., Buylaert, J.P., Murray, A.S., Terhorst, B., Tsukamoto, S., Frechen, M. in press. Luminescence The chronostratigraphy of prominent palaeosols in Lower Austria: testing the performance of two post-IR IRSL dating protocols. *Eiszeitalter und Gegenwart*.
- Timar, A., Vandenberghe, D., Panaiotu, E.C., Panaiotu, C.G., Necula, C., Cosma, C., Van den haute, P., 2010. Optical dating of Romanian loess using fine-grained quartz. *Quaternary Geochronology*, 5, 143-148.
- Thomsen, K.J., Murray, A.S., Jain, M., Bøtter-Jensen, L., 2008. Laboratory fading rates of various luminescence signals from feldspar-rich sediment extracts. *Radiation Measurements*, 43, 1474-1486.
- Visocekas, R., 1985. Tunnelling radiative recombination in labradorite: Its association with anomalous fading of thermoluminescence. *Nuclear Tracks and Radiation Measurements*, 10 (4-6), 521-529.
- Wintle, A.G, Murray, A.S. 2006. A review of quartz optically stimulated luminescence characteristics and their relevance in single-aliquot regeneration dating protocols. *Radiation Measurements*, 41, 369-391.

Wintle, A.G., 1973. Anomalous fading of thermoluminescence in mineral samples. *Nature*, 245, 143-144.

## **Appendix**

One of the co-authors (Frank Sirocko) has a different chronostratigraphical interpretation, which he describes in detail in a paper under submission. F. Sirocko interprets the luminescence dates from this study as result of a mixture of an eolian fraction with grains from the wave-generated erosion of soil material, which is again a mixture from the Devonian bedrock and loess of MIS6 or older.

According to Sirocko et al. (unpublished) the stratigraphical framework for JW2 and JW3 is as follows:

Scoria from the Laacher See eruption is apparent in the soil at 1 m depth, correlating to an eruption age of about 12.9 ka. Sediments from 1-22 m are free of clay and are regarded as a mixture from eolian deposition and wave generated suspensions. These sediments are free of pollen and correlate to the last glacial maximum (LGM). The relative paleointensity variation of sediment magnetisation places the Mono Lake Event at 24 m indicating an age of 30 ka according to the GLOPIS paleomagnetic stack, which is based on a GISP2 derived age model. A tuning of the greyscale variations between 25 and 41 m reproduces almost perfectly the succession of the Greenland Interstadials GI3-17. The second minimum of the relative paleointensity is at 32.5 m and correlates most likely to the Laschamps Event. The MIS3 sections of JW2 and JW3 have been studied by several  $^{14}\text{C}$  dates giving ages around 50 ka representing the upper dating limit of the  $^{14}\text{C}$  method. This would imply that all organic particles in JW3 are derived from soils of GI14, which was the warmest period of MIS3.

The markers of MIS5 start with a prominent step in the paleomagnetic inclination record at 81 m representing a principle change that was dated in the Monticchio record to 75 ka. The end of this inclination maximum is at 99 m, representing 86 ka. A tephra consisting of the same geochemical composition as the Roucourt tephra in France is visible in JW3 at 107.4 m, which would place this depth at around 90 ka. The sediments below yield two IRSL ages of 93 ka and 100 ka (Degering & Krbetschek, 2007a). The greyscale record between 75 m and 130 m can be perfectly tuned to the Greenland ice core stadial/interstadial succession and also the North Atlantic C-events. A tephra with an identical zonation to the Dümpelmaar tephra is visible at 139 m; this tephra was dated at the Herchenberg section to  $116 \pm 10$  ka. The

succession of the markers of core JW3 ends with the occurrence of interglacial pollen at depth below 145 m most likely representing the Eemian.

# Chapter 7

Quaternary Science Journal, 2011 (60).

## **Luminescence dating of the loess/palaeosol sequence at the gravel quarry Gaul/Weilbach, Southern Hesse (Germany)**

**E.D. Schmidt<sup>1\*</sup>, A. Semmel<sup>†</sup>, M. Frechen<sup>1</sup>**

<sup>1</sup>*Leibniz Institute for Applied Geophysics (LIAG), Section 3: Geochronology and Isotope  
Hydrology, Stilleweg 2, 30655 Hannover, Germany*

*\* corresponding author: Esther.Schmidt@liag-hannover.de,  
Estherdorothe.Schmidt@googlemail.com*

*Key words: loess, luminescence dating, IRSL, fading, Weilbach, chronostratigraphy*

Einen Tag nach Erhalt eines Briefes mit Korrekturen an unserem gemeinsamen Manuskript, erreichte uns völlig überraschend die traurige Nachricht vom Tode Arno Semmels. Wir werden ihn als Mensch, Kollegen und Wissenschaftler vermissen.

### **Abstract**

A thick Middle and Late Pleistocene loess/palaeosol sequence is exposed at the gravel quarry Gaul located east of Weilbach in the southern foreland of the Taunus Mountains. The loess/palaeosol sequence correlates to the last three glacial cycles. Seven samples were dated by luminescence methods using an elevated temperature IRSL (post-IR IRSL) protocol for polymineral fine-grains to determine the deposition age of the sediment and to set up a more

reliable chronological framework for these deposits. The fading corrected  $IR_{50}$  and the  $pIRIR_{225}$  age estimates show a good agreement for almost all samples. The fading corrected IRSL ages range from  $23.7 \pm 1.6$  ka to  $>350$  ka indicating that the oldest loess was deposited during marine isotope stage (MIS) 10 or earlier and that the humic-rich horizon (Weilbacher Humuszone) was developed during the late phase of MIS 7. Loess taken above the fCc horizon was most likely accumulated during MIS 6 indicating that the remains of the palaeosol are not belonging to the last interglacial soil. The two uppermost samples indicate that the youngest loess accumulated during MIS 2 (Upper Würmian). Age estimates for the loess-palaeosol sequence of the gravel quarry Gaul/Weilbach could be obtained up to  $\sim 350$  ka using the  $pIRIR_{225}$  from feldspar.

## 7.1. Introduction

Loess records are sensitive archives of climate change and provide important information on local and regional environmental processes and conditions for the Middle and Late Pleistocene period in Europe. The southern foreland of the Taunus mountains (Fig.1), which are part of the Rhenish Massif in Germany, consists mainly of Pleistocene terraces of the river Main covered by thick loess/palaeosol sequences.

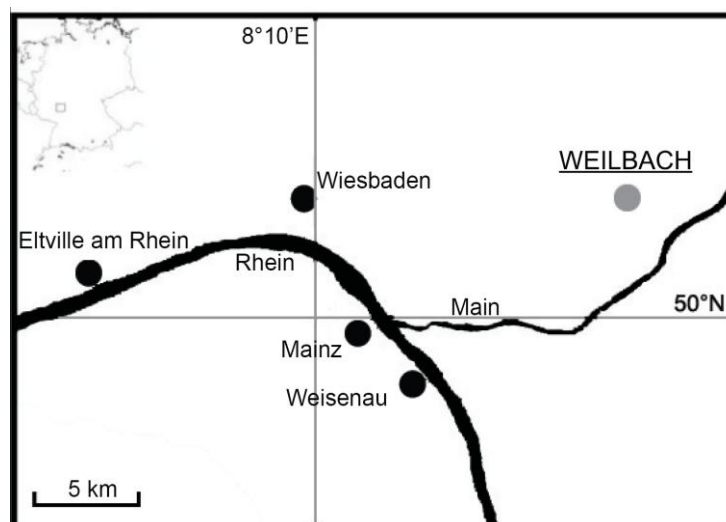


**Figure 7.1:** Location of the loess/palaeosol sequence exposed at the gravel quarry Gaul/Weilbach.

For these deposits it was suggested that each palaeosol or fossil Bt horizon (= fossil argillic B horizon) correlates to an interglacial *sensu stricto* (Fink, 1973). Semmel (1967, 2005) questioned this suggestion because there are loess sequences in Western Europe which

contain much more fossil Bt horizons than evidenced by palynological studies. The Upper Pleistocene Lower terraces of the river Main (t6 and t7 sensu Semmel, 1969) are not covered by such argillic horizons. The stratigraphically older terraces t5 and t4 are covered by loess and intercalated by a fossil Bt horizon and by two Bt horizons, respectively.

In contrast to the studies of Semmel (1969), only one buried Bt horizon, intercalating the loess covering terrace t4, was found at the gravel quarry Gaul located east of Weilbach during the excavation of the past years (Semmel, 2005). The latter Bt horizon is covered by two humic horizons (“Humuszonen”). A significant hiatus truncates the uppermost humic horizon followed by the typical Late Weichselian loess succession including Lohne Soil, tundra gleys (“Naßböden”) E2 and E3, and the Eltville Tephra (Semmel, 1967; stratigraphy after Schönhals et al., 1964; local description after Semmel, 2005a). This loess/palaeosol sequence was studied along of an about 1 km long exposed wall at the gravel quarry Gaul. However, below a weak palaeosol designated to correlate to the Middle Weichselian Lohne Soil, a continuous fCc horizon including large, mainly vertical exposed carbonate concretions (“loess dolls”) of about 20 cm length, sometimes with remains of brown clayey loam, was exposed. It is likely that these remains belong to a fossil Bt horizon (Semmel, 2005). Independent stratigraphical age control is provided by the occurrence of the Eltville Tephra, a widespread marker horizon in this region which most likely resulted from an eruption of the Eifel volcanic field (Semmel, 2007). The Eltville Tephra has been investigated by several dating studies at different sections. The mean luminescence age values are between 19.2 ka and 20.6 ka for this tephra horizon (Wintle and Brunnacker, 1982; Zöller, 1989; Frechen and Preusser, 1996; Antoine et al., 2009). Zöller and Semmel (2001) provided mean TL age estimates of 21 ka for loess above the Eltville Tephra and 25 ka below. So far numerical age estimates are still lacking for the loess deposits from the Weilbach section making it still difficult to interpret the terrestrial climate archives as well as to correlate the loess/palaeosol sequences with other loess records. The nearby loess record from Mainz-Weisenau was described in detail by Semmel (1995). Thermoluminescence (TL) age estimates for the deposits of the Mainz-Weisenau section were presented by Buschbeck (1993) and Zöller (1995). Frechen and Preusser (1996) provided thermoluminescence (TL) and infrared stimulated luminescence (IRSL) age estimates. These previous studies provided TL and IRSL ages up to about 100 ka, which was thought to be the upper dating limit that time (Frechen, 1999).

This study presents the first optically stimulated luminescence (OSL) dating results from the loess/palaeosol sequence at the gravel quarry Gaul located east of Weilbach based on a post-IR IRSL measurement sequence. The IRSL signal measured at 50°C and the subsequent

post-IR IRSL signal measured at 225°C using the latter sequence are hereafter referred to as IR<sub>50</sub> and pIRIR<sub>225</sub>, respectively. Our study aims to set up a more reliable chronological framework for this loess/palaeosol sequence. Furthermore, we want to answer the question whether the oldest Bt horizon correlates to the Middle Pleistocene (antepenultimate or penultimate interglacial) or to the Upper Pleistocene.

## 7.2. Loess/palaeosol sequence at the gravel quarry Gaul/Weilbach

The loess/palaeosol sequence with indicated sample positions for luminescence dating is shown in Fig. 2.

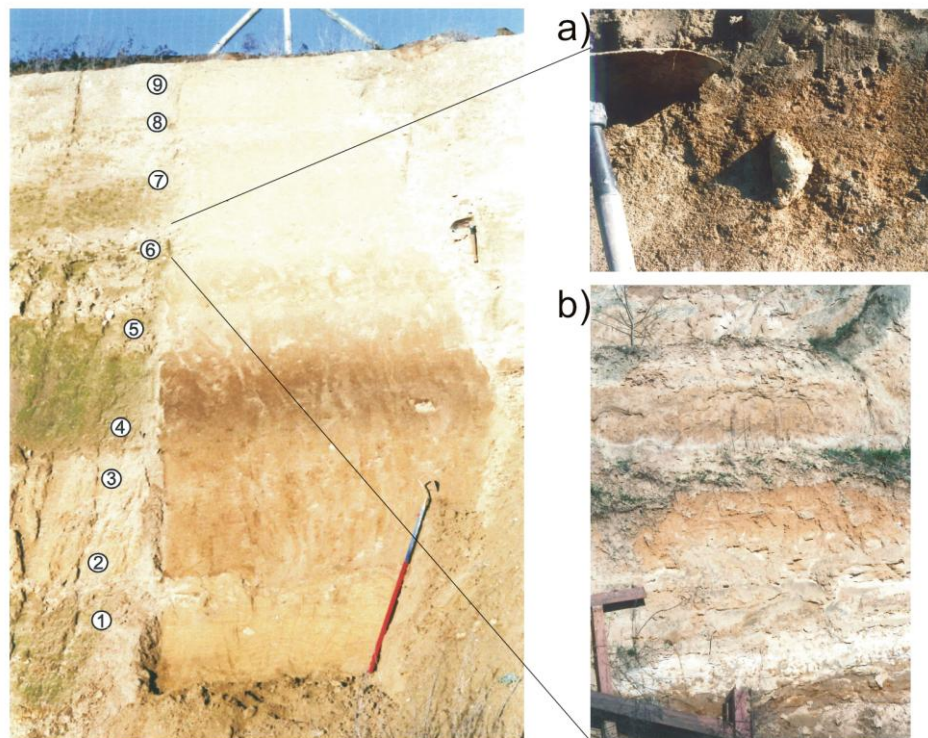


**Figure 7.2: Loess/palaeosol sequence at the gravel quarry Gaul/Weilbach with a) loess concretions of the fCc horizon with remains of brown Bt material from the quarry Gaul near Weilbach and b) Two fossil Bt-horizons near the profile of Fig.2 situated at the Gaul quarry near Weilbach.**

9 = E3 tundra gley, above the Eltville tephra (Wei1 was taken below)

8 = E2 tundra gley, greyish compact loess (Wei2 was taken below)

7 = Löhne soil (Wei3 was taken below)

6 = fCc-horizon with carbonate concretions (Wei4 was taken below)

5 = reworked humic-rich material (Wei5)

4 = humic-rich horizon (“Weilbacher Humuszone”) (Wei6)

3 = reworked carbonate-rich loess loam

2 = fBt-horizon

1 = oldest loess (Wei7)

The coordinates of the section under study are 55°46'28,7" N and 8°44'35,5" E. The location of the profile under study within the terrace sequence of river Main is shown in Fig. 3.

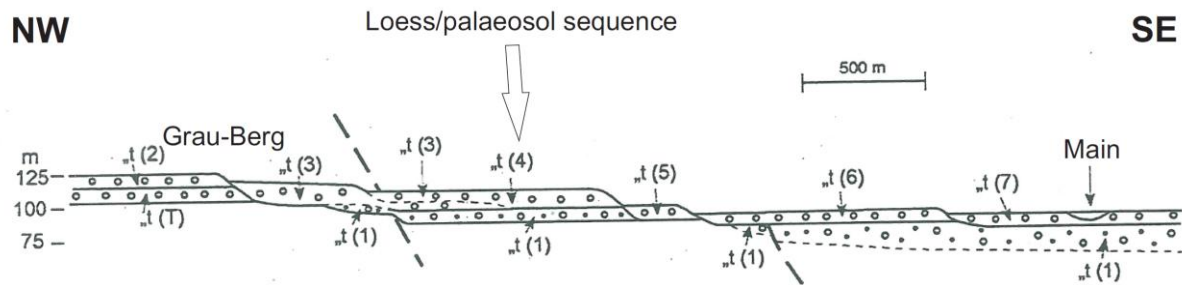


**Figure 7.3: Terraces of the river Main in the southern foreland of the Taunus mountains. The Loess/palaeosol sequence is located close to the symbol “t4”.**

The gravel of terrace t4 is covered by carbonate-free flood loam, which changes to the top into calcareous loess (1 in Fig. 2). Sample Wei 7 was taken from this loess unit. This layer is covered by a 30 cm thick fCc horizon including large carbonate concretions, which form the bottom of a reddish brown fBt horizon (2 in Fig. 2). The colour of the truncated palaeosol is pale coloured owing to secondary carbonate infiltration. In the profile under study the fBt horizon is about 90 cm thick but varies strongly in thickness along the quarry wall owing to erosion postdating the soil forming processes. The truncated palaeosol is covered by carbonate-rich, greyish brown loess loam (about 30 cm thick) below a brown spotted dark humic-rich horizon (“Weilbacher Humuszone”) (4 in Fig. 2, about 70 cm thick). Sample Wei6 was taken from this horizon. The humic-rich horizon is covered by a solifluction layer of reworked humic-rich material including loess loam and calcareous loess, which is about 60 cm thick. Sample Wei5 was taken from this unit (5 in Fig. 2). This layer is covered by light brown about 50 cm thick loess with carbonate pseudomicelium including a truncated fCc horizon with up to 20 cm large carbonate concretions (6 in Fig. 2). Sample Wei4 was taken from this reworked loess. Along the quarry wall, reddish brown remains of loam are found around these carbonate concretions (Fig. 2a). Close to the profile from Fig.2 a truncated Bt horizon about 60 cm thick is exposed along the quarry wall above the fCc horizon in a dell filled with loess (Fig. 2b). The uppermost part of the loess/palaeosol sequence includes weak palaeosols correlating to the Middle Weichselian Lohne Soil (7 in Fig. 2) and to the Upper Weichselian sequence including tundra gley E2 (8 in Fig. 2), tundra gley E3 and the Eltville Tephra (9 in Fig. 2). Sample Wei3 was taken below the Lohne Soil, sample Wei2 below the tundra gley E2 and sample Wei1 below the tundra gley E3.



The stratigraphic interpretation of the profile is based on the local stratigraphical loess scheme (Semmel, 1968; 2005) suggesting that the oldest exposed fBt horizon (2 in Fig. 2) correlates to the antepenultimate or penultimate interglacial designated to be older than ~200 ka. The humic-rich horizon correlates most likely to the “Weilbacher Humuszone”, which correlates to an interstadial period during the early penultimate glacial period (Semmel, 1968) and the fCc horizon (6 in Fig. 2) most likely correlates to the last interglacial. The loess sequence covering the fCc horizon correlates most likely to the Middle and Upper Weichselian, as indicated by the exposed typical marker horizons.

### 7.3. Experimental details

The samples were taken in light-tight plastic cylinders and the sediment was extracted under subdued red light and pretreated with 10% hydrochloric acid to remove carbonates, sodium oxalate to dissolve aggregates and 30% hydrogen peroxide to remove organic matter. The material was then refined to a fine silt (4-11  $\mu\text{m}$ ) fraction. Finally, samples were prepared for measurement by settling the polymineral grains (4-11  $\mu\text{m}$ ) from acetone onto aluminium discs. All OSL/IRSL measurements were performed using an automated Risø TL/OSL-DA20 equipped with a  $^{90}\text{Sr}/^{90}\text{Y}$  beta source. Feldspar IRSL signals were detected through Schott BG-39 and Corning 7-59 filters (passing 320 to 460 nm; i.e. blue).

Radionuclide concentrations for all samples were obtained using high resolution gamma spectrometry of sediment collected from the immediate surrounding of the samples. A water content of  $20 \pm 5$  % was estimated for all samples. It has to be mentioned that the estimation of water content since the loess was deposited is associated with a high degree of uncertainty. Mean  $a$ -values of  $0.08 \pm 0.02$  for polymineral IRSL were used to derive the effective alpha dose rate (Rees-Jones, 1995). The concentrations of uranium, thorium and potassium were converted into infinite-matrix dose rates using the conversion factors of Adamiec and Aitken (1998) and water-content attenuation factors (Aitken, 1985). Estimation of the cosmic-ray dose rate was calculated according to Prescott and Stephan (1982) and Prescott and Hutton (1994) from knowledge of burial depth, altitude, matrix density, latitude and longitude for each sample. The uranium, thorium, potassium content and total dose rates are shown in Table 1.

Sample	Uranium (ppm)	Thorium (ppm)	Potassium (%)	Cosmic dose rate (Gy/ka)	IRSL dose rate (Gy/ka)
Wei 1	3.03 ± 0.03	10.09 ± 0.06	1.23 ± 0.01	0.19 ± 0.02	3.00 ± 0.16
Wei 2	3.40 ± 0.03	11.24 ± 0.06	1.38 ± 0.01	0.18 ± 0.02	3.32 ± 0.18
Wei 3	3.24 ± 0.02	11.41 ± 0.06	1.30 ± 0.01	0.14 ± 0.01	3.18 ± 0.17
Wei 4	2.76 ± 0.02	9.38 ± 0.05	1.18 ± 0.01	0.13 ± 0.01	2.72 ± 0.15
Wei 5	2.80 ± 0.03	11.12 ± 0.06	1.31 ± 0.01	0.12 ± 0.01	3.01 ± 0.16
Wei 6	3.33 ± 0.03	13.55 ± 0.06	1.43 ± 0.01	0.09 ± 0.01	3.45 ± 0.18
Wei 7	2.92 ± 0.03	10.73 ± 0.06	1.30 ± 0.01	0.06 ± 0.01	2.94 ± 0.16

**Table 7.1: Dose rate data from potassium, uranium and thorium content, as measured by gamma spectrometry.**

#### 7.4. Luminescence dating

Luminescence dating enables to determine the depositional age of various sediments such as loess over a range from a few decades to several hundred thousand years by dating the time that has passed since the last exposure of the minerals to daylight (Aitken, 1998). Quartz or feldspar grains (the most common minerals in sediments) are used as natural dosimeters. They are able to store energy within their crystal structure, which is coming mainly from an omnipresent ionising radiation (alpha, beta and gamma) as well as from cosmic radiation. The charge can be stored in imperfections in the crystal lattice for long periods. In the laboratory the grains are first heated, and then stimulated with IR or blue LEDs which release the electrons from their traps in the form of visible light (luminescence). Such a measurement allows estimating the dose of radiation (palaeodose or equivalent dose,  $D_e$ ) which the crystal has absorbed since the last exposure to daylight. The luminescence signals from feldspars grow to much higher doses than those from quartz, which offers the possibility of significantly extending back the age range. However, luminescence dating of feldspars has a tendency to underestimate the geological age, because of anomalous fading (Wintle, 1973) which is caused by quantum-mechanical tunnelling (Visocekas, 1985). Feldspar dating is normally carried out using a 50° C IR stimulation with detection in the blue (-violet) spectrum. IRSL ages underestimate often consistently the quartz OSL ages most likely due to anomalous fading. Several methods of age corrections have been proposed (e.g. Huntley & Lamothe, 2001; Lamothe et al., 2003) and many studies show corrected IRSL ages which are in good agreement with quartz OSL ages. But these corrections rely on different assumptions, including e.g. the fact that the logarithmic time dependence is relevant to geological time (Huntley and Lamothe, 2001) and there is no general consensus which correction method

should be used. Furthermore, the correction method is strictly applicable only for natural doses in the linear region of the growth curve (Huntley and Lamothe, 2001), although Buylaert et al. (2009; in press) have shown that the correction can give accurate ages outside this range. However, if the fading rate can be reduced, feldspar dating will be more reliable.

#### **7.4.1. Post-IR IRSL measurement sequence**

Thomsen et al. (2008) found out, that stimulation at elevated temperatures significantly reduces the fading rate. Based on this work BUYLAERT et al. (2009) proposed a new single aliquot regenerative dose (SAR) protocol, with detection in the blue (320-460 nm). This protocol which includes elevated temperature stimulation with IR for 100 s at 225°C, following stimulation with IR for 100 s at 50°C, is called post-IR IRSL measurement sequence and is presented in Table 2.

<b>Step</b>	<b>Treatment</b>	<b>Observed</b>
1	Dose	
2	Preheat, 60s at 250°C	
3	IR stimulation, 100s at 50°C	Lx
4	IR stimulation, 100s at 225°C	<b>Lx</b>
5	Test dose	
6	Preheat, 60s at 250°C	
7	IR stimulation, 100s at 50°C	Tx
8	IR stimulation, 100s at 225°C	<b>Tx</b>
9	IR stimulation, 40s at 290°C	
10	Return to step 1	

**Table 7.2: Elevated temperature post-IR IRSL measurement sequence.**

Buylaert et al. (2009) have shown that the observed fading rates for the post-IR IR signal are significantly lower than from the conventional IR<sub>50</sub> and that the signal is bleachable in nature. Buylaert et al. (submitted) measured a mean residual dose value of  $10 \pm 2$  Gy on polymineral fine-grains extracted from modern Chinese loess. This post-IR IRSL measurement protocol is applied to the polymineral fine-grains from the Weilbach section. The initial 2.0 s of the post-IR IR signal is used for calculating the D<sub>e</sub> values, with a background subtraction based on the signal observed in the last 10 s of the decay curve. All dose response curves were fitted using an exponential saturating function. Tests were carried out on the same aliquots as for D<sub>e</sub> measurement to check for anomalous fading and to compare the fading rates of the IR<sub>50</sub> and the pIRIR<sub>225</sub>. The aliquots were dosed, preheated and then stored for various delays after irradiation and before measurement. This sequence was

repeated several times on each aliquot. The fading rates are expressed in terms of the percentage of the decrease of intensity per decade of time (g-value; Aitken, 1985; Auclair, Lamothe and Huot, 2003). The g-values were calculated according to Huntley and Lamothe (2001) using the same integration limits as for the  $D_e$  calculation. The g-values were used to correct the ages.

#### 7.4.2. Luminescence characteristics and performance in SAR

Figure 4 shows the dose response curves and the decay curves for the  $IR_{50}$  and the  $pIRIR_{225}$  for the stratigraphically oldest samples Wei6 (Fig. 4a) and Wei7 (Fig. 4b). These curves are selected to be representative for all samples.

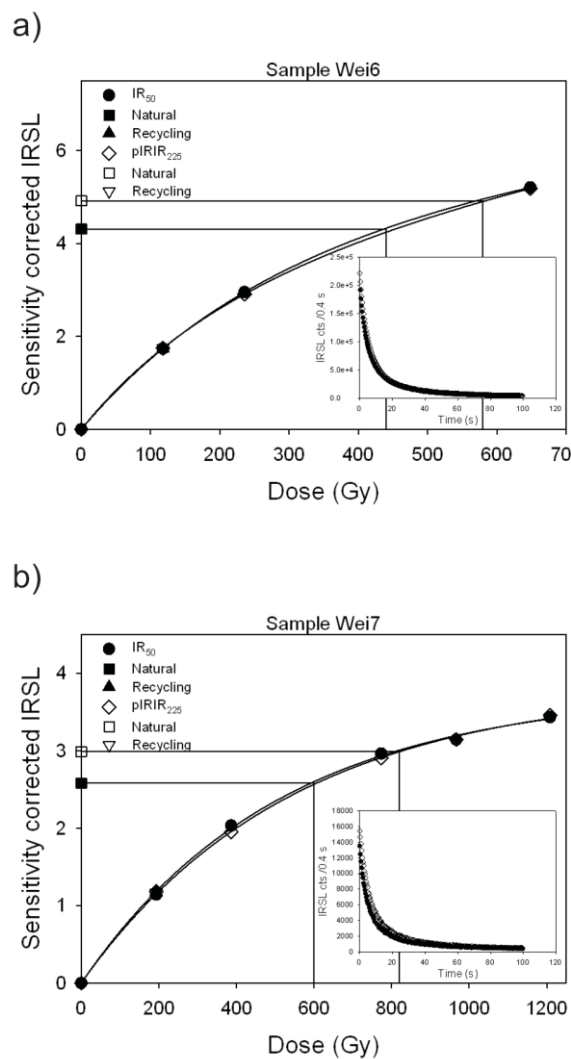
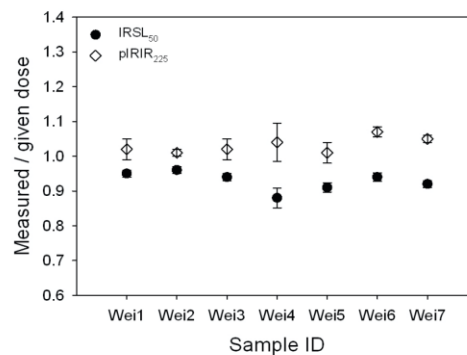


Figure 7.4: Dose response and decay curves for samples a) Wei 6 and b) Wei 7 showing the  $IR_{50}$  (filled symbols) and the  $pIRIR_{225}$  signal (open symbols).

The natural  $IR_{50}$  has about 10-15% lower signal intensity than the natural  $pIRIR_{225}$ . The growth curves for the  $pIRIR_{225}$  lies above the curve for the  $IR_{50}$  for all samples. However, the shapes of the growth curves are indistinguishable. Buylaert et al. (2009) observed also that the shape of the growth curves for the  $IR_{50}$  and the  $pIRIR_{225}$  are indistinguishable for their samples. The  $pIRIR_{225}$  of all the measured samples is much brighter (~10-15%) than for the  $IR_{50}$  (inlay of Fig. 4a and b) confirming the results of Buylaert et al. (2009). Recycling ratios for the samples range from  $0.98 \pm 0.03$  to  $1.01 \pm 0.003$  for the  $IR_{50}$  and from  $0.91 \pm 0.04$  to  $0.99 \pm 0.003$  for the  $pIRIR_{225}$ . Recuperation is below 5% of the natural signal. To test the applicability of the post-IR IRSL protocol using a stimulation temperature of  $225^{\circ}C$ , the dose recovery ratio was measured for all samples (Murray and Wintle, 2003). The aliquots were bleached for 4 hours in a Hönle SOL2 solar simulator before giving a dose approximately equal to the natural dose, except for sample Wei7, where a smaller dose was chosen. This dose was then measured in the same manner as the equivalent dose in order to confirm that the protocol is able to recover a known dose successfully. If the SAR protocol is suitable, the measured to given dose ratio should be close to 1. Fig. 5a shows the results of the dose recovery test for all samples for the  $IR_{50}$  and the  $pIRIR_{225}$ .

a)



b)

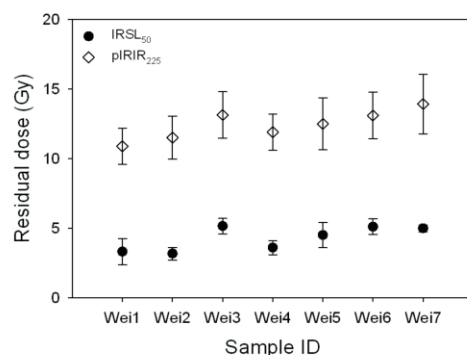


**Figure 7.5: Dose recovery test (a) and the residual doses (b) for the post-IR IR protocol at  $225^{\circ}C$  for all samples. Three aliquots were measured per sample. Error bars represent 1 standard error.**

The obtained ratios of the measured to given dose range from  $0.88 \pm 0.02$  to  $0.94 \pm 0.01$ , with a mean of  $0.93 \pm 0.01$  Gy ( $n = 21$ ) for IR<sub>50</sub> and from  $1.01 \pm 0.03$  to  $1.07 \pm 0.01$ , with a mean of  $1.03 \pm 0.01$  Gy ( $n = 21$ ) for pIRIR<sub>225</sub>. This data indicates the applicability of the post-IR IRSL protocol. To confirm that the IRSL and the post-IR IRSL are bleachable by natural daylight we exposed three aliquots per sample for four hours to a Hönle SOL2 solar simulator and then measured the apparent dose in the usual manner. The results are shown in Fig. 5b and Table 3. The residual doses range from  $3.2 \pm 0.5$  Gy to  $5.6 \pm 0.2$  Gy, with a mean of  $4.4 \pm 0.9$  Gy ( $n = 7$ ) for IR<sub>50</sub> and from  $10.9 \pm 1.3$  Gy to  $14.9 \pm 2.1$  Gy, with a mean of  $12.7 \pm 0.5$  Gy ( $n = 7$ ) for pIRIR<sub>225</sub>.

#### ***7.4.3. Equivalent Dose ( $D_e$ ), fading rates and age estimates***

In Table 3 the equivalent doses, dose recovery results, residual doses, g-values and the resulting luminescence ages, both uncorrected as well as fading corrected, are summarized for all samples.

Sample	Depth (m)	Measurement	$D_e$ (Gy)	Recycling	Measured/given dose	Residual doses (Gy)	g-value (%/decade)	Uncorrected age (ka)	Corrected age (ka)
Wei 1	0.33	IR <sub>50</sub>	52.9 ± 1.3	0.99 ± 0.01	0.95 ± 0.01	3.3 ± 0.9	3.2 ± 0.2	17.6 ± 1.1	23.7 ± 1.6
		pIRIR <sub>225</sub>	64.9 ± 2.3	1.02 ± 0.01	1.02 ± 0.03	10.9 ± 1.3	1.7 ± 0.1	21.6 ± 1.4	25.2 ± 1.6
Wei 2	0.75	IR <sub>50</sub>	65.5 ± 0.9	0.99 ± 0.01	0.96 ± 0.01	3.7 ± 0.5	2.9 ± 0.3	19.8 ± 1.1	25.9 ± 1.9
		pIRIR <sub>225</sub>	78.3 ± 3.5	1.01 ± 0.01	1.01 ± 0.01	11.5 ± 1.6	1.9 ± 0.2	23.5 ± 1.7	28.1 ± 2.3
Wei 3	2.15	IR <sub>50</sub>	331 ± 4	1.01 ± 0.01	0.94 ± 0.01	5.2 ± 0.6	3.0 ± 0.1	104 ± 9	140 ± 8
		pIRIR <sub>225</sub>	393 ± 3	0.98 ± 0.01	1.02 ± 0.03	13.1 ± 1.7	1.8 ± 0.2	123 ± 6	146 ± 9
Wei 4	2.75	IR <sub>50</sub>	337 ± 2	1.01 ± 0.003	0.88 ± 0.02	3.6 ± 0.5	3.1 ± 0.1	123 ± 9	177 ± 14
		pIRIR <sub>225</sub>	454 ± 10	0.98 ± 0.01	1.04 ± 0.06	11.9 ± 1.3	1.6 ± 0.3	167 ± 9	203 ± 22
Wei 5	3.25	IR <sub>50</sub>	388 ± 3	1.00 ± 0.003	0.91 ± 0.01	4.6 ± 0.9	2.9 ± 0.1	129 ± 9	178 ± 12
		pIRIR <sub>225</sub>	503 ± 10	0.99 ± 0.003	1.01 ± 0.03	12.5 ± 1.9	1.6 ± 0.2	167 ± 9	202 ± 14
Wei 6	5.00	IR <sub>50</sub>	423 ± 4	1.00 ± 0.003	0.94 ± 0.01	5.6 ± 0.2	3.1 ± 0.2	122 ± 7	169 ± 10
		pIRIR <sub>225</sub>	557 ± 7	0.99 ± 0.003	1.04 ± 0.06	14.9 ± 2.1	2.0 ± 0.1	162 ± 9	198 ± 12
Wei 7	7.48	IR <sub>50</sub>	411 ± 18	0.98 ± 0.03	0.92 ± 0.01	5.00 ± 0.5	2.9 ± 0.4	139 ± 8	>190
		pIRIR <sub>225</sub>	921 ± 41	0.91 ± 0.04	1.05 ± 0.01	13.9 ± 1.1	2.0 ± 0.4	313 ± 22	>350

**Table 7.3. Summary of equivalent dose ( $D_e$ ), recycling ratio, dose recovery, residual doses, fading and luminescence ages. Six aliquots were measured per sample for  $D_e$  determination. For the fading tests three aliquots/sample were measured.**

The  $D_e$ -s obtained using the  $IR_{50}$  from feldspar range from  $52.9 \pm 1.3$  Gy to  $423 \pm 4$  Gy. The obtained equivalent doses gave uncorrected age estimates between  $17.6 \pm 1.1$  ka and  $139 \pm 8$  ka.  $D_e$  values obtained for the  $IR_{50}$  increase clearly with depth from sample Wei1 to sample Wei5. The values obtained for sample Wei6 and Wei7 do not increase considerably with depth indicating that this signal is in field saturation at  $\sim 400$  Gy. The  $D_e$ -s calculated using the  $pIRIR_{225}$  from feldspar range from  $64.9 \pm 2.3$  Gy to  $921 \pm 41$  Gy. The  $D_e$  values are all in average  $\sim 20\%$  higher than those obtained using the  $IR_{50}$ . The  $pIRIR_{225}$  does not show evidence of field saturation (equilibrium between the accumulation of new charge and the loss by anomalous fading), and increases with depth. The characteristic saturation doses ( $D_0$ ) are about  $\sim 450$  Gy for the  $IR_{50}$  and the  $pIRIR_{225}$ . According to Wintle and Murray (2006) it is only possible to obtain reliable equivalent doses ( $D_e$ ) up to a dose value of  $2D_0$  and therefore it is important to test if the equivalent dose values exceed  $2D_0$ . Following this suggestion it is possible to measure  $D_e$  values up to about  $\sim 900$  Gy for our material. Fading tests were carried out for all samples using the post-IR IRSL measurement sequence. The  $g$ -values are shown in Fig. 6 for the  $IR_{50}$  and the  $pIRIR_{225}$ .

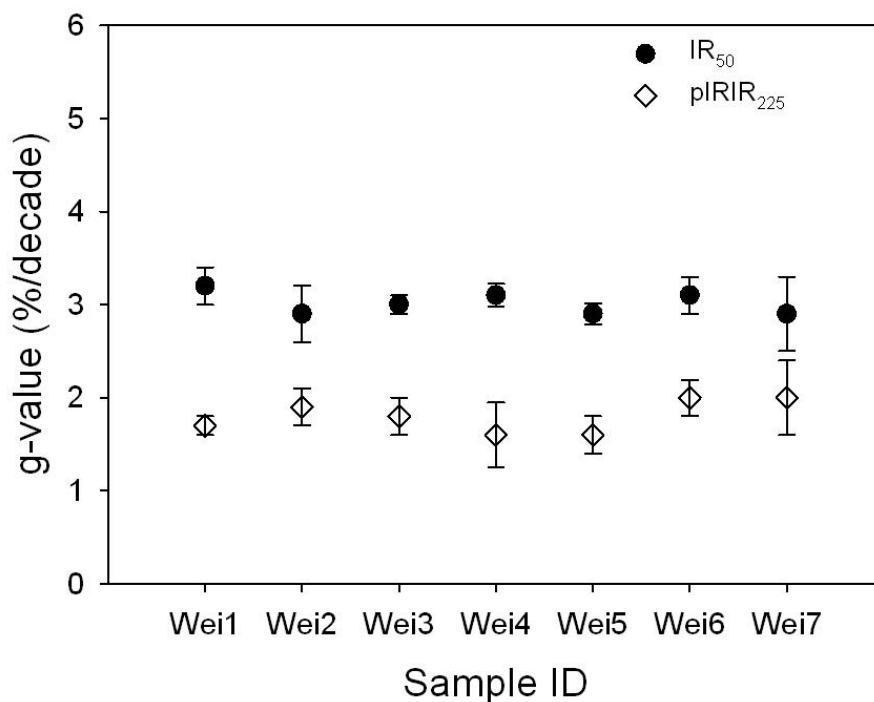


**Figure 7.6: Fading rates for the post the  $IR_{50}$  and  $pIRIR_{225}$  signals for all samples. Three aliquots were measured per sample. Error bars represent 1 standard error.**



The g-values range from  $2.9 \pm 0.3\%$ /decade to  $3.2 \pm 0.2\%$ /decade, with an average of  $3.01 \pm 0.04\%$ /decade ( $n = 7$ ) for the  $IR_{50}$  and from  $1.6 \pm 0.3\%$ /decade to  $2.0 \pm 0.4\%$ /decade, with an average of  $1.8 \pm 0.1\%$ /decade ( $n = 7$ ) for the  $pIRIR_{225}$  indicating that the  $pIRIR_{225}$  fades ~40% less than the  $IR_{50}$ . The fading corrected ages are listed in Table 3. Fading corrections use the methods proposed in Huntley and Lamothe (2001). The fading corrected age estimates for the  $IR_{50}$  range from  $23.7 \pm 1.6$  ka to  $>190$  ka and from  $25.2 \pm 1.6$  ka to  $>350$  ka for the  $pIRIR_{225}$ . The  $IR_{50}$  and the  $pIRIR_{225}$  are in agreement for samples Wei1-Wei6. For sample Wei7 the  $IR_{50}$  underestimates the  $pIRIR_{225}$ . We assume that the fading corrected  $pIRIR_{225}$  values yield more reliable age estimates. The  $IR_{50}$  is most likely in field saturation for sample Wei7. The  $pIRIR_{225}$  age estimate for sample Wei7 ( $>350$  ka) can be regarded as minimum age only, as the  $D_e$  value of  $921 \pm 41$  Gy is in the range of  $2D_0$ .

## 7.5. Discussion

Our study presents the first luminescence age estimates for the loess/palaeosol sequence of the gravel quarry Gaul located east of Weilbach based on an elevated temperature infrared stimulated luminescence (IRSL) signal which has been shown to fade at a very much lower rate than the conventional IRSL signal (Thomsen et al., 2008, Buylaert et al., 2009). The fading corrected  $IR_{50}$  and the  $pIRIR_{225}$  show good agreement for samples Wei1-Wei6. For sample Wei7 the  $IR_{50}$  underestimates the  $pIRIR_{225}$ . Our interpretation is hence based on the fading corrected  $pIRIR_{225}$  age estimates (Fig. 7). Sample Wei7, which was taken from the calcareous loess covering the gravel of terrace t4 (1 in Fig. 2) yielded an age estimate of  $>350$  ka indicating loess deposition during marine Isotope Stage (MIS) 10 or earlier and suggesting that terrace t4 has a minimum deposition age of ~350 ka. The calcareous loess is covered by a fCc horizon which forms the bottom of a reddish brown fBt horizon (2 in Fig. 2). This truncated palaeosol is covered by about 30 cm thick loess loam and a brown dark humic-rich horizon (4 in Fig. 2).

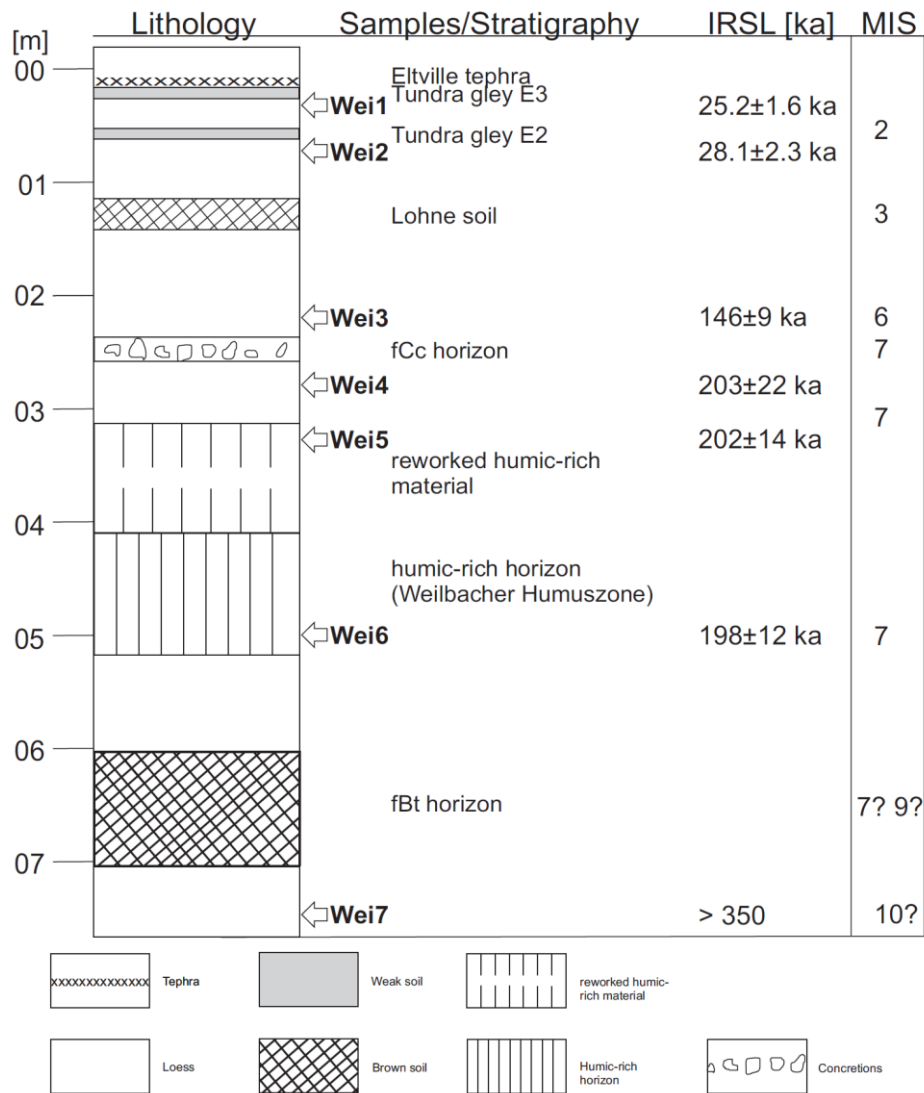


**Figure 7.7: Lithology and luminescence ages of the loess/palaeosol sequence exposed at the gravel quarry Gaul/Weilbach. Fading corrected pIRIR<sub>225</sub> age estimates are presented.**

Sample Wei6 was taken from this layer and yields an age estimate of  $198 \pm 12$  ka indicating a formation of the “Weilbacher Humuszone” during the late phase of MIS 7. Thus the oldest reddish brown fBt horizon (2 in Fig. 2) is older than ~200 ka and was most likely developed during the antepenultimate or penultimate interglacial. The humic-rich horizon is covered by a solifluction layer of reworked humic-rich material including loess loam and calcareous loess (Sample Wei 5 was taken from this horizon, 5 in Fig. 2). This layer yielded an age estimate of  $202 \pm 14$  ka and is covered by about 50 cm thick reworked loess (Wei4) with macroscopically visible pseudomicelium, which gives an age estimate of  $203 \pm 22$  ka. These layers can probably be correlated with a cold phase during MIS 7. It has to be mentioned that samples Wei5 and Wei4 were taken from reworked material. They could eventually be contaminated with older material, which would lead to an age overestimation.

Therefore the ages have to be regarded more carefully. The reworked loess is covered by a fCc horizon with up to 20 cm large carbonate concretions (6 in Fig. 2). Reddish brown remains of loam are found around these carbonate concretions (Fig. 2a). Above the fCc horizon loess accumulated; sample Wei3 was taken from this horizon and yielded an age estimate of  $146 \pm 9$  ka indicating accumulation during the penultimate glaciation (MIS 6). This result shows that the remains of the palaeosol very likely do not correlate to the last interglacial period but very likely correlate to a warm phase of MIS 7. The last interglacial soil (MIS 5) and the deposits of the lower Weichselian are missing in this profile. Bibus et al. (1996, 2002) provided a detailed description of the latter ones from the Mainz-Weisenau section and Frechen and Preusser (1996) provide TL and IRSL age estimates ranging from 68-113 ka for these deposits. The results of Bibus et al. (1996, 2002) show that there is evidence for three warmer phases after the last interglacial, revealing the significant hiatus for our profile. Above the loess layer the Middle Weichselian Lohne Soil (7 in Fig. 2) is developed followed by an Upper Weichselian sequence including tundra gley E2 (8 in Fig. 2), tundra gley E3 and the Eltville Tephra (9 in Fig. 2). Sample Wei2 was taken below the tundra gley E2 giving an age estimate of  $28.1 \pm 2.3$  ka and Sample Wei1 below the tundra gley E3 yielding an age estimate of  $25.2 \pm 1.6$  ka indicating accumulation during the last Pleniglacial (Upper Weichselian) correlating to MIS2. Frechen and Preusser (1996) obtained age estimates of  $\sim 20$  ka for the Eltville tephra and Zöller and Semmel (2001) provided mean TL age estimates of 21 ka for loess above the Eltville Tephra and 25 ka below. According to Frechen (1999) an eruption age between 17-23 ka for the Eltville tephra is most likely, which is in good agreement with our results.

Our results are not in complete agreement with the loess stratigraphy proposed by Semmel (1968, 2005). However, they support the assumption that the oldest exposed fBt horizon (2 in Fig. 2) correlates to the antepenultimate or penultimate interglacial and that the humic-rich horizon most likely correlates to the “Weilbacher Humuszone”, designated to be an interstadial period during the early penultimate glacial period (Semmel, 1968). But contrary to the suggestion that the fCc horizon (6 in Fig. 2) most likely correlates to the last interglacial, an age estimate of  $146 \pm 9$  ka was obtained for the loess sediments accumulated above the fCc horizon and the carbonate concretions. This age estimate indicates that the soil formation correlates most likely to a warm phase of MIS 7. Sample Wei1 and Wei 2 are in good agreement with the stratigraphical loess scheme (Semmel, 1968; 2005) and support the assumption that this loess deposits correlates to the Upper Weichselian, which is also indicated by the exposed typical marker horizons.

## 7.6. Conclusion

In our study we applied an elevated temperature IRSL (post-IR IRSL) protocol for polymineral fine-grains of the loess/palaeosol sequence at the gravel quarry Gaul/Weilbach (i) to set up a more reliable chronological framework for this loess/palaeosol sequence and (ii) to answer the question whether the oldest Bt horizon correlates to the Middle Pleistocene (antepenultimate or penultimate interglacial) or to the Upper Pleistocene (last interglacial). Performance tests such as dose recovery and residual checks were carried out to confirm the suitability of our SAR protocol. The IR<sub>50</sub> and the pIRIR<sub>225</sub> signals are in good agreement for samples Wei1-Wei6. For sample Wei7 the IR<sub>50</sub> underestimates the pIRIR<sub>225</sub>. Fading corrected IR<sub>50</sub> and pIRIR<sub>225</sub> ages range from  $23.7 \pm 1.6$  to  $>350$  ka. These age estimates indicate that the oldest loess was deposited during marine isotope stage (MIS) 10 or earlier suggesting that the terrasse t4 yield a minimum age of  $\sim 350$  ka. According to our results the humic-rich horizon was developed during the late phase of MIS 7 and can hence be correlated to the “Weilbacher Humuszone”. The oldest exposed fBt horizon most likely correlates to the antepenultimate or penultimate interglacial. Loess above the fCc horizon most likely accumulated during MIS 6 indicating that the remains of the palaeosol do not correlate to the last interglacial soil. The two uppermost samples indicate that the youngest loess was accumulated during MIS 2 (Upper Weichselian). This is in good agreement with the results of other dating studies regarding the Eltville tephra.

## Acknowledgements

This research is part of a PhD study in the frame of the “Leibniz Pakt für Forschung und Innovation” at the LIAG-Institute in Hanover. Ludwig Zöller and Lara Wacha are thanked for the useful comments on the manuscript.

## References

- Ademic, M. and Aitken, M.J., 1998. Dose-rate Conversion Factors: Update. *Ancient TL*, 16, 37-50.
- Aitken, M.J., 1985. *Thermoluminescence Dating*, London.
- Aitken, M.J., 1998. *An Introduction to Optical Dating*, Oxford.
- Antoine, P., Rousseau, D.-D., Moine, O., Kunesch, S., Hatté, C., Lang, A., Tissoux, H., Zöller, L., 2009. Rapid and cyclic eolian deposition during the Last Glacial in European loess: a high-resolution record from Nussloch, Germany. *Quaternary Science Reviews*, 28, 2955–2973.
- Auclair, M., Lamothe, M., Huot, S., 2003. Measurement of anomalous fading for feldspar IRSL using SAR. *Radiation Measurements*, 37, 487–492.
- Bibus, E., Rähle, Wedel, J., 2002. Profilaufbau, Molluskenführung und Parallelisierungsmöglichkeiten des Altwürmabschnitts im Lößprofil Mainz-Weisenau. *Eiszeitalter und Gegenwart*, 5, 1-14.
- Bibus, E., W. Bludau, W., C. Bross, C., Rähle, W., 1996. Der Altwürm- und Rissabschnitt im Profil Mainz-Weisenau. *Frankfurter geowissenschaftliche Arbeiten*, D20, 21–52.
- Buschbeck, H.M., 1993. *Thermolumineszenz und ihre Anwendung zu Altersbestimmungen in Geologie und Archäologie*. Diss. Univ. Frankfurt, p.155.
- Buylaert, J.-P., Thiel, C., Murray, A.S., Vandenberghe, D.A.G., Yi, S., Lu, H., submitted. IRSL and post-IR IRSL residual doses recorded in modern dust samples from the Chinese Loess Plateau. *Geochronometria*.
- Buylaert, J.P., Murray, A.S., Thomson, K.J., Jain, M., 2009. Testing the potential of an elevated temperature IRSL signal from K-feldspar. *Radiation Measurements*, 44, 560-565.

- Fink, J., 1973. Internationale Lößforschung, Bericht der INQUA-Lößkommission. *Eiszeitalter & Gegenwart*, 23/24, 415-426.
- Frechen, M., 1999. Upper Pleistocene loess stratigraphy in Southern Germany. *Quaternary Science Reviews*, 18, 243-269.
- Frechen, M. and Preusser, F., 1996. Kombinierte Lumineszenz-Datierungen am Beispiel des Lößprofils Mainz-Weisenau. *Frankfurter geowissenschaftliche Arbeiten, D 20*, 53-66.
- Huntley, D.J. and Lamothe, M., 2001. Ubiquity of anomalous fading in K-feldspars and the measurement and correction for it in optical dating. *Canadian Journal of Earth Sciences*, 38, 1093-1106.
- Lamothe M., Auclair M., Hamzaoui C., Huot S., 2003. Towards a prediction of long-term anomalous fading of feldspar IRSL. *Radiation Measurements*, 37, 493-498.
- Murray, A.S. and Wintle, A.G., 2003. The single regenerative dose protocol: potential for improvements in reliability. *Radiation Measurements*, 37, 377-381.
- Murray, A.S. and Olley, J.M., 2002. Precision and accuracy in the optically stimulated luminescence dating of sedimentary quartz: a status review. *Geochronometria*, 21, 1-16.
- Prescott, J.R. and Hutton, J.T., 1994. Cosmic ray contribution to dose rates for luminescence and ESR dating: large depths and long-term time variations. *Radiation Measurements*, 23, 497-500.
- Prescott, J.R. and Stephan, L.G., 1982. The contribution of cosmic radiation to the environmental dose for thermoluminescence dating. *PACT*, 6, 17-25.
- Rees-Jones, J., 1995. Optical dating of young sediments using fine-grain quartz. *Ancient TL*, 13, 9-14.

- Roberts, H.M., 2008. The development and application of luminescence dating to loess deposits: a perspective on the past, present and future. *Boreas*, 37, 483-507.
- Schönhals, E., Rohdenburg, H., Semmel, A., 1964. Ergebnisse neuerer Untersuchungen zur Würmlöß-Gliederung in Hessen. *Eiszeitalter & Gegenwart*, 15, 199–206.
- Semmel, A., 1967. Neue Fundstellen von vulkanischem Material in hessischen Lössen.- *Notizbl. hess. L.-Amt Bodenforschung*, 94, 104-108.
- Semmel, A., 1968. Studien über den Verlauf jungpleistozäner Formung in Hessen. *Frankfurter geogr. Hefte*, 45, 133 S.
- Semmel, A., 1969. Quartär.- *Erl. geol. Kte. Hessen*, Bl. 5916 Hochheim a.M., 51-99, Wiesbaden.
- Semmel, A., 1995. Quarry of the Portlandzementwerke Heidelberg at Mainz-Weisenau.- In: Schirmer, W. (ed.): *Quaternary field trips in Central Europe*, 1, 452-454, München.
- Semmel, A., 2005. Probleme der Abgrenzung und Datierung pleistozäner Terrassen - erörtert an Beispielen aus dem Untermaingebiet. *Geologisches Jahrbuch Hessen*, 132, 113-129.
- Semmel, A., 2005a. 7. Exkursionshalt IV Paläopedologische Probleme im Löß am Mainzer Dreieck S Hofheim a.Ts.- 51 S., Selbstverlag Hofheim/Ts.
- Semmel, A., 2007. Löss als Indikator der Landschaftsentwicklung in der Wetterau und am Untermain.- *Jahresberichte der Wetterauischen Gesellschaft für die gesamte Naturkunde*, 153-157, 7-35.
- Thomsen, K.J., Murray, A.S., Jain, M., Bøtter-Jensen, L. (2008): Laboratory fading rates of various luminescence signals from feldspar-rich sediment extracts. *Radiation Measurements*, 43, 1474-1486.

- Visocekas, R., 1985. Tunnelling radiative recombination in labradorite: Its association with anomalous fading of thermoluminescence. *Nuclear Tracks and Radiation Measurements*, 10, 521-529.
- Wintle, A.G., 1973. Anomalous fading of thermoluminescence in mineral samples. *Nature*, 245, 143-144.
- Wintle, A.G. & Brunnacker, K., 1982. Ages of volcanic tuff in Rheinhessen obtained by thermoluminescence dating of loess. *Naturwissenschaften*, 69, 181–183.
- Wintle, A.G. & Murray, A.S., 2006. A review of quartz optically stimulated luminescence characteristics and their relevance in single-aliquot regeneration dating protocols. *Radiation Measurements*, 41, 369-391.
- Zöller, L., 1989. Geomorphologische und geologische Interpretation von Thermolumineszenz-Daten.- *Bayreuther Geowissenschaftliche Arbeiten*, 14,103-112.
- Zöller, L. (1995): Würm- und Rißlößstratigraphie und Thermolumineszenz-Datierung in Süddeutschland und angrenzenden Gebieten. - *Habil.schrift Fak. f. Geowiss. Univ. Heidelberg*, (unpublished).
- Zöller, L. & Semmel, A. (2001): 175 years of loess research in Germany – long records and “uncon-formities“.- *Earth Science Reviews* **54**: 19-28



# Chapter 8

## Conclusion

The following pages present the general conclusion for luminescence dating, separated in the chapters “quartz” and “feldspar” and its application concerning loess stratigraphy.

### 8.1. Quartz

A modified single aliquot regenerative dose (SAR) protocol was proposed by Banerjee et al. (2001) for polymineral fine-grains. This protocol was applied to polymineral fine grains from the Stari Slankamen section. Performance tests like dose recovery, recycling ratio and recuperation gave satisfying results. However, the shape of the decay curve of the post-IR OSL signal was clearly different from quartz OSL. It decays much slower and is very similar to the decay curves from feldspar. Therefore it was concluded that the double SAR protocol was not capable of isolating a quartz signal but it is dominated by feldspar, and hence it also suffers from anomalous fading resulting in an age underestimation, when no fading correction is applied. Subsequently the polymineral fine grain fraction from the Stari Slankamen section was treated with 20 % hydrofluoric acid (HF) for 20 minutes (Mauz and Lang, 2004) or with fluorosilicic acid ( $\text{H}_2\text{SiF}_6$ ) for 6 days to obtain fine-grained quartz. In this thesis the optically stimulated luminescence (OSL) from quartz has been used to estimate the deposition age of loess from the Stari Slankamen loess/palaeosol sequence, from various loess sections of the Middle Rhine area and from maar lake sediments from the Jungfernweiher. For the loess deposits from Stari Slankamen age estimates of  $4.6 \pm 0.3$  ka to  $63.5 \pm 4.3$  ka were obtained. The calculated age estimates range for the loess sections in the Middle Rhine from  $16.6 \pm 1.4$  ka to  $86.1 \pm 5.9$  ka. The latter age estimate underestimate the IRSL age estimate ( $115 \pm 9$  ka) showing that the OSL is already in saturation although the growth curve does not yet saturate in this dose range. Reliable age estimates, which were in good agreement with the IRSL results, are obtained up to  $\sim 70$  ka. The characteristic saturation doses ( $D_0$ -values) for the loess samples from the Middle Rhine area and the maar lake sediments from the Jungfernweiher are about  $\sim 120$ - $150$  Gy. These are very similar to the values reported by Wintle and Murray

(2006); they suggested equivalent dose ( $D_e$ ) values should only be reported up to  $\sim 2D_0$ . Thus in our case it is possible to measure doses up to about  $\sim 240$ - $300$  Gy resulting in an upper limit of  $\sim 70$ - $80$  ka by taking into account the average dose rate of  $\sim 3.5$  Gy/ka. However, equivalent doses ( $D_e$ ) for maar lake sediments from the Jungfernweiher range from  $440 \pm 30$  Gy to  $580 \pm 40$  Gy. The laboratory-generated dose response curves continue to grow up to  $\sim 1000$  Gy for the maar lake sediments. Previous studies (Timar et al., 2010; Lowick et al., 2010) made similar observation for their fine-grain quartz samples and concluded that equivalent doses larger than  $2D_0$  were not very reliable. Taking all these observations into account, the equivalent doses for the maar lake sediments are considered to be in or close to saturation, and it is concluded that they only provide minimum dose estimates and so minimum age estimates. Due to the comparatively low saturation level the optically stimulated luminescence (OSL) is not suitable to date Middle Pleistocene deposits. Another possibility to use quartz as dosimeter is measuring the thermally transferred OSL (TT-OSL; Wang, et al. 2006, 2007; Tsukamoto et al., 2008). Unfortunately TT-OSL age estimates could not be obtained for all of the samples, due to the lack of signal. Some samples from the Tönchesberg section showed different luminescence characteristics compared to the other samples which could arise if the loess originated from different sources. While the loess deposits from the nearby Rhine area showed a weak TT-OSL signal, the loess from two marker horizons yielded a signal up to 10 times stronger with much smaller residuals. This suggests well bleached mineral grains after a long transport i.e. a distal source, different from the other loess horizons. These results imply that the TT-OSL from quartz is not suitable to date Middle Pleistocene loess deposits with a Rhenish source from the Middle Rhine area, but it could be used to identify loess deposits that originate from a different source.

## **8.2. Feldspar**

Feldspar has the potential to date Middle Pleistocene deposits as the signal grows to much higher doses than quartz but it suffers from a spontaneous loss of signal, the so-called anomalous fading, which leads to an age underestimation. In this study a double SAR protocol (Banerjee et al., 2001) was applied on polymineral fine grains from the Stari Slankamen and the Weilbach section; an infrared stimulation (IRSL) was carried out prior to a stimulation with blue LEDs (post-IR OSL) detected in the UV. The protocol was not capable to isolate a quartz OSL signal – the obtained post-IR OSL was still dominated by feldspar and

hence also affected by anomalous fading. Laboratory fading tests were carried out for both, the IRSL and post-IR OSL. The results showed that the fading rates obtained for the post-IR OSL were about 50% smaller than for the IRSL. Unfortunately the signals reached field saturation at around 300-500 Gy; therefore it was only possible to provide minimum age estimates for the penultimate glacial deposits.

In this thesis the post-IR IRSL protocol with a stimulation at 225°C (pIRIR<sub>225</sub>) was carried out on polymineral fine grains from loess of the Weilbach section and from maar lake sediments of the Jungfernweiher. Performance tests, i.e. dose recovery, recycling ratio and recuperation gave satisfying results. For both sections the IR<sub>50</sub> is in field saturation at doses of ~350-500 Gy. The pIRIR<sub>225</sub> is not in field saturation and increases with depths. The laboratory measured fading rates are around 40-50% smaller for the pIRIR<sub>225</sub> but still above 1.5%/decade. These results show that the applied protocol allows the determination of much higher equivalent doses (D<sub>e</sub>) and showed reduced fading rates. The pIRIR<sub>290</sub> signal was measured for two samples from the Jungfernweiher and a fading rate below 1%/decade was observed. Furthermore, the uncorrected pIRIR<sub>290</sub> age estimates are consistent with the corrected pIRIR<sub>225</sub> age estimates. Subsequently this protocol was applied to polymineral fine grains from loess of the Stari Slankamen section and from various sections in the Eifel area. Quality criteria like recycling ratio and recuperation were satisfactory. In contrast there were problems with the dose recovery ratio. The ratio of the measured to given dose yielded underestimation for the IR<sub>50</sub> and overestimation for the pIRIR<sub>290</sub> signal. Bleaching was carried out either for 4h in the Hönle SOL2 solar simulator or for three sunny days at the window. The obtained equivalent doses (D<sub>e</sub>) using the pIRIR<sub>290</sub> are between ~30-45% higher than those obtained using the IR<sub>50</sub>. The resulting uncorrected IR<sub>50</sub> ages underestimated the uncorrected pIRIR<sub>290</sub> age estimates by about 35-40% on average. Fading tests were carried out to confirm that this underestimation is due to anomalous fading. For the pIRIR<sub>290</sub> signal almost all calculated g-values were below 1%/decade while the IR<sub>50</sub> from the loess samples from the Eifel area shows fading rates around ~3%/decade. To get confidence about the reliability of the age estimates samples from the sites Wannenköpfe and Dachsbusch/Middle Rhine area were measured. For a sample taken from the reworked loess between two tephra deposits which yield <sup>40</sup>Ar/<sup>39</sup>Ar-age estimates of 215 ± 4 ka and 151 ± 11 ka, respectively, an age estimate of 147 ± 14 ka was calculated. Two sample taken below the 215 ± 4 ka tephra yielded age estimates of 228 ± 14 ka and 290 ± 17 ka. These results are in good agreement with the independent age control showing that the pIRIR<sub>290</sub> signal gives reliable age estimates for the polymineral fine grains from loess. Eight samples of the Stari Slankamen section and

nine samples from the sections in the Eifel area were found to be in saturation using both signals – the IR<sub>50</sub> as well as the pIRIR<sub>290</sub> signal. To test if there is a relation between the laboratory saturation level and the field saturation the ratio of the sensitivity-corrected natural signal to the laboratory saturation level was calculated for the IR<sub>50</sub> and for the pIRIR<sub>290</sub>. The obtained ratio is for all of the 17 samples close to unity showing that field saturation is equal to laboratory saturation for the pIRIR<sub>290</sub> signal. While the IR<sub>50</sub> was in field saturation at doses of about ~600 Gy, the dose corresponding to ~0.86 of saturation (2D<sub>0</sub> for a single exponential growth curve) was used to calculate minimum age estimates; these are of the order of ~300 ka, indicating an upper limit for dating loess of ~300 ka.

The equivalent doses D<sub>e</sub> obtained using the pulsed pIRIR<sub>150</sub> range from 52.2 ± 1.2 Gy to 645 ± 63 Gy, giving ages between 17.1 ± 1.1 and 189 ± 16 ka, which are in good agreement with the quartz OSL ages back to ~70 ka. One sample was taken from loess-like sediments above the Tönchesberg scoria, which yielded an <sup>40</sup>Ar/<sup>39</sup>Ar-laser-single grain age of 202 ± 14 ka and gave an pulsed pIRIR<sub>150</sub> age estimate of 186 ± 22 ka. This result is in good agreement with the independent age control and proves the reliability of the measurements.

It is concluded that the pIRIR<sub>290</sub> signal as well as the pulsed pIRIR<sub>150</sub> signal have the potential to date Middle Pleistocene deposits. The pIRIR<sub>290</sub> signal could be used to calculate age estimates up to ~300 ka while the pulsed pIRIR<sub>150</sub> signal provided age estimates up to ~200 ka.

### **8.3. Chronology for the investigated Aeolian sediments**

Based on the results of this thesis, a more reliable chronological framework could be established for the investigated loess/palaeosol sequences. The luminescence age estimates obtained for the loess deposits were in general underestimating previous results of other studies up to ~100 ka. In this thesis age estimates up to ~300 ka were obtained. For the first time it was possible to obtain more geochronological information about Middle Pleistocene deposits from the Vojvodina region and the Middle Rhine area based on luminescence dating.

A detailed loess/palaeosol sequence was investigated at Stari Slankamen in the Vojvodina region/Serbia, applying for the first time optically stimulated luminescence. This section is regarded as one of the most important sites for understanding Middle Pleistocene palaeoclimatic evolution in Central and Southeastern Europe (Marković et al., submitted). For the lower part of the sequence the results show that the TL age estimates of previous studies

of Singhvi et al. (1989) and Butrym et al. (1991) were all significantly underestimated the true deposition age, presumably because of anomalous fading. The age estimates of this thesis showed that palaeosols V-S3, V-S4 and V-S5 yielded minimum ages of ~230-390 ka which is considerably older than proposed by many previous studies. It could be also revealed that the loess unit V-L2 accumulated during marine isotope stage (MIS) 6 and that an erosional event marked out by an unconformity and gravel layer has a minimum age of ~170 ka. Furthermore the data of this thesis suggested that pedocomplex V-S1 can be correlated with the complete MIS 5 period which is in contrast to the finding of Bronger et al. (2003) who correlated palaeosol F2 (V-S1) with MIS 5a. The results for the upper part of the profile were generally in good agreement with the age estimates obtained by previous studies confirming that there were two major loess accumulation phases during the last Glacial, during MIS 4 and 2 and that the weak pedocomplex was developed during MIS 3.

For the older deposits from the sections at Kärlich and Ariendorf only minimum age estimates of the order of ~300 ka were obtained confirming the results for the Serbian loess about the upper age limit. The results of this thesis revealed significant underestimation of previous studies. The obtained age estimates show that there was loess accumulation during MIS 8 as indicated at the sections Ariendorf and Wannenköpfe. During warm phases of MIS 7, weak soils (Tönchesberg) up to red-brown forest soil (“parabraunerde”, remaining Bt-horizon; Ariendorf) developed. These finding could be also confirmed by results from the gravel quarry Gaul in Weilbach, where the luminescence age estimates indicate a formation of a strongly developed palaeosol (only the fCc-horizon with reddish brown remains of loam was left over) during a warm event of MIS 7. The results from samples from the sections of Ariendorf, Tönchesberg and Dachsbusch show a major phase of loess accumulation during the transition MIS 6/7 and during the whole MIS 6. Loess samples taken from the nearby southern foreland of the Taunus Mountains gave the same results. During MIS 5 a red-brown forest soil (“parabraunerde”) was developed. Remainings of this soil could only be found at the Tönchesberg and at the Wannenköpfe (Frechen and Justus, 1998); at all other sections it was missing due to erosional events. Two marker loess were accumulated in the transition MIS 4/5 according to the obtained luminescence ages. Kukla and Koci (1972) interpreted them as deposits from long-distance dust storms indicating the abrupt end of the interstadial and the first strong cold event of this glacial cycle. In this thesis different luminescence characteristics were observed from the Rhenish loess from this section and the loess from the marker horizons indicating a different source of these marker loess. Two weak brown soils (Tönchesberg section) are developed during MIS 3. During MIS 2 another major phase of

loess accumulation took place as revealed at the sections Tönchesberg, Kärlich, Ariendorf, Wannenköpfe (Frechen and Justus, 1998) and Weilbach.

Besides the loess/palaeosol sequences, maar lake sediments of the Jungfernweiher were also investigated in this thesis as aeolian dust (loess) makes up often a large part of the sediment inventory. The results proved the applicability of luminescence dating to maar lake sediments. In contrast there was a discrepancy between the established stratigraphy and all the IRSL data obtained in this thesis. However the stratigraphy is based (1) on radiocarbon ages, which are in the range ~43-55 ka (except for one of ~35 ka); all at or close to the upper limit of the method, (2) on luminescence age estimates of Degering and Krbetschek (2007) which underestimate the results of this thesis significantly most likely owing to field saturation of their signal and (3) on an association of the tephra at 107 m with a known age event (Rocourt Tephra; Lenaz et al. 2010) which is not secure. The results of this thesis showed that the Jungfernweiher was effectively filled up with sediments until ~250 ka, and there has either been very little deposition since then, or younger sediments have been eroded.

It is generally concluded that the obtained luminescence results of the investigated samples from the different sections does significantly improve the geochronological framework for the deposits of the Vojvodina region and the Middle Rhine area covering the last ~300 ka. In both areas it was for the first time possible to obtain reliable luminescence ages for the penultimate glacial deposits. Hopefully it will be possible in future to extend the age range beyond the ~300 ka limit in luminescence dating to access the further potential of the loess/palaeosol sequences.

## References

- Banerjee, D., Murray, A.S., Bøtter-Jensen, L., Lang, A., 2001. Equivalent dose estimation using a single aliquot of polymineral fine grains. *Radiation Measurements* 33, 73–94.
- Bronger, A., 2003. Correlation of loess/palaeosol sequences in East and Central Asia with SE Central Europe: towards a continental Quaternary pedostratigraphy and paleoclimatic history. *Quaternary International* 106-107, 11-31.

- Butrym, J., Maruszczak, H., Zeremski, M., 1991. Thermoluminescence stratigraphy of Danubian loess in Belgrade environs. *Annales, Universite Marie-Curie Sklodowska, B* 46, 53–64.
- Buylaert, J.P., Murray, A.S., Thomson, K.J., Jain, M., 2009. Testing the potential of an elevated temperature IRSL signal from K-feldspar. *Radiation Measurements*, 44, 560-565.
- Degering, D., Krbetschek, M. R., 2007. Dating of Interglacial Deposits by Luminescence Methods.- In: Sirokko et al. (Eds.): *The Climate of Past Interglacials*, Elsevier, 157-172
- Frechen, F., Justus, A., 1998. Zur Geologie der Wannenvulkangruppe in der Osteifel *GeoArchaeoRhein*, 2, 213–240.
- Kukla, G.J., Koci, A., 1972. End of the last interglacial in the loess record. *Quaternary Research*, 2, 374-383.
- Lenaz, D., Marciano, R., Veres, D., Dietrich, S., Sirocko, F. 2010. Mineralogy of the Dehner and Jungfernweiher maar tephra (Eifel, Germany). *N.Jb.Geol.Palaont.Abh. Fast track* DOI:10.1127/0077-7749/2010/0062.
- Lowick, S.E., Preusser, F., Pini, R., Ravazzi, C. 2010. Underestimation of fine grain quartz OSL dating towards the Eemian: comparison with palynostratigraphy from Azzano Decimo, northeastern Italy, *Quaternary Geochronology*, 5, 583-590.
- Marković, S.B., Hambach, U., Stevens, T., Kukla, G.J., Heller, F., McCoy, W.D., Oches, E.A., Bugge, B., Zöller, L. in press. The last million years recorded at the Stari Slankamen loess/palaeosol sequence: revised chronostratigraphy and long-term environmental trends. *Quaternary Science Reviews*. doi:10.1016/j.quascirev.2011.02.004.

- Mauz, B., Lang, A., 2004. Removal of the feldspar-derived luminescence component from polymineral fine silt samples for optical dating applications: evaluation of chemical treatment protocols and quality control procedures. *Ancient TL* 22, 1-8.
- Schmidt, E.D., Frechen, M., Murray, A.S., Tsukamoto, S., Bittmann, F., 2011. Luminescence chronology of the loess record from the Tönchesberg section – a comparison of using quartz and feldspar as dosimeter to extend the age range beyond the Eemian. *Quaternary International*, 234, 10-22.
- Schmidt, E.D., Murray, A.S., Jain, M., Tsukamoto, S., Frechen, M., 2009. Testing recuperated OSL dating on quartz and polymineral fine-grains. Poster, UK Meeting on Luminescence And Electron Spin Resonance Dating, Royal Holloway, 26.-28.08.2009.
- Singhvi, A.K., Bronger, A., Sauer, W., Pant, R.K., 1989. Thermoluminescence dating of loess/palaeosol sequences in the Carpathian basin (east-central Europe): a suggestion for a revised chronology. *Chemical Geology* 73, 307-317.
- Timar, A., Vandenberghe, D., Panaiotu, E.C., Panaiotu, C.G., Necula, C., Cosma, C., Van den haute, P., 2010. Optical dating of Romanian loess using fine-grained quartz. *Quaternary Geochronology*, 5, 143-148.
- Tsukamoto, S., Duller, G.A.T., Wintle, A.G., 2008. Characteristics of thermally transferred optically stimulated luminescence (TT-OSL) in quartz and its potential for dating sediments. *Radiation Measurements*, 43, 1204-1218.
- Wang, X.L., Wintle, A.G., Lu, Y.C., 2006. Thermally transferred luminescence in fine-grained quartz from Chinese loess: Basic observations. *Radiation Measurement*, 41, 649-658.
- Wang, X.L., Wintle, A.G., Lu, Y.C., 2007. Testing a single-aliquot protocol for recuperated OSL dating. *Radiation Measurements*, 42, 380-391.



Wintle, A.G, Murray, A.S. 2006. A review of quartz optically stimulated luminescence characteristics and their relevance in single-aliquot regeneration dating protocols. *Radiation Measurements*, 41, 369-391.

## **Acknowledgements**

First of all I want to express my deepest acknowledgements to Prof. Dr Manfred Frechen for his guidance, permanent support, encouragement and confidence during my whole thesis.

This thesis was carried out in the frame of the “Leibniz Pakt für Forschung und Innovation” at the Leibniz Institute for Applied Geophysics (LIAG) in Hannover. I am grateful for the financial support and the laboratory facilities.

To acknowledge everyone who contributed with his help, support and encouragements to this work would fill many pages. Therefore I just concentrate on several persons. But I am very, very grateful to all of you!!

I want to thank a lot Dr. Sumiko Tsukamoto for introducing me into luminescence dating, for her assistance and support, the nice discussions about work and other issues and especially that she was never tired to answer to all my questions.

Many thanks to Prof. Dr. A.S. Murray (Nordic Laboratory for Luminescence Dating) for his excellent guidance, support and timely discussions.

I wish to thank all the co-authors of my paper for the collaboration.

I am so much grateful to Dr. Tobias Lauer for all his help and that he always supported me to get back the confidence in me and in my work. All the fieldwork and the whole thesis would have not been possible without you Tobi.

I am much obliged to the other PhD students and friends at the LIAG for many fruitful discussions and help: Dr. Tony Reimann, Dr. Lara Wacha, Dr. Christine Thiel, Dr. Alexander Kunz, Dr. Paul Königer and Dr. Linto Alappat. Special thanks to Alex for introducing me into the gamma spectrometry. I wish to thank the technicians from the section S3 at the LIAG Sonja Riemenschneider, Frank Oppermann, Karsten Vollmer, Gudrun Drewes, Petra Posimowski and Sabine Mogwitz for their timely help and for training me in the laboratory.

I am greatly indebted to Dr. Mayank Jain, Dr. Jan-Pieter Buylaert and all the members of the Nordic Laboratory for Luminescence Dating/ Risø National Laboratory for the great help during my two stays there. At this place I also want to mention Cilia Derese and Reza Sohbaty, with whom I could share the office for several months during my thesis. Thanks a lot to both of you for all your support and your friendship.

Great acknowledgements is made to Prof. Dr. Frank Sirocko and his co-workers for welcoming me at the Sedimentology group of the Institute for Geosciences in Mainz, for integrating me in their working group and for carrying always the heavy cores. Special thanks to Stephan Dietrich, Dr. Klemens Seelos, Stephanie Grimm, Simone Illig and Christoph Wagner for your help, the nice time together and unforgettable evenings...

I want to thank Prof. Dr. Erhard Bibus for many discussions and his advices about the loess sections in the Eifel area.

Many thanks to Dr. Matthias Krbetschek for his help and the timely discussions.

I thank my family and my friends for their support.

Last but not least I deeply thank Guillaume Car, Sarah Fuchs and Katrin Stimmler for supporting me especially during the last hard working months. Your help, care and your deep friendship gave me so much energy to finish this work.

# **Curriculum Vitae**

**For reasons of data protection,  
the curriculum vitae is not included in the online version**



## **Publications**

- Schmidt, E.D., Murray, A.S., Tsukamoto, S., Frechen, M., submitted. Elevated temperature IRSL dating of loess sections in the Eifel region of Germany. *Quaternary International*.
- Schmidt, E.D., Murray, A.S., Stevens, T., Buylaert, J.P., Markovic, S.B., Tsukamoto, S., Frechen, M., submitted. Elevated temperature IRSL dating of the lower part of the Stari Slankamen loess sequence (Vojvodina, Serbia) – investigating the saturation behaviour of the pIRIR<sub>290</sub> signal. *Quaternary Geochronology*.
- Schmidt, E.D., Semmel, A., Frechen, M., 2011. Luminescence dating of the loess/palaeosol sequence at the gravel quarry Gaul/Weilbach. *Quaternary Science Journal*, 60 (1).
- Schmidt, E.D., Murray, A.S., F. Sirocko, Tsukamoto, S., Frechen, M., 2011. IRSL signals from maar lake sediments stimulated at various temperatures. *Quaternary Science Journal*, 60 (1).
- Schmidt, E.D., Frechen, M., Murray, A.S., Tsukamoto, S., Bittmann, F., 2011. Luminescence chronology of the loess record from the Tönchesberg section – a comparison of using quartz and feldspar as dosimeter to extend the age range beyond the Eemian. *Quaternary International*, 234, 10-22.
- Schmidt, E.D., Machalett, B., Marković, S.B., Tsukamoto, S., Frechen, M., 2010. Luminescence chronology of the upper part of the Stari Slankamen loess sequence (Vojvodina, Serbia). *Quaternary Geochronology*, 5: 137-142.
- Schmidt, E.D., Machalett, B., Marković, S.B., Milojkovic, N., Tsukamoto, S., Frechen, M. 2008. Luminescence dating of the upper part of the Stari Slankamen loess sequence (Vojvodina, Serbia). *Abhandlungen der geologischen Bundesanstalt*, 62, 217-218 .
- Schmidt, E.D., Lauer, T., Bibus, E. 2007. Die Bedeutung des oberflächennahen Untergrundes für Boden und Relief an der Bauland-Odenwald-Grenze. *Mitteilungen der Deutschen Bodenkundlichen Gesellschaft*, 110, 535-536.

## Oral presentations

- Schmidt, E.D., Murray, A.S., Stevens, T., Buylaert, J.P., Markovic, S.B., Tsukamoto, S., Frechen, M. 2010. Investigating the saturation behaviour of the pIRIR<sub>290</sub> signal from loess. – oral presentation, Final Workshop of Leibniz Pakt Project, 25.-26.10.2010.
- Schmidt, E.D., Murray, A.S., Stevens, T., Buylaert, J.P., Markovic, S.B., Tsukamoto, S., Frechen, M. 2010. Elevated temperature IRSL dating of the lower part of the Stari Slankamen loess sequence (Vojvodina, Serbia) – investigating the saturation behaviour of the pIRIR<sub>290</sub> signal. – UK Meeting on Luminescence And Electron Spin Resonance Dating, Oxford, 07.-10.09.2010.
- Schmidt, E.D. 2010. Luminescence dating of loess deposits - a Comparison of using Quartz and Feldspar as Dosimeter to extend the Age Range beyond the Eemian. - Doktorandenkolloquium Geographisches Institut, Freie Universität Berlin, 28.04.2010; Berlin.
- Schmidt, E.D., Frechen, M., 2010. Aktuelle Entwicklungen im Bereich der Lumineszenzdatierungen. – Workshop Forschungsbohrung Rodderberg, 08.-09.03.2010; Bonn.
- Schmidt, E.D. Recent developments in luminescence dating Loess chronology of the Tönchesberg section (Eifel area/Germany). – Université de Bordeaux, 09.03.2010; Bordeaux.
- Schmidt, E.D. Recent developments in luminescence dating. – Laboratoire de Géographie Physique Meudon, 27.02.2010; Meudon, Paris.
- Schmidt, E.D., Murray, A.S., Ankjaergaard, C., Tsukamoto, S., Frechen, M., 2009. Potential of a pulsed signal from feldspar to date old loess. German Meeting on Luminescence And Electron Spin Resonance Dating, Hannover, 9.-11.10.2009.

Schmidt, E.D., Murray, A.S., Tsukamoto, S., Frechen, M., 2009. Potential of Quartz and Feldspar in OSL to date Middle Pleistocene loess from the Eifel area/Germany. Oral presentation, Loessfest09, Novi Sad, Serbia, 31.08-03.09.2009.

Schmidt, E.D., Murray, A.S., Ankjaergaard, C., Tsukamoto, S., Frechen, M., 2009. Potential of a pulsed signal from feldspar to date old loess. Oral presentation, UK Meeting on Luminescence And Electron Spin Resonance Dating, Royal Holloway, 26.-28.08.2009.

Schmidt, E.D., Murray, A.S., Tsukamoto, S., Frechen, M., 2009. Potential von Quartz als Dosimeter für die Lumineszenzdatierung mittelpleistozäner Löss. Vortrag, 8. Jahrestagung der AG Paläopedologie der DBG, Wien, 21.-23.05.2009.

Schmidt, E.D., Frechen, M., Tsukamoto, S., Machalet, B., Marković, S.B., Sirocko, F. 2008. Luminescence Chronology of Loess and Maar Lake Sediments of the Vojvodina/Serbia & the Eifel area. Hauskolloquium Geozentrum Hannover, Dezember 2008.

Schmidt, E.D., Binot, F., Frechen, M., 2008. Forschungsbohrung Rodderberg-Vulkan bei Bonn. Austauschsitzung GGA-Institut Hannover, 12.-13.11.2008.

Schmidt, E.D., Machalet, B., Marković, S.B., Tsukamoto, S., Frechen, M. 2008. Luminescence Chronology of the Upper Part of the Stari Slankamen Loess Sequence (Vojvodina, Serbia). German Meeting on Luminescence And Electron Spin Resonance Dating, Leipzig, 31.10.-02.11.2008.

## **Poster**

Schmidt, E.D., Frechen, M., Murray, A.S., Tsukamoto, S., 2009. Luminescence chronology of a detailed terrestrial loess record of the past 200 ka exposed at the Tönchesberg section. Austauschsitzung LIAG Hannover, 04.-05.11.2009.



- Schmidt, E.D., Frechen, M., Murray, A.S., Tsukamoto, S., 2009. Luminescence chronology of the loess record from the Tönchesberg section – a comparison of using quartz and feldspar as dosimeter to extend the age range beyond the Eemian. Poster, EGU General Assembly 2010, Vienne, Austria, 02.-07.05.2010.
- Schmidt, E.D., Murray, A.S., Jain, M., Tsukamoto, S., Frechen, M., 2009. Testing recuperated OSL dating on quartz and polymineral fine-grains. Poster, UK Meeting on Luminescence And Electron Spin Resonance Dating, Royal Holloway, 26.-28.08.2009.
- Schmidt, E.D., Sirocko, F., Tsukamoto, S., Frechen, M. 2009. OSL Dating of Maar Lake Sediments - Application of Different Methods on Temporal Successions of Dust Storm Events. Poster, EGU General Assembly 2009, Vienne, Austria, 19.-24.04.2009.
- Schmidt, E.D., Machalett, B., Marković, S.B., Milojkovic, N., Tsukamoto, S., Frechen, M. 2008. OSL Dating of Aeolian Sediments from the Stari Slankamen Loess Site (Vojvodina, Serbia). Poster, 12th International Conference On Luminescence And Electron Spin Resonance Dating (LED 2008), 18.-22.09.2008.
- Schmidt, E.D., Lauer, T., Bibus, E. 2007. Die Bedeutung des oberflächennahen Untergrundes für Boden und Relief an der Bauland-Odenwald-Grenze. Poster, Jahrestagung 2007 der Deutschen Bodenkundlichen Gesellschaft, Dresden, 02.-09.09.2007.